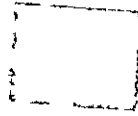


2



NASA CR-72773
SU-SEL-70-075



The Design and Development of a Low-Cost Microwave Adaptor Suitable for Television Reception from High-Power Communications Satellites

by

B B Lusignan, P. Z. Bulkeley, J M Janky, and R. B. Taggart, Jr.

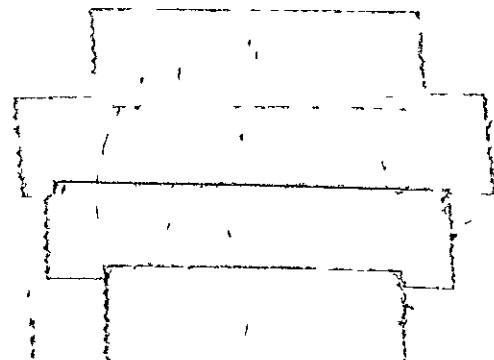
CENTER FOR RADAR ASTRONOMY
Stanford University
Stanford, California

Technical Report No 3682-1

Prepared for
NATIONAL AERONAUTICS AND SPACE ADMINISTRATION

NASA Lewis Research Center
Contract NAS 12-690

FACILITY FORM 602	<u>N71-17707</u> (ACCESSION NUMBER)	(THRU)
	<u>196</u> (PAGES)	<u>G3</u> (CODE)
	<u>CR-72773</u> (NASA CR OR TMX OR AD NUMBER)	<u>07</u> (CATEGORY)



107

NOTICE

This report was prepared as an account of Government-sponsored work. Neither the United States, nor the National Aeronautics and Space Administration (NASA), nor any person acting on behalf of NASA

- A) Makes any warranty or representation, expressed or implied, with respect to the accuracy, completeness, or usefulness of the information contained in this report, or that the use of any information, apparatus, method, or process disclosed in this report may not infringe privately-owned rights, or
- B.) Assumes any liabilities with respect to the use of, or for damages resulting from the use of, any information, apparatus, method or process disclosed in this report.

As used above, "person acting on behalf of NASA" includes any employee or contractor of NASA, or employee of such contractor, to the extent that such employee or contractor of NASA or employee of such contractor prepares, disseminates, or provides access to any information pursuant to his employment or contract with NASA, or his employment with such contractor

FINAL REPORT

THE DESIGN AND DEVELOPMENT OF A LOW-COST MICROWAVE ADAPTOR SUITABLE
FOR TELEVISION RECEPTION FROM HIGH-POWER COMMUNICATIONS SATELLITES

by

B B Lusignan, P Z Bulkeley, J. M Janky, and R B. Taggart, Jr

Center for Radar Astronomy
Stanford University
Stanford, California 94305

Prepared for

National Aeronautics and Space Administration

October 31, 1970

Contract NAS 12-690

NASA Lewis Research Center
Cleveland, Ohio

PRECEDING PAGE BLANK NOT FILMED

ABSTRACT

This report presents the design of a mass-producible microwave adaptor which is capable of detecting wideband FM television signals broadcast from a synchronous satellite. A complete communications system design at 2.62 GHz is included. Performance criteria are formulated, and the appropriate alternatives are evaluated. A novel design for the antenna is presented, which is estimated to cost \$32 in quantities of 100,000 units. The electronics package is estimated to cost \$60 for the same production quantity. The design details of working prototypes of both the antenna and electronics package are included. The trends for higher frequencies are discussed, and a design for a 12 GHz system is discussed.

CONTENTS

	<u>Page</u>
I INTRODUCTION AND SUMMARY	1
II DETERMINATION OF SYSTEM PARAMETERS	5
A. Basic System Description	5
B. General Receiver Requirements	6
C. Quantity of Receivers	7
D. Frequency Range	7
E. Receiver Figure of Merit and Costs	8
F. System Parameters	9
G. Maximum Antenna Diameter	14
H. Maximum Figure of Merit A_e/T_e	14
I. Determination of A_e and T_e from Required A_e/T_e	16
J. Availability of Satellite Power	16
K. Satellite Power Generation	18
L. Adaptor Specifications and Functional Block Diagram	20
M. Design Philosophy	22
III THE ANTENNA	25
A. Design Objectives	25
B. Design Approach and Alternatives	26
C. Preliminary Design	27
D. Final Design and Cost Estimates	40
E. Testing the Antenna Gain Measurement Method	48
F. Antenna Costs and Assembly Procedure	50
IV THE ELECTRONICS PACKAGE	57
A. Development of System Requirements for the "Front End"	57
B. The Mixer	60
C. The Local Oscillator	70
D. Preselector Filter	70
E. The IF Amplifier	100
F. The Limiter	108
G. The Discriminator	110

CONTENTS (Cont)

	<u>Page</u>
H The Detector	112
I. The Remodulator	113
J The Power Supply and Voltage Regulator	113
K. The Working Model Layout and Performance	114
 V COST ESTIMATES OF ELECTRONICS PACKAGE	 133
A Origin of Costs	133
B Learning Curves	134
C Component Costs	135
D. Mixer-Feed Housing	137
E Microwave Diode Costs	140
F. Step Recovery Diode Costs	144
G Imported Components and Duty Considerations	144
H. Production Costs Assembly, Overhead, Profit, and Taxes	145
I. Alternative Configuration Costs	147
J. Low-Volume Production Cost Estimates	147
K. Cost Implications for a Brazilian Satellite System	150
 VI. TRENDS FOR HIGHER FREQUENCIES	 153
A Configuration as a Function of Frequency Range	153
B 12 GHz System Specifications and Cost Estimate	154
 VII CONCLUSIONS	 157
 APPENDIX	
A. Program for Optimizing the Petal Shape, Calculating the Feed Horn Illumination Constants, and Calculating the Gain of the Antenna	159
B Petal Plotting Program	163
C. Antenna Diameter vs Noise Figure Tradeoff	165
D Delay Line Oscillator	166
E Alternate Layouts for Mixer-Feed Housing	172
F Circular Waveguide Accessories and the "Perfect" Transition	174
G. The 2.62 GHz Wideband FM Test Signal Source	177
H Discriminator Design	179
 REFERENCES	 185

ILLUSTRATIONS

<u>Figure</u>		<u>Page</u>
I-1	Assembled antenna and electronics package	1
II-1	The basic direct broadcasting system	5
II-2	Growth rate of the effective radiated power for commercial satellites since 1963	17
II-3	Block diagram of adaptor	21
III-1	Cartesian representation of antenna surface	28
III-2	Antenna components	29
III-3	First antenna prototype	37
III-4	Mounting structure for first prototype	37
III-5	Antenna seam--first prototype	38
III-6.	Second prototype with feedhorn and adjustable feed supports	39
III-7	Close-up of box rim construction of second prototype	39
III-8	Three rim designs	41
III-9	Extrusion for rim	42
III-10	Third prototype and final antenna design	43
III-11	Cross-sectional view through the antenna at petal centerline	45
III-12	Top view of antenna petal	45
III-13	Feed horn gain pattern	45
III-14	Antenna gain vs feed horn pattern	47
III-15	Gain measurement test setup	49
III-16	Antenna during gain measurement	50
III-17	Assembly procedure	52
IV-1.	"Front end" of adaptor	58
IV-2	Balanced mixer in circular waveguide	63

ILLUSTRATIONS (Cont)

<u>Figure</u>	<u>Page</u>
IV-3 Single-diode mixer in circular waveguide . . .	69
IV-4 Three local oscillator configurations	73
IV-5. Fractional long-term stability vs frequency	76
IV-6 Basic oscillator circuit	78
IV-7 FM noise density vs apparent modulation frequency for various oscillators	80
IV-8 Typical LC oscillator	83
IV-9. Equivalent circuit of LC oscillator	83
IV-10 Typical LC oscillator circuit	86
IV-11. Complete local oscillator circuitry	87
IV-12 Step-recovery diode multiplier circuit	88
IV-13 Interdigital filter structure realized by a sandwich construction technique	93
IV-14 Cutaway view of a filter rod with capacities	95
IV-15. Experimental local oscillator assembly	96
IV-16 3.8 GHz filter response as a function of rod length	98
IV-17 2.5 GHz filter response as a function of rod length	99
IV-18 Lerner filter circuit	102
IV-19. Complete IF amplifier circuitry	104
IV-20 Signal processor circuitry filter, limiter, discriminator, and remodulator	109
IV-21. Measured discriminator response	112
IV-22. Power supply and voltage regulator schematic	114
IV-23. The die-castable mixer-feed housing	115
IV-24. Disassembled mixer-feed housing	116
IV-25 Mixer-feed housing with circuit boards installed	117

ILLUSTRATIONS (Cont)

<u>Figure</u>		<u>Page</u>
IV-26	Mechanical drawing of mixer-feed housing	119
IV-27	Mechanical drawing of filter insert	121
IV-28	Crystal controlled local oscillator board layout	124
IV-29	Sketch of proposed changes in layout of mixer-feed housing	126
IV-30.	IF amplifier layout	127
IV-31	Signal processor board layout	129
IV-32	Discriminator board layout	130
V-1.	Reduction factor versus quantity	135
V-2	Production cost of mixer-feed housing versus quantity	138
V-3	Filter insert costs versus quantity	139
V-4	Parts cost versus quantity	141
V-5	Price range of mixer diodes versus noise figure	142
B-1.	Petal dimension orientation	163
C-1	Antenna and diode cost vs system noise figure	166
D-1	Two-stage delay line oscillator	168
E-1	Wraparound configuration	173
E-2	Complete electronics compartment, half cylinder	174
E-3	Split housing with circuit boards mounted in a horizontal plane	175
F-1	Coax-to-waveguide transition	175
F-2	Alignment setup for the "perfect" transition	176
G-1	Schematic diagram for the 2 62 GHz wideband FM test signal source	178
H-1	Circuit diagram of the transmission line discriminator	179

TABLES

<u>Number</u>		<u>Page</u>
I-I	Adaptor characteristics . .	3
II-I	Communications system parameters for direct broadcasting via satellite	15
III-I	Antenna gain vs number of petals $f_0 = 3.0$ GHz	32
III-II	Petal tolerance vs antenna gain . .	34
III-III	Antenna costs as quoted from manufacturers .	54
III-IV.	Antenna costs for various quantities	55
IV-I	Stripline substrate material prices (1969) .	61
IV-II	Step-recovery diode multiplier circuit parameters	90
IV-III	120 MHz filter element values	105
V-I	2.62 GHz _Z FM receiver parts cost	136
V-II	Mixer-feed housing mold costs	138
V-III	Filter insert costs	140
V-IV	Mixer hardware cost	140
V-V	Cost projections for mixer diodes	144
V-VI	Total cost estimates of the adaptor (dollars 100,000 units)	146
V-VII	Module parts cost (100,00 units)	147
V-VIII	Alternative module costs (100,000 units)	148
V-IX	Total factory costs	149
VI-I	12 GHz communication system parameters	155
VI-II	12 GHz receiver cost estimates	155
VII-I	Factory cost summary for adaptor	157
C-I	Costs for various antenna-mixer diode pairs for constant figure of merit	166

TABLES (Cont)

<u>Number</u>		<u>Page</u>
D-I	Fractional stability for delay line oscillator $f_o = 270\ 338\ \text{MHz}$	169
D-II	Fractional setting error for oscillator in Fig IV-9 for $\Delta L = \pm 1\ \text{nh}$, $\Delta C = \pm 1\ \text{pf}$	171
H-I	Average distortion vs line length	183

I. INTRODUCTION AND SUMMARY

The purpose of the research effort sponsored by NASA Contract NAS 12-690 is to design a low-cost mass-producible adaptor system capable of detecting television signal broadcast directly from high-powered synchronous satellites. It must render the satellite signal acceptable to an ordinary television set. The adaptor consists of a seven-foot diameter antenna of novel design and an electronics package which mounts at the focus of the antenna, as shown in Fig. I-1.



Fig. I-1. ASSEMBLED ANTENNA AND ELECTRONICS PACKAGE.

One of the major motivations for the study is the potential such a system offers for improving the educational systems in remote areas of the United States and in developing nations, by providing supplementary instructional material from more experienced teachers. Other uses include a distribution system for broadcasts of community interest and entertainment. It has been shown that a satellite distribution system can be the least expensive method of reaching all remote areas in a

developing nation, if suitable low-cost receiving equipment is available. This study demonstrates that such low-cost equipment is technically and economically feasible and could be mass-produced in the United States and in developing nations for their own use.

Although the original intention was to determine the best receiver configuration over a frequency range from 1 to 12 GHz, it soon became obvious that only a few bands in or near this range could become available for the intended use: 800 MHz, 2.5 GHz, and 12 GHz. We have concentrated on the design of a 2.62 GHz adaptor, and have considered the needs and alternatives for a 12 GHz adaptor. The receiver techniques described herein are applicable over a wide frequency range. Several versions of the adaptor have been built and tested, including three antennas, an electronics package breadboard, and a working prototype of the mass-producible electronics package. Although additional improvements can be made, enough work has been done with each adaptor subsystem to develop a good understanding of the design requirements for a mass-producible adaptor. An initial, but extensive, cost analysis indicates that the 2.62 GHz adaptor could be built in Brazil, for example, for a factory cost of \$92, in production quantities of 100,000 units. This includes an overhead and profit margin for the manufacturer. In this quantity, the antenna costs \$32 and the electronics package costs \$60.

These very low costs are due in part to the fact that the adaptor is designed to be mass-produced, and great care has been taken in choosing the method of fabrication from the various alternatives. The antenna differs from other small antennas (less than 10 feet in diameter) in that it can be fabricated almost entirely by mass-production machinery, using very little labor. It can be shipped disassembled as a kit and assembled at the installation site by one or two men in less than two hours. No technical training beyond instructions in assembly is needed. Since a deployment crew will be necessary for proper installation in rural areas, the additional cost of assembling the antenna is minor in comparison with the overall installation costs. Several of the electronics package functions are integrally combined in a die-castable mixer-feed housing which needs no subsequent machining. Most receiver designs do not use die-casting techniques as extensively as is done here, because the quantity

being produced is not sufficient to warrant the cost of the dies. The last factor in achieving the low cost is the economy of scale which results when a large quantity of any item is produced. The price for many of the components is substantially lower for the large quantity. A summary of the adaptor characteristics is given in Table I-I.

Table I-I

ADAPTOR CHARACTERISTICS

Center Frequency	2.62 GHz
Modulation	Wideband FM
Signal Bandwidth	25.2 MHz
System Noise Figure	7 dB
Antenna Diameter	7 feet
Antenna Efficiency	50%
Antenna Gain	32.85 dB
Receiver Figure of Merit (G/T)	2.2 dB
Output Frequency	Channel 2-5 (54-76 MHz)

The second section develops the communications system parameters needed to specify the performance requirements of the adaptor. The third and fourth sections describe the 2.62 GHz antenna design and the electronics package design, respectively. The cost analysis is given in the fifth section. The sixth section describes the essentials of a 12 GHz receiver design. Several appendices are included which contain important design details, computer programs, and summaries of work which was not covered in the main text.

II. DETERMINATION OF SYSTEM PARAMETERS

A. Basic System Description

The components of the basic satellite transmission system shown schematically in Fig II-1, include the following.*

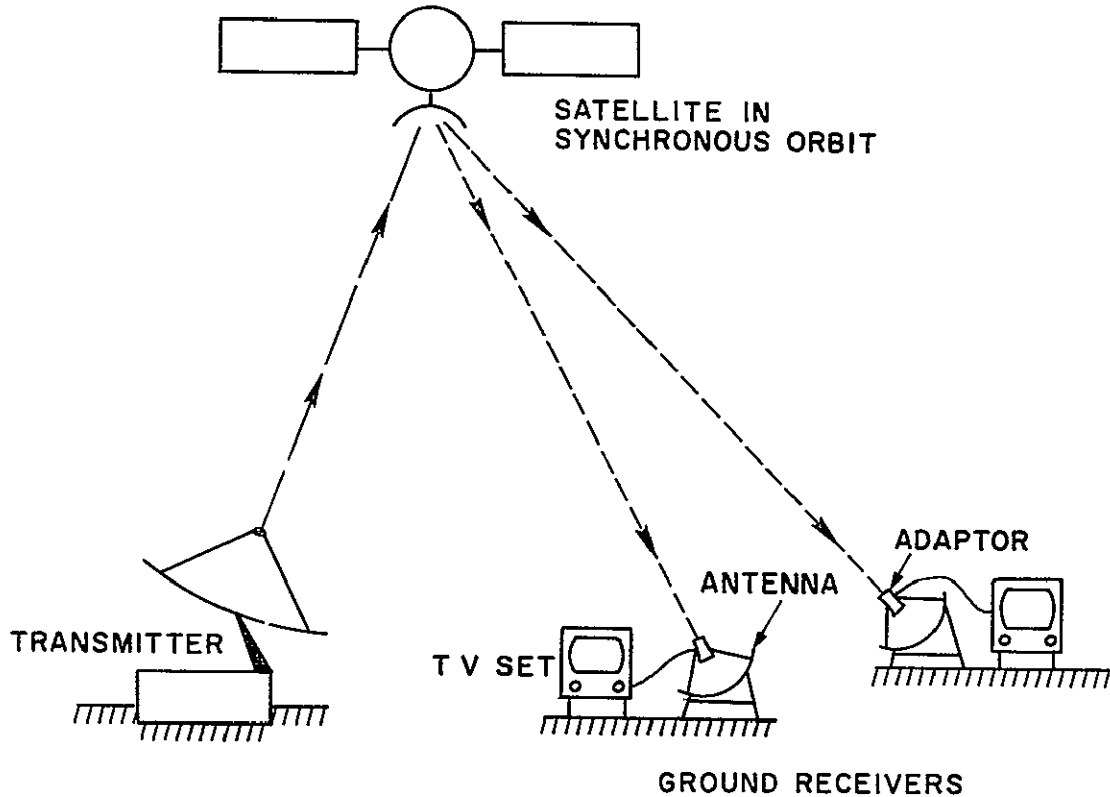


Fig. II-1. THE BASIC SATELLITE TRANSMISSION SYSTEM

1. A central programming studio in which instructional material may be prepared, and a transmitting facility which beams the instructional material to a synchronous satellite.

* This description is given primarily for illustrative purposes, quite a number of variations are possible, such as the addition of retransmission facilities for urban areas and two-way communications capabilities for more remote areas

2. A high-powered satellite which acts as a repeater and retransmits the ETV signals back down to a given geographical region, such as the entire country of Brazil, or a single time-zone of the United States.
3. A small, low-cost receiver consisting of an antenna and an electronics package, capable of detecting the satellite broadcasts and rendering them acceptable to ordinary television sets, would be located at every primary school throughout the country

B General Receiver Requirements

The antenna and electronics package must be inexpensive as well as easily transportable and require neither special skills for installation nor operational adjustments after they are installed. The antenna and electronics package should provide a sensitivity which is compatible with the power levels available from satellites which could be launched with existing technology. It is appropriate at this point to discuss the reasons why an antenna and electronics package are necessary.

Granting the limitation placed on the amount of power a satellite can transmit to a given area on earth,* an ordinary television set with the normal television antenna is not sufficiently sensitive to detect the maximum signal allowed by the regulation. Thus a larger antenna is necessary.

The electronics package is needed because of some constraints on the satellite design related to transmitter power and modulation methods. The television signal is a composite of amplitude-modulated (AM) and frequency-modulated (FM) signals. However, strictly-FM transmitters

* The restriction set forth by the Xith Plenary Assembly of the ITU in CCIR recommendation 358 gives an upper bound on the effective radiated power from a satellite as follows: (1) $\psi = -152 + \theta/15$ dBw/m², in any 4 KHz band, where θ is the angle of arrival at the earth's surface, measured in degrees from the horizontal. This CCIR limitation is used as a starting point for the system design from the interference standpoint because it is the only regulation in existence. However, it was enacted with interference to telephone communications in mind. The likelihood of interference with terrestrial ITFS systems has not yet been thoroughly examined.

are capable of providing a high-quality signal-to-noise ratio with significantly less prime power than the corresponding AM transmitter. Since prime power is a scarce resource on a satellite, FM transmitters are preferred. Consequently, the electronics package is necessary to detect, demodulate, and process the satellite signal to make it compatible with the ordinary television set. This reduction in transmitter power afforded by using FM is obtained at the expense of greater RF bandwidth.

C Quantity of Receivers

In order to make an effective contribution to improving the educational facilities of a country, the ASCEND study[†] estimated that at least 152,000 such receivers would be needed in Brazil for full coverage of the primary school-age population, and 20% coverage of the secondary school age group. Similarly, 980,000 receivers are needed in India. The ASCEND estimate for the cost of the adaptor is \$195, and the cost for a Brazilian television set was \$170 in 1969. Thus the hardware cost alone (not including the installation and operation costs or the satellite and launch costs) for a Brazilian system is \$55.5 million. The cost for the Indian ground system was estimated in the ASCEND study at over \$400 million. This is considerably more than the cost for the satellite, launched, or for any other component of the system.* Since the system cost is very sensitive to the microwave receiver cost, it is very important to obtain as inexpensive a design as possible. The results of this present study indicate that the manufactured cost could be less than \$100 for the antenna and electronics package.

D. Frequency Range

The frequency range specified for consideration of this receiver design is 1-13 GHz.** However, there are only a few bands within this range in which direct transmission for educational purposes could

[†] Reference 27 at end of report.

* The launched cost for one Intelsat IV is \$29 million.

** Contractual obligation.

conceivably be licensed the upper UHF band from 600-900 MHz, the ITFS band from 2500-2690 MHz, and 11.7-12.4 GHz. The lower band is not within the specified range of this study, but is being considered elsewhere.* A complete development is presented for a 2620 MHz receiver, including a working model. Basic paper designs for a 12 GHz receiver are presented, but no working model is supplied.

E Receiver Figure of Merit and Costs

The generally accepted measure of a receiver's ability to detect signals is called its figure of merit. The weaker the signal, to be detected, the greater the figure of merit must be. The standard figure of merit is defined as the ratio of receiver antenna gain to system noise temperature, G_r/T_e . For a given transmission frequency, the antenna gain is proportional to its effective area. At the proposed microwave frequencies, the best type of antenna is a parabolic reflector.** Historically, antenna cost has been exponentially proportional to the desired gain,*** and therefore the area. The system noise temperature is a measure of how much electrical noise is being added to the signal by the receiver itself. For the case of the simplest equipment, the noise temperature cost is inversely related to the temperature desired. Thus a rough first approximation to the cost of a microwave receiver has been exponentially proportional to G_r/T_e .

Given the large number of receivers needed, and this exponential cost dependence, it is obvious that the satellite should radiate as much power as possible, in order that the ground receiver have the lowest possible figure of merit. In order to determine the minimum figure of merit, some additional aspects of the communications system design must be considered.

* The General Electric Co. is pursuing a UHF design, as well as the Computer Sciences Corporation.

** This choice is based on the criteria of effective area and structural integrity. For a more detailed discussion, see ASCEND, Appendix G.

*** D. L. Pope, BSTJ, "Parametric Representation of Ground Antennas for Communications Systems Studies," December 1968.

F. System Parameters

Since an FM system is under consideration, the essential relationship between the figure of merit and a performance constraint is the carrier-to-noise ratio (CNR). This is the ratio of the carrier signal strength to noise power in a specified bandwidth. This ratio must be greater than the FM detector threshold, nominally 10 dB. Further, there should be some additional margin to allow for rain loss (2 dB) and the normal attenuation at the edge of the satellite antenna pattern (3 dB). Thus a CNR of 15 dB at the beam center is proposed.

The general relationship among the variables of satellite transmitter power, bandwidth, carrier to noise ratio, and others is given by

$$\text{CNR} = \frac{\text{Received Power}}{kT_e \text{ BW}_{\text{if}}} \quad (1)$$

$$= \frac{\lambda^2}{4\pi} \frac{P_t G_t G_r}{4\pi d^2 kT_e \text{ BW}_{\text{if}}} \quad (2)$$

where

P_t = satellite transmitter power in watts

G_t = satellite antenna gain

G_r = receiver antenna gain

d = distance to synchronous orbit (36,000 km from equator)

λ = wavelength at carrier frequency, in meters

BW_{if} = noise bandwidth of receiver

T_e = receiver system noise temperature in degrees Kelvin

k = Boltzman's constant, 1.38×10^{-23} joules/°K

Some simplifications can be made to this formula in view of the given system. The product $P_t G_t$ is called the effective radiated power (ERP). The flux density ψ is given by

$$\psi = \frac{P_t G_t}{4\pi d^2} = \frac{ERP}{4\pi d^2} \quad (3)$$

The maximum permissible flux density thus determines the ERP

The figure of merit G_r/T_e is included in Eq. (2). Because the downlink carrier frequency is limited to a specified band, 2500-2690 MHz, the figure of merit can be simplified to remove this frequency dependence. Recognize that the receiver antenna gain G_r is given by

$$G_r = \eta \left(\frac{\pi D}{\lambda} \right)^2 \quad (4)$$

where

η = the overall efficiency of the antenna, nominally 50% for antenna diameters of 3 meters or less

D = the diameter of the parabola in meters

λ = the wavelength of the carrier frequency in meters

After substitution of this expression and of Eq. (3) into Eq. (2), we have

$$CNR = \psi \cdot \frac{\eta \pi D^2}{4kT_e BW_{if}} \quad (5)$$

We now propose that the modified figure of merit be defined as

$$\text{Modified Figure of Merit} = \frac{A_e}{T_e} = \frac{\eta \pi D^2}{4T_e} \quad (6)$$

where A_e is the effective area of the parabola. Thus the CNR is given by

$$CNR = \psi \frac{A_e}{T_e} \frac{1}{kBW_{if}} \quad (7)$$

We have a relationship between two constrained variables, ψ and CNR, and two other variable, BW_{if} and A_e/T_e . The noise bandwidth term BW_{if} is not independent, but is related to the maximum flux density by another parameter, f_m , the maximum modulating frequency of the television signal. Thus, for a given kind of information, modulation type, and maximum flux density, the modified figure of merit A_e/T_e can be specified for any desired CNR. We may now find the minimum A_e/T_e needed to provide a 15 dB CNR for the maximum flux density permitted under the regulation.

The CCIR flux density limitation is

$$\psi \leq (-152 + \theta/15) \text{ dBw/m}^2 \text{ per 4 KHz band} \quad (8)$$

For the case of Brazil, θ is assumed to be as low as 45° . Thus,

$$\psi \leq -149 \text{ dBw/m}^2 \text{ per 4 KHz band} \quad (9)$$

The total rf bandwidth of the wideband signal depends on the modulation index β and the maximum modulating frequency f_m , and is approximated by Carson's rule* as

$$BW_{rf} = 2(\beta + 1) f_m \quad (10)$$

The spectral density of this wideband signal may be assumed to be approximately uniform, and thus the total flux density limitation is given by

$$\psi < -149 + 10 \log \left[\frac{2(\beta + 1)f_m}{4\text{KHz}} \right] \text{ dBw/m}^2 \quad (11)$$

For $f_m = 4.2$ MHz, this expression reduces to

* Carson's rule is described in Signals and Noise in Communications Systems, H. E. Rowe, D. Van Nostrand, Princeton, N. J., 1965

$$\psi < -115.78 + 10 \log (\beta + 1) \text{ dBw/m}^2 \quad (12)$$

This is the total allowable flux density. The only remaining parameter to be specified is the noise bandwidth of the IF amplifier, BW_{if} . This bandwidth is slightly larger than the rf signal bandwidth BW_{rf} for reasons to be discussed in the section on the electronics package design. The following approximation is valid

$$B_{if} = 2.5 (\beta + 1) f_m \quad (13)$$

This approximation gives a 25% increase over the signal bandwidth. Substituting this expression and the maximum flux density from Eq. (12) in the CNR Eq. (7), we obtain

$$\begin{aligned} \text{CNR} &= -115.78 + -10 \log k - 10 \log (2.5 f_m) + 10 \log \left(\frac{A_e}{T_e} \right) \\ &= -115.78 + 228.60 - 70.21 + 10 \log (A_e/T_e) \\ \text{CNR} &= 42.61 + 10 \log (A_e/T_e) \end{aligned} \quad (14)$$

The CNR must be 15 dB, and thus

$$\begin{aligned} A_e/T_e &= 1/577 \text{ m}^2/\text{°K} \\ &= 1.735 \times 10^{-3} \text{ m}^2/\text{°K} \end{aligned} \quad (15)$$

In decibels, this is -27.61 dB.

The problem of finding a particular A_e and T_e for minimum cost is considered in a following section. To complete the design of the communications system, it remains only to specify the modulation index β .

The modulation index determines the magnitude of the improvement in signal-to-noise ratio provided by a wideband FM system. This signal-

to-noise ratio (SNR) is defined as the ratio of the peak-to-peak picture signal amplitude (black to white) to the rms voltage in a 5 MHz band and is given by

$$\text{SNR} = \text{CNR} \cdot \text{PPF} \cdot \text{FMI}_1 \left[\frac{\text{BW}_{\text{rf}}}{f_m} \right] \text{FMI}_2 \cdot \text{NWF} \quad (16)$$

where

CNR = the carrier to noise ratio, 15 dB

PPF = 9 dB, a conversion factor which changes the rms signal power to the required peak-to-peak power

$\text{FMI}_1 = 3\beta_{\text{picture}}^2 = 1.5\beta^2$, the FM improvement factor, the picture information uses only 0.7 of the complete peak-to-peak video signal excursion

$\frac{\text{BW}_{\text{rf}}}{f_m} = (\beta + 1)$, by Carson's rule, this expression is often lumped with the expression for FMI_1

FMI_2 = the additional improvement due to pre-emphasis, and for television signals, amounts to 2.8 dB

NWF = 10.2 dB, a noise weighting factor for the triangular noise from an FM discriminator, this factor accounts for the measurable improvement in SNR due to inherent filtering of both the picture tube response and the human eye response.

A Television Allocation Study Organization (TASO) grade 1 picture is one in which 50% of the test subjects call an "excellent" picture and 93% call a "fine" picture, such a picture requires an rms video SNR of 44 dB,* or an rms picture SNR of at most 41 dB. This is the same as a peak-to-peak SNR of 50 dB. The sum of the factors given a value in the defining text is 37 dB, therefore, the β -dependent terms must provide 13 dB further improvement

$$1.5^2(\beta + 1) = 20 \quad (17)$$

Choosing $\beta = 2$, the resulting improvement is 12.55 dB, which is adequate for an initial system specification

* C. E. Dean, "Measurements of the Subjective Effects of Interference in Television Reception," Proc IRE, TASO ISSUE, June 1960, p 1042, figures 8 and 9

The total flux density ψ can now be determined, and then the satellite ERP. The flux density becomes -111 dBW/m^2 , and the corresponding ERP is 51.35 dBW for a $37,000 \text{ km}$ path length to synchronous orbit.* A complete list of the calculated parameters appears in Table II-I.

G. Maximum Antenna Diameter

The antenna must be simple to transport and install, and the receiver should require little or no adjustments after installation. This implies that the beamwidth must be large enough to accommodate variations in satellite position (due to drift) and perturbations from wind without undue loss of signal. The expected variation in satellite position is $\pm 0.8^\circ$, or a total of 1.6° . If the satellite movement is to cause no more than 1 dB loss in signal strength, then the 1-dB beamwidth is 1.6° , and the 3-dB beamwidth is 2.8° . This corresponds to a 3-meter (10 foot) diameter antenna for the 2.5 GHz band, and gives an effective area of 3.53 m^2 . The corresponding permissible perturbation of the antenna body is $\pm 2.1 \text{ cm}$ (0.84 in) about any radial axis. 3 meters is the maximum antenna diameter for a 1-dB degradation criterion, other factors, such as the cost tradeoff between effective aperture and system noise temperature, and fringe area reception needs, will dictate that a smaller diameter antenna will be more desirable for regions near the beam center.

H. Maximum Figure of Merit A_e/T_e **

The lowest system noise temperature obtainable in a mass-production design should be at least 1 dB higher than the lowest noise figure available in a mixer diode, with no preamplifier. Diodes are available with

* This is 1000 km more than the distance from the equator to synchronous orbit, and adds 0.10 dB to the ERP.

** For the sake of completeness, the corresponding figure of merit, $(G/T)_{r,e \text{ max}}$ is 5.3 dB , and the minimum is 2.2 dB .

Table II-I

COMMUNICATIONS SYSTEM PARAMETERS FOR DIRECT BROADCASTING VIA SATELLITE

Equation Element	Value
Satellite Effective Radiated Power	51.35 dBW (136,000 watts)
Transmission Frequency	2620 MHz
Flux Density	-111.0 dBW/m ²
Modulation Index β	2
Maximum Modulation Frequency	4.2 MHz
Signal RF bandwidth	25.2 MHz
Noise Bandwidth	31.5 MHz
Required Carrier to Noise Ratio	15 dB
Required Adaptor $\frac{A_e/T_e}{(G_r/T_e)}$	$1.735 \times 10^{-3} \text{ m}^2/\text{°K}$ (2.2 dB)
Maximum Available Adaptor $\frac{A_e/T_e}{(3 \text{ m dia.}, 1000\text{°K})}$	$3.53 \times 10^{-3} \text{ m}^2/\text{°K}$
FM Improvement in SNR $1.5\beta^2(\beta+1)$	12.55 dB
Improvement in SNR due to Pre-Emphasis	2.8 dB
Noise Weighting Factor	10.2 dB
Peak-to-Peak Conversion Factor	9 dB
Peak-to-Peak Picture SNR, weighted, beam center	49.55 dB
CNR Margin over Detector Threshold, beam edge	2.00 dB

5.5 dB noise figures, and so the total system noise figure should be no lower than 6.5 dB, or 1000°K. Thus the best figure of merit possible is

$$\left(\frac{A_e}{T_e}\right)_{\max} = 3.53 \text{ m}^2/1000\text{°K} = 3.53 \times 10^{-3} \text{ m}^2/\text{°K}$$

In decibels, this is -24.5 dB, which is about 3 dB better than the minimum A_e/T_e needed on the basis of maximum flux density. Consequently, we have an upper and a lower limit on receiver figure of merit, on the basis of maximum flux density and maximum permissible signal degradation.

I. Determination of A_e and T_e from the Required A_e/T_e

In order to make a start on the design of the antenna and electronics package, it is necessary to specify the system noise temperature T_e and the effective area A_e . Based on the previous discussion, we have chosen a system noise temperature of 1160°K (7 dB noise figure) and an effective area of 2.02 m² as a feasible solution. We can now say that this solution is very nearly optimum, because of the extensive cost information which has been compiled. A brief discussion of the tradeoff between antenna diameter and system noise temperature is included as an appendix.

J. Availability of Satellite Power

The effective radiated power required for a Brazilian program is 51.35 dBW, or 136,000 watts. While it is true that no satellite has yet been flown with an effective radiated power (ERP) of this magnitude, there are no technological obstacles which would prevent the realization of a satellite with such a power level. The most critical aspect of obtaining this ERP lies with the solar cell power supply and the satellite transmitter. The remaining problems of launch and spacecraft housekeeping can be routinely performed.

The growth rate of satellite ERP since 1963 is shown in Fig. II-2. The satellites listed represent two nonmilitary families. The Syncom, built by the Hughes Aircraft Company, and the commercially built Intelsats I, II, III, and IV and the Applications Technology Satellites (ATS) 1, 3, and E, flown by NASA for scientific experiments. The ERP needed for direct transmission to low-cost receivers equipped with the 7-foot antenna of the previous example and for a 10-foot antenna are shown for the year 1975. There is a clear trend in capability towards an ERP which will make possible direct reception by a low-cost receiver system

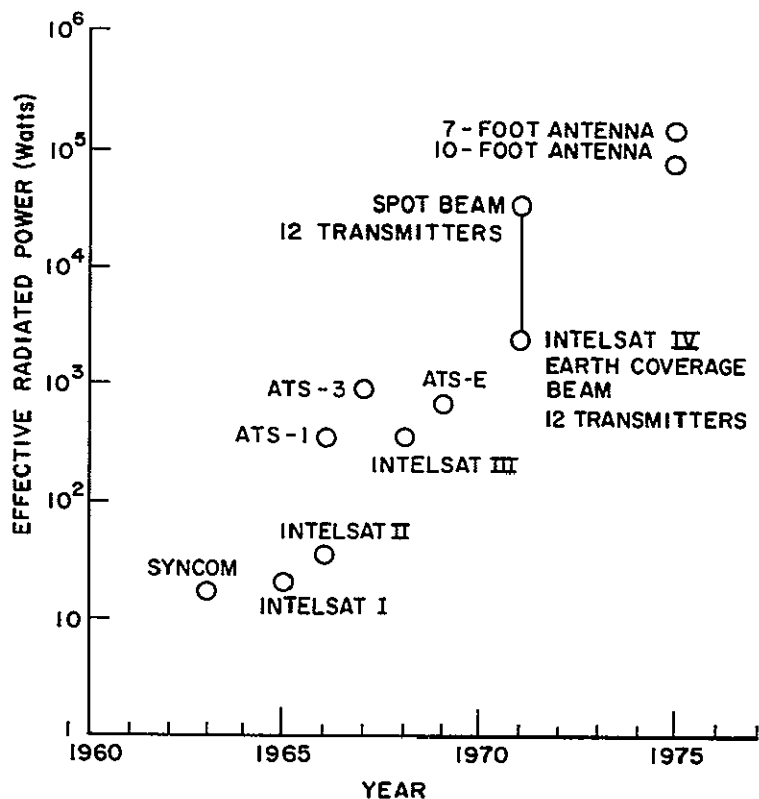


Fig. II-2. GROWTH RATE OF THE EFFECTIVE RADIATED POWER FOR COMMERCIAL SATELLITES SINCE 1963.

The introduction of the Intelsat IV with its spot beam and all 12 transmitters sending the same signal demonstrates that the technical capability now exists for direct transmission to limited areas. At 4000 MHz, the 10-foot antenna could receive the transmission from the Intelsat IV, but there would be no safety margin in the carrier-to-noise ratio (CNR = 11.5:1). With the 7-foot antenna, the Intelsat IV's 27,000 watt ERP is insufficient for adequate reception. The Intelsat IV is not intended for direct transmission. Using 12 or more transmitters is an undesirable way to achieve the needed ERP since it is an inefficient use of the available power, is more complex, and has a potential for distorting the signal. For best performance, a single transmitter should be used. The amplifier must then deliver at least 275 watts.*

* Additional capability is usually provided to allow for reduction in output power due to aging, a 300 watt level will be assumed for the sake of discussion.

K Satellite Power Generation

The principal component of the amplifier which converts the direct current power to radio frequency power is a traveling wave tube (TWT). From a field of three possible tube types, it is used primarily because of its high reliability, long life, and demonstrated performance in a space environment * The \$20 million investment, involved in building and launching a commercial satellite, imposes a severe constraint on the probability of success and on the lifetime of the satellite. Traveling wave tubes with a 300-watt capability exist, but further development is needed to make them operational in space. This qualification testing usually takes several years Lloyd Derr estimates that the cost of developing a tube in the 100- to 500-watt range would be under \$1 million and would take less than 3 years for complete qualification **

The Watkins-Johnson Company and Varian Associates, both of Palo Alto, California, are presently engaged in developing high-efficiency tubes in the 100-watt range for scientific deep-space explorations Watkins-Johnson has a 100-watt TWT, Varian has a power amplifier tube, an electrostatically-focused Klystron (ESF), capable of 20- to 100-watt operation. At present, Varian is negotiating with NASA to extend the power level to 500 watts and to perform the necessary development work †

The operating lifetime requirement for the tubes used by Jet Propulsion Laboratories is 20,000 hours, 2.25 years, with no failure of any kind Such performance has already been obtained with a number of tubes in spacecraft. ‡ Statistically, this implies that the probability of successful operation over a 5-year period is quite high. An extra transmitter is often included on satellites to improve the reliability and increase the expected lifetime

* Feldman, Communications Satellite Output Devices, 8 Microwave J., Dec 1965, at 87-97

** Interview with Lloyd Derr, Head, Microwave Power Tube Development, Jet Propulsion Laboratories, Dec 1969, in Pasadena, Calif Dr H. G Kosmal, Head of the Tube Development Section at NASA Lewis RC, agrees with this estimate, for tubes with efficiencies of less than 50%.

† Interview with Richard D Nelson, Chief Engineer, Tube Division, Varian Associates, Dec 1969, in Palo Alto, Calif

‡ Interview with Mr Derr, supra note **.

In a recent proposal to NASA, the Hughes Aircraft Company suggested that either a 100-watt klystron or a 100 watt TWT be included on the Applications Technology satellite-G for experiments in direct transmission to limited areas* Thus the feasibility of providing a single high-power transmitter is beyond the stage of academic discussion

A 300-watt transmitter will require about 700 watts of direct current power which must be supplied by the solar cells Allowing for other power requirements on a spacecraft, 800 watts is a conservative estimate of the needs of a single channel direct transmission satellite The Air Force is presently planning to fly an experimental satellite with a Flexible Rolled-Up Solar Array (FRUSA) capable of supplying 500 watts in September 1971 ** Thus, the power supply will pose no problem The successful completion of these experiments will demonstrate the feasibility of direct transmission of television from satellites by 1975

The single transmitter, together with the satellite antenna, provides the effective radiated power This effective radiated power is the product of the antenna gain and the radio frequency power delivered by the transmitter. The antenna gain is determined by the desired area coverage on earth.† To obtain total coverage of Brazil at 7° beamwidth is needed. Adjusting for various losses, the gain of such an antenna is 500

* Proposal from Hughes Aircraft Company, Space Systems Division, El Segundo, California, to National Aeronautics and Space Administration, Washington, D C., dated Dec 31, 1969, containing plans for a 100-watt S-Band transmitter for the ATS-G spacecraft (Hughes Reference No 69 (22)12157/C0693)

** "Oriented Flexible Rolled-Up Solar Array," George Wolff, presented at 3rd Communications Satellite Conference, sponsored by the AIAA in Los Angeles, April 8, 1970, paper 70-738

† The expression for antenna gain in terms of the solid angle subtended from the antenna is given by

$$\text{Gain} \approx \frac{27,000}{\theta^2}$$

where θ is the half-power beamwidth in degrees

L. Adaptor Specifications and Functional Block Diagram

The communications system parameters for the adaptor are summarized in Table II-I. The functions which the adaptor must perform and the element which performs each function are given in Table II-II. A block diagram is shown in Fig. II-3.

Table II-II

FUNCTIONAL REQUIREMENTS

Adaptor Element	Function
Antenna	Collects sufficient signal flux to provide the desired CNR
Feed	Matches signal from free space to waveguide mixer
Mixer	Partially determines system noise figure and translates signal to IF
Local Oscillator	Generates beat signal for mixer at 2500 MHz
IF Amplifier	Increases signal amplitude, sets noise bandwidth, and partially determines noise figure
Limitter	Removes all in-phase noise components to provide FM improvement
Discriminator-Detector	Converts FM into original AM signal
Remodulator	Translates demodulated video signal to appropriate channel for ordinary television set
Power Supply	Supplies dc power for other circuits
Housing	Houses and protects electronic circuits

The details of each element's performance requirements are discussed in the following two major sections.

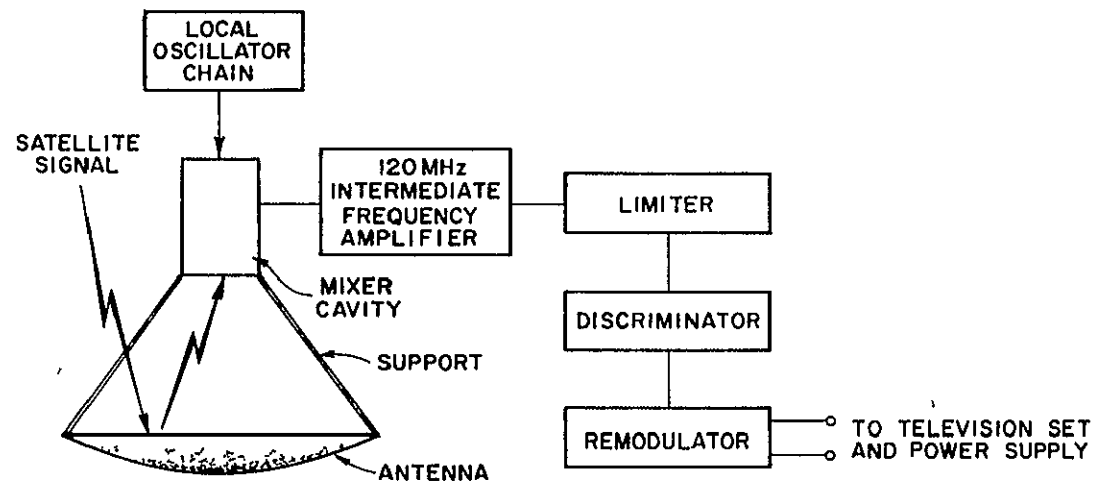


Fig. II-3 BLOCK DIAGRAM OF ADAPTOR.

M. Design Philosophy

The major goal is to design a microwave receiver and antenna which can be mass-produced inexpensively, preferably in a developing nation such as Brazil. The antenna must be easy to transport, assemble, and aim in the field by semi-skilled labor. The electronics package must be reliable and capable of outdoor operation, in the event of failure, it must be easy to service, or at least replace. The electronics package should also be inexpensive to manufacture and easy to assemble and align.

These basic performance criteria, including the electrical requirements, must be expanded into much more detail in order to evaluate the existing alternatives and to help examine new designs when nothing satisfactory presently exists.

Of course, all of these constraints do not provide the answer to the question, what is the best way to build this adaptor? The designer's responsibility is to choose the most promising alternatives on the basis of the present definition of the performance criteria and his understanding of the alternatives. However, because of limited knowledge in new areas, and because our objective is to provide a working model of a mass-producible adaptor, it is necessary to obtain concrete answers by model simulation or actual fabrication and testing. This results in refinement of the performance criteria and a more precise definition of what is actually needed and what is unnecessary. To that end, we have considered a large number of alternative designs for the antenna and electronic circuitry and have built prototypes of the most promising alternatives. Through extensive measurement and analysis, significant improvements have been made. In the case of the antenna, three prototypes were constructed, and a satisfactory design is now available. In the case of the electronics, the most promising alternatives were chosen, and a breadboard experimental model was first constructed to assess the various critical parameters. An engineering model was next constructed incorporating the basic designs. Extensive testing and some modifications has resulted in a satisfactory design, but has also revealed a few unforeseen difficulties, and suggestions are made to improve the overall performance of the first prototype.

The following two chapters on the antenna and the electronics describe the formulation of the more detailed performance criteria, the evaluation of alternatives, the fabrication of prototypes, and the final design. A complete cost analysis for quantities from 10 to 100,000 units is included

III THE ANTENNA

A Design Objectives

This section discusses the antenna design for the adaptor including the design objectives, the reasons for choosing this particular antenna design, the theoretical methods used to predict performance and establish the geometry, the mechanical hardware design, the methods for mass production, the manufacturing costs, and the testing procedures with results

The main design objectives for the antenna are

- (1) Nearly parabolic geometry
- (2) Adequate gain
- (3) Low cost--under \$50 in production of 100,000 units
- (4) Durability and ruggedness--capability of withstanding wind loading, corrosion, and human factors
- (5) Simple fabrication and assembly
- (6) Manufacturable in the developing area where it will be used
- (7) Ease of transportation and deployment to the site of operation
- (8) Ease of aligning and aiming

The main idea is to design a rugged, inexpensive antenna which has adequate performance. One measure of performance, antenna gain, is determined by geometric factors such as diameter, surface tolerance, and also by the wavelength of the received signal. The antenna cost is also related to geometric factors such as the diameter (surface area and material cost) and tolerances on the components which relate to production methods, precision, and costs. Other performance and cost factors must be taken into consideration, but a reasonable approach is to formulate the general relationship between gain, diameter, tolerances, and frequency, and then relate diameter and tolerance to production methods and costs to compare and evaluate the most feasible design alternatives.

Preceding page blank

B. Design Approach and Alternatives

A useful first step for getting an accurate cost estimate for the antenna is to actually design and build a working model. This makes one familiar with many of the details which could be overlooked in a paper-and-pencil design. One main objective was to produce working hardware and production cost information.

The function of the antenna is to collect a wideband FM signal transmitted from a satellite. This satellite has a maximum amount of radiated power and it is the function and purpose of the receiver to collect enough of this radiated power on the ground to produce a clear television picture and intelligible sound. To achieve this at high frequency a high gain antenna is required, much higher than can be achieved by an ordinary television antenna. The ASCEND study concluded that the best type of antenna for this purpose is a parabolic dish about six to ten feet in diameter.

We examined several alternative parabolic antenna designs, and selected one made out of petals which are mass produced in a simple stamping operation. These petals would attach to a circumferential rim structure and would fold in to be fastened along their seams forming a quasi-paraboloidal surface.

Other alternatives considered were as follows: (1) One possibility is a beach umbrella folding structure having a shape close to that of a paraboloidal antenna. The umbrellas themselves are in widespread use in the six to eight foot sizes, made in collapsible form out of canvas and vinyl with metal ribs. (2) Another type of umbrella which is non-collapsible is made of sheet metal petals attached to an aluminum tubular support structure. (3) A third type of umbrella is formed of plastic fiberglass. These first three alternatives were found to be in about the same retail price range for small quantities in the U. S., \$35 to \$100 depending primarily on their diameter. (4) A fourth alternative is to mass produce the antenna in a single stamped piece of aluminum or steel using a compound die and hydraulic presses. (5) A fifth alternative is to stretch form the entire antenna. (6) A sixth alternative is to spin form the antenna. It can be shown that the material cost in the antenna is the dominant fabrication cost in production of 100,000 or more.

antennas * In these quantities the material cost for alternatives (4), (5), and (6) is \$25 to \$30. However, these last three alternatives would be more costly than \$35 to \$100 in small quantities due to higher tooling costs than in the first three alternatives. (7) A seventh alternative is to form the antenna surface in the face of a large rectangular block of polyurethane and then coat the surface with metal or metal paint This large block could then be cut up into smaller segments for shipment (8) An eighth alternative is to design a transportable mold for the antenna and then cast the antenna out of concrete or other material which should be available in rural areas (9) A ninth alternative would be to fabricate a parabolic support structure and cover it with a fine metal screen

The cost of antennas fabricated by almost all of these alternatives fall into the same range for high volume production No one alternative stands out as having a significantly lower cost than the others

Our approach has been to choose a promising design alternative which requires low tooling costs and which can be shipped in a small carton for assembly at the site By requiring low tooling costs we plan to assure that the total cost will remain low over a wide range of production quantities This is of particular advantage when building a prototype system of a few hundred receivers for initial evaluation Shipping a six to ten foot dish can be a major problem which would be eliminated by shipping the antenna disassembled in a carton and assembling it in the field.

We have completed the detailed design and development of one antenna type with production costs and a working model This design is near the optimal for low cost and it will serve as a basis for further evaluation

C Preliminary Design

The antenna which was developed is quasi-paraboloidal. It consists of ten petal-shaped flat sheets of aluminum shaped so that when the petals are joined together along the seams, they must bend along their centerline into the shape of an approximate parabola, as illustrated in

* ASCEND study, p 3-22 to 3-32.

Figure III-1 Because the petals bend along their centerline only, the resulting antenna surface is not a perfect paraboloid of revolution. That is, it diverges from the ideal paraboloidal section increasingly from the centerline of the petal to the seam. This surface deviation causes a reduction in the gain of the antenna. However a computer optimizing study, which will be discussed later, has resulted in a design which minimizes this loss in gain. The resulting antenna and matching feed horn have a predicted gain only one-half the theoretical maximum. This is less than 1 db below the gains obtainable from true paraboloidal antennas.

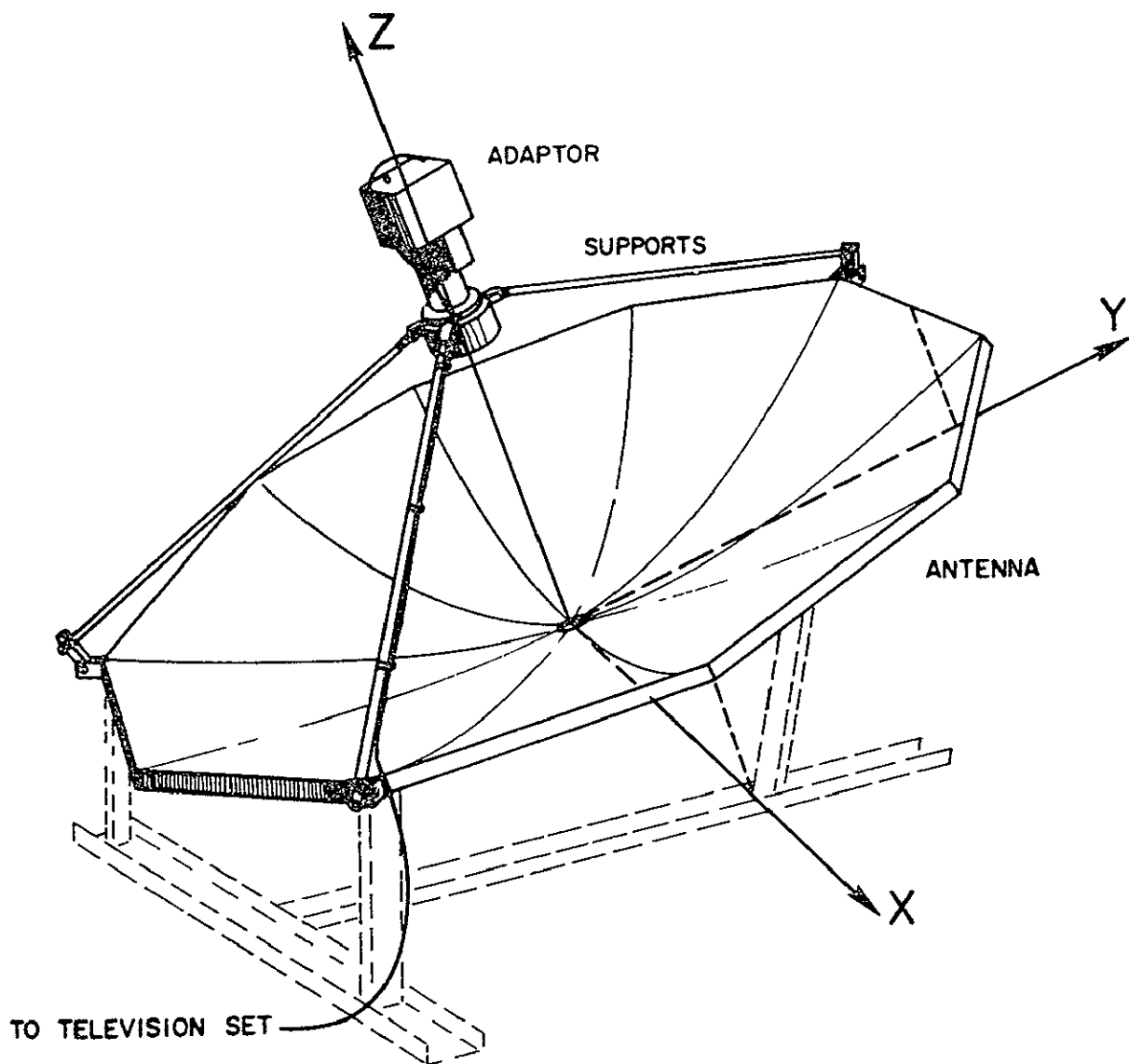


Fig III-1 CARTESIAN REPRESENTATION OF ANTENNA SURFACE.

The structural rigidity of the antenna comes from ten aluminum hollow section segments formed by an extrusion process. Each segment is snapped to a petal during assembly as shown in Fig III-2 (and in Fig III-17). First the extruded segments are fastened together with stamped corner brackets which slip over adjoining segments, this forms the rim. Then the flat petals are slipped into the rim, folded in, and fastened along the seams with pop rivets or screws, this completes the antenna structure.

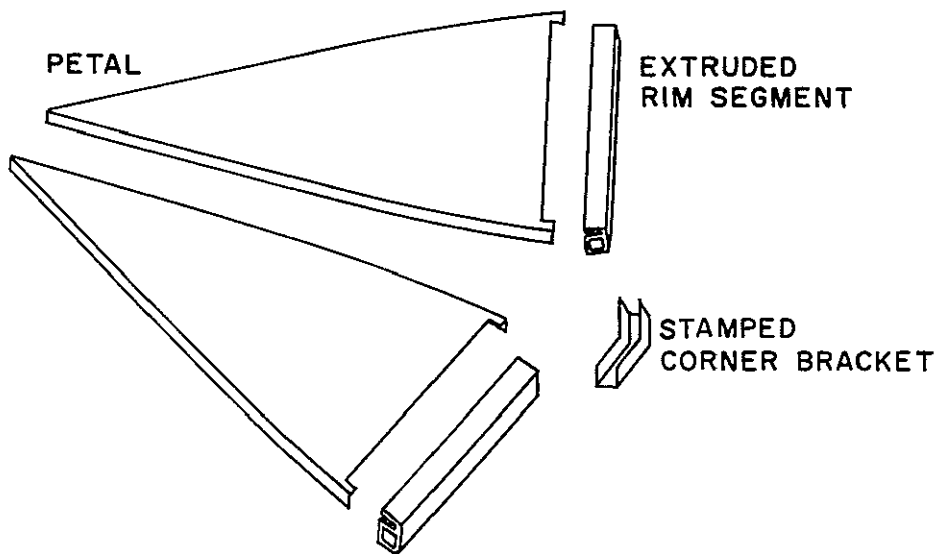


Fig. III-2 ANTENNA COMPONENTS

The use of extrusions and stamped corner brackets evolved from a series of prototypes. Similarly the optimizing scheme was devised in detail after two prototypes had been built. However, before any prototypes were built, calculations were made to estimate the performance of the design. These are described below.

For an antenna with random surface deviations, a measure of performance, the gain, is determined in part by geometric factors such as the antenna area, the surface deviation from an ideal paraboloid antenna,

and the wavelength of the received signal. The gain of an antenna is given by the following expression,*

$$\text{Gain} = \left[\frac{4\pi A}{\lambda^2} \right] \times \left[\text{Tolerance Factor} \right] \times \left[\text{Aperture Efficiency} \right] \times \left[\text{Reflection Coefficient} \right]^2 \quad (1)$$

where

A = receiving area of the antenna

λ = wavelength

The tolerance factor is given by [24]

$$\text{Tolerance Factor} = \frac{1}{1 + \left[\frac{2\pi\delta}{\lambda} \right]^2} \quad (2)$$

where

δ = root mean square value of the surface deviation from the desired paraboloidal shape defined below by Eq (3).

The aperture efficiency is the ratio of the power in the terminating impedance to the total power received by the antenna from the incident wave. The aperture efficiency normally has a value between 0.5 and 0.7. As a beginning estimate a value of 0.6 is assumed.

The reflection coefficient for aluminum sheets is close to unity

To calculate an initial estimate for antenna gain it is necessary to know δ , the root mean square value of the surface deviation. The definition for δ is taken to be

$$\delta = \sqrt{\frac{1}{m} \sum_{i=1}^m \delta_i^2} \quad (3)$$

* Direct communication with R. N. Bracewell, Center for Radar Astronomy, Stanford University, Stanford, California, October 1968

The minimum distance from any point i on the antenna surface to the surface of a paraboloid which has the same focal length as the antenna is taken to be δ_1 . The focal length is defined below. The quantity m is the number of points where δ_1 is measured over the entire antenna surface.

An approximation for δ_1 can be obtained from a study of antenna geometry. From a cartesian coordinate system fixed to the antenna as shown in Fig III-1 we obtain a relation $z = f(x,y)$ representing the ideal paraboloidal surface and a second relation $z = g(x,y)$ representing one petal shaped surface. It can be assumed that the actual δ_1 at any point is less than or equal to the distance between these two surface heights measured in the axial or z direction.

$$\delta_1 \leq [f(x,y) - g(x,y)] \quad (4)$$

where

$$f(x,y) = \frac{x^2 + y^2}{4z_0}$$

$$g(x,y) = \frac{y^2}{4z_0}$$

and z_0 is defined to be the focal length. An upper bound estimate for δ_1 is obtained by adding up these squared differences at a specified number of points, dividing by m , and taking the square root.

$$m = \frac{A}{\Delta x \Delta y}$$

$$\delta = \sum_{i=1}^m [g(x,y) - f(x,y)]^2 \frac{\Delta x \Delta y}{A} \quad (5)$$

Taking the limit as $m \rightarrow \infty$ and carrying out the indicated integration, we get

$$\delta = \frac{D^2}{80z_0} \left[\tan\left(\frac{180^\circ}{n}\right) \right]^2 \quad (6)$$

where

D = antenna diameter

z_0 = focal length of the antenna

n = number of petals in the antenna

For a 6 foot diameter antenna and a focal length/diameter ratio of 0.4*

$$\delta = 2.25'' \left[\tan\left(\frac{180^\circ}{n}\right) \right]^2$$

Table III-I

ANTENNA GAIN VS NUMBER OF PETALS $f_0 = 3.0$ GHz

n =	4	5	6	8	10	12	18
$\delta =$	2.25"	1.19"	0.75"	0.385"	0.236"	0.162"	0.070"
Gain =	---	---	29.0	31.6	32.4	32.7	33.0

Equations (1), (2), and (6) provided enough initial information to establish the geometry, diameter, focal length, and number of sections to achieve acceptable performance. After that prototypes were built for the purposes of evaluating such factors as structural rigidity, ease of assembly, rim design, and mounting methods.

The calculations above were performed assuming no blockage effects** from the feed and its supports. This makes the values of gain obtained

* The selection of 0.4 is arbitrary for the purposes of this example, but practical justification is given below.

** The feed and feed supports affect the antenna gain because they partially block the incoming signal from reaching the antenna surface.

higher than can be achieved in practice. However, the analysis implied in Eqs (1) and (2) was developed for antennas having random surface deviations. But in our petal antenna the surface deviations have a regular pattern and are not randomly distributed across the antenna face, the largest deviations are near the seams at the outer edge. Because of the regular variations and because of the increasing deviation near the rim where the feed horn gain is low, a more detailed analysis was undertaken to predict the antenna performance and to optimize the petal shape to minimize the loss of gain. This analysis will be explained below.

Some further calculations were performed to determine the necessary tolerances on the seam fastening method. The hole locations punched into the petals will largely define the antenna shape when it is assembled. If these holes are not where they should be then the entire antenna surface will deviate from what it is supposed to be and this will effect the gain.

We now describe the method used to establish tolerances on the holes or any seam fastening technique by assessing the change in gain for hole location change δx .

We assume that for some reason the rivet hole locations are not in their proper place but are displaced by an amount δx away from the center of the petal (refer to Fig. III-1). Further, we assume that this displacement of each hole is proportional to its distance y from the apex of the petal such that δx is a maximum at the rim and zero at the apex. For positive values of δx the assembled antenna will be flatter and will have a longer focal length. Because the assembled antenna has flattened out, it now has a new longer focal length z_0 . An approximate method for determining the effect of the displaced rivet holes would be to find the equation for the height of the new surface and compare that the ideal paraboloid ($z = x^2 + y^2 / 4z_0$) to see how much this hole displacement has increased the overall root mean square surface deviation. The change in RMS deviation can be related readily to changes in gain, referring back to Eq. (2).

For a seven foot diameter antenna with a focal length/diameter ratio of 0.4, 10 petals, at a frequency of 2.6 GHz some gain calculations were

made for different values of δx_{\max} where δx_{\max} is the value of δx at the rim. One can perform a similar set of calculations for δy changes in the rivet hole locations and in this way allowable tolerances can be established. For negative values of δx_{\max} the antenna gain is increased because the petal surface has more curvature and the RMS deviation from the ideal paraboloid is diminished. This fact has led us, later, to develop a scheme to optimize gain by changing the shape of the petal. From examination of the results in Table III-II the δx tolerance on the rivet hole location was taken to be ± 20 mils at the rim, decreasing to ± 10 mils at half the distance to the antenna center. The allowable δy tolerance is larger by a factor of 3 for a 10 section antenna. In normal stamping and sheet metal operations hole tolerances of ± 0.005 inch can be achieved on this size stamping and therefore the antenna petals can be manufactured by stamping and be within acceptable tolerance range.

Table III-II

PETAL TOLERANCE VS ANTENNA GAIN

δx_{\max} in inches	Gain db
0.000	32.4
0.010	32.3
0.020	32.2
0.050	31.7
0.100	30.8
0.250	27.8

For high volume production the major cost is for materials. This cost is directly related to the diameter, focal length, and number of petals. The antenna is also subject to the following constraints in order for it to achieve acceptable performance.

$$\text{Gain} = \left[\frac{4\pi A}{\lambda^2} \right] \times \left[\frac{\text{Tolerance}}{\text{Factor}} \right] \times \left[\frac{\text{Aperture}}{\text{Efficiency}} \right] \times \left[\frac{\text{Reflection}}{\text{Coefficient}} \right]^2 \quad (1 \text{ repeated})$$

where

A = receiving area of the antenna

λ = wavelength.

$$\text{Tolerance Factor} = \frac{1}{1 + \left[\frac{2\pi\delta}{\lambda} \right]^2} \quad (2 \text{ repeated})$$

where

δ = root mean square value of the surface deviation from the desired paraboloidal shape, defined in Eq (3)

$$\delta = \frac{D^2}{80z_o} \left[\tan \frac{180^\circ}{n} \right]^2 \quad (6 \text{ repeated})$$

where

D = antenna diameter

z_o = focal length of the antenna

n = number of petals in the antenna

$$0.35 \leq \frac{z_o}{D} \leq 0.45 \quad (7)$$

$$\delta \leq \frac{\lambda}{10} \quad (8)$$

Relation (7) puts a bound on the focal length/diameter ratio to between 0.35 and 0.45. This range is established by electrical considerations comparing feed design efficiency with minimum effects of feed blockage. Relation (8) is derived empirically from antenna design, and represents "good practice" for adequate electrical performance.*

* Direct communication with R. N. Bracewell, Stanford University.

Equations (1), (2), (6), (7), and (8) combined with the data in Table III-II formed the basis for the first prototype design and construction.

The first prototype antenna was designed to have a gain of 35 db at 4 GHz. In this design the focal length-to-diameter ratio was chosen to be 0.40. Restricting the root-mean-square surface deviation to be less than one-tenth of the wave length yields an RMS surface deviation of $\delta = 0.295$ inches. From the RMS surface deviation, the frequency, and gain, the diameter is found from the first constraint. It is 6.7 feet. From Eq. (6) the number of sections is found to be ten.

A full-size computer plot was made of the shape of each section, and from this plot a sheet metal template was made at Peninsula Metal Fabrication in Mountain View, California. In petals made from this template ± 0.020 inches was established as the δx locational tolerance for the rivet holes near the antenna rim in each section. At half the radius the tolerance was reduced to ± 0.010 inches, at one-fourth the radius it was ± 0.005 inches.

A template was made which would rest exactly on the contour of the assembled antenna at the junction between two adjacent sections. After final assembly it was found that this template followed the contour of the seam within 1/8 inch or less when the rim was planar.

This first prototype antenna was constructed from 0.040-inch thick aluminum with the sections fastened together by pop rivets spaced at three-inch intervals along each seam.

One design objective is to make the antenna as rigid as possible without additional supporting structure. Although this prototype supports itself and provides adequate performance under normal conditions, additional rigidity was needed for it to withstand extreme service conditions. This additional rigidity was obtained by a redesign of the antenna rim.

As is shown in Figs III-3, III-4, and III-5, the present rim extends outward 1-1/2 inches perpendicular to the antenna axis, then downward 1-1/2 inches parallel to the antenna axis and inward 1/2 inch normal to the antenna axis. At the junction between two sections the rims are joined by a piece of aluminum bar stock and four self-tapping screws.

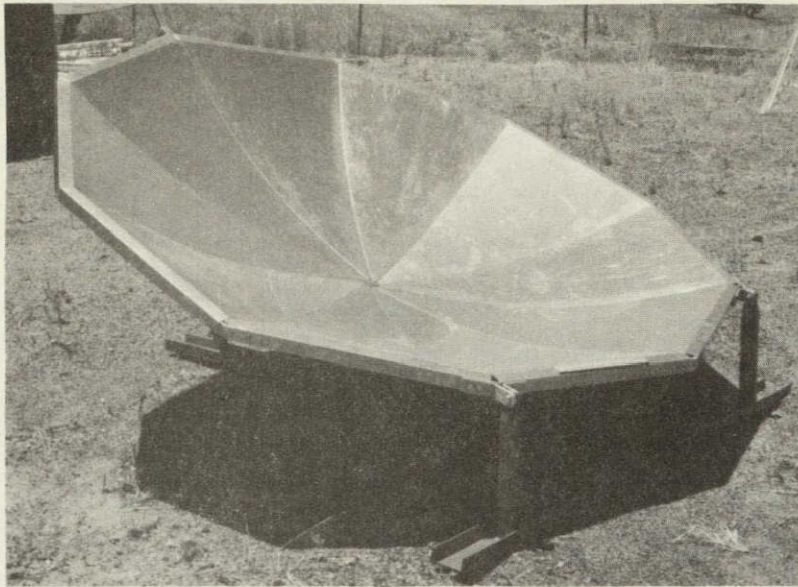


Fig. III-3. FIRST ANTENNA PROTOTYPE.

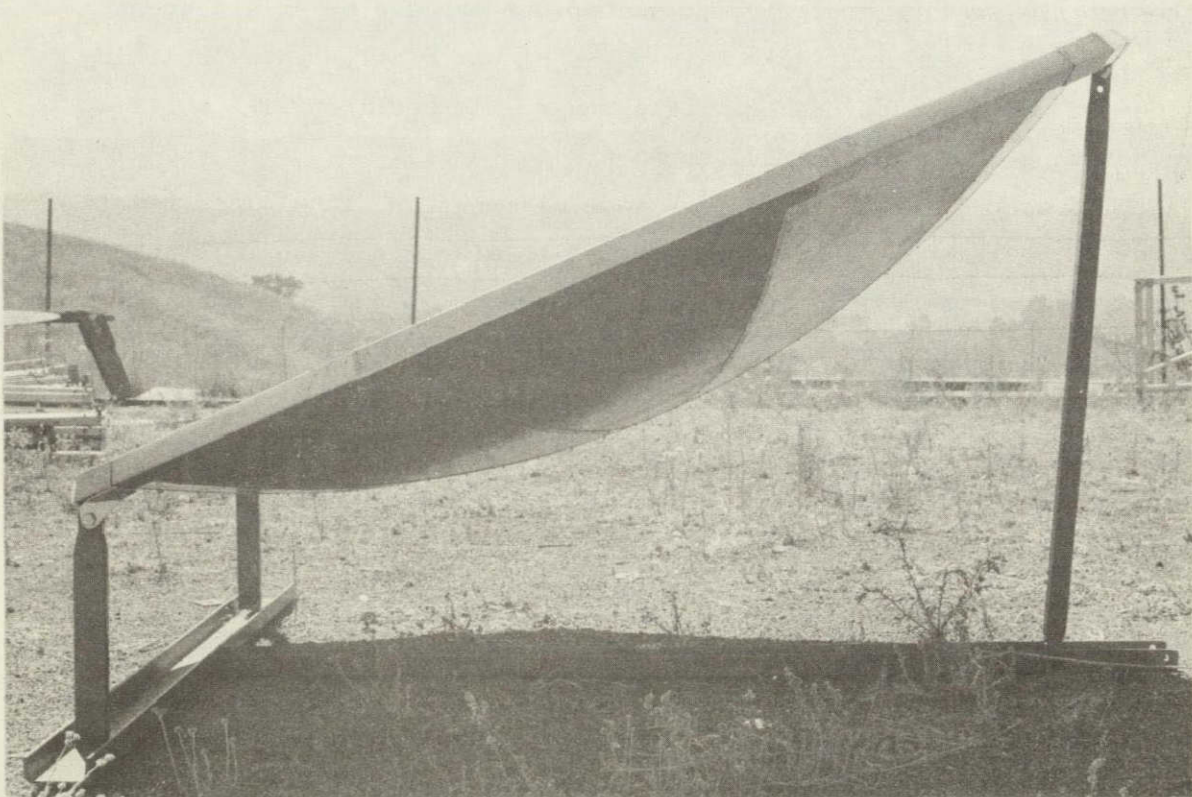


Fig. III-4. MOUNTING STRUCTURE FOR FIRST PROTOTYPE.

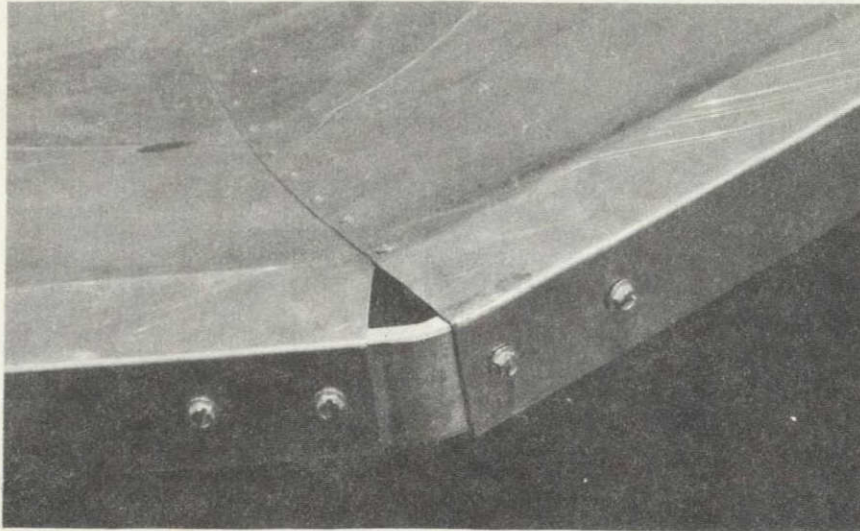


Fig. III-5. ANTENNA SEAM--FIRST PROTOTYPE.

If one presses down firmly on the rim at the seam the rim deforms 1 to 2 inches in a direction parallel to the antenna axis. It appears that the total deformation is composed of a displacement and a rotation of the two rim sections relative to each other through an axis tangent to the riveted seam. This deformation was almost eliminated by building a second prototype antenna having a square rim section $1\text{-}1/2 \times 1\text{-}1/2$ inches tangent to the antenna surface.

The second prototype has the same diameter and focal length as the first. The rim box sections are joined together by a square bracket clamp which fits over adjoining rim segments at the appropriate angles.

The second prototype, shown in Figs. III-6 and III-7, has the improved rim design. This design meets mechanical performance requirements for stiffness and torsional rigidity. However, this box rim required a series of four brake press operations which would be costly in a high volume production operation. The aluminum sheet metal thickness in the second prototype is 0.050 inch. Most of the rim distortion under load was confined to elastic buckling of the corner brackets near their welded seam.

From the second prototype, we concluded that the flat petal antenna is a workable solution to the problem of designing a low-cost antenna.

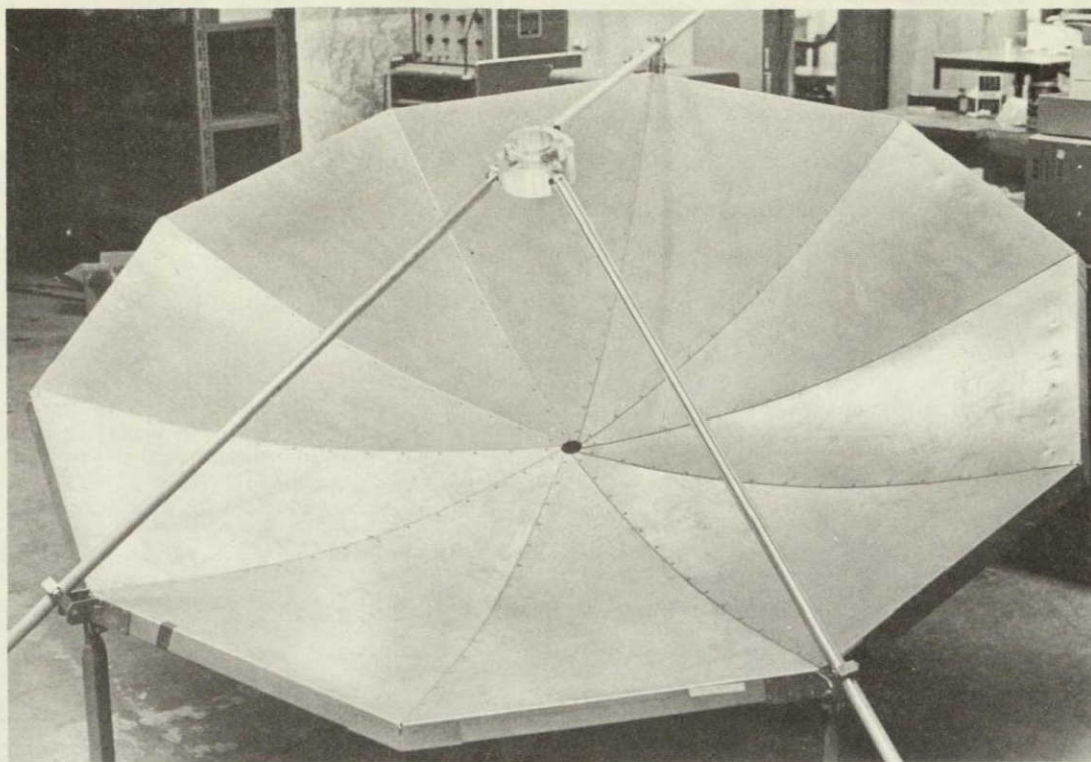


Fig. III-6. SECOND PROTOTYPE WITH FEEDHORN AND ADJUSTABLE FEED SUPPORTS.

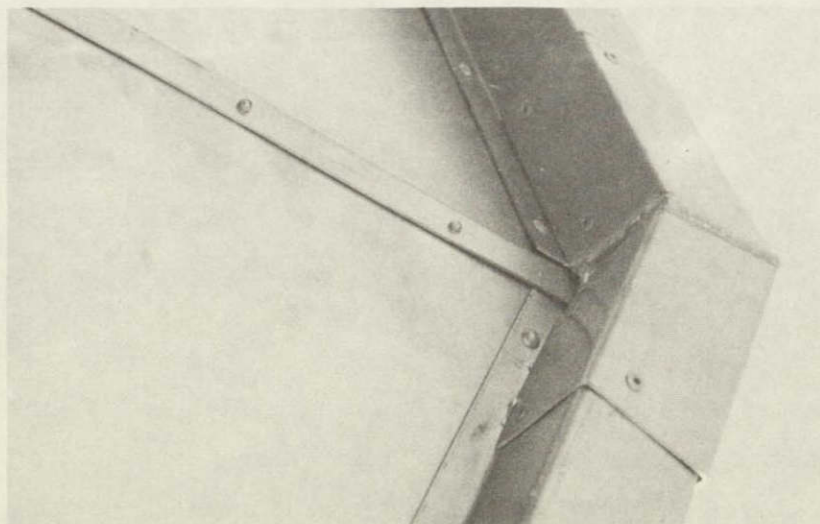


Fig. III-7. CLOSE-UP OF BOX RIM CONSTRUCTION OF SECOND PROTOTYPE.

D. Final Design and Cost Estimates

A third prototype was designed and built to eliminate problems found in the first two prototypes. Particular effort has been put into redesigning the rim structure around the edge of the 10 petal design and the corner bracket stampings which join the rim segments together. An optimizing program was developed for the petal shape to provide for maximum electrical performance.

The rim is one of the most important parts of the antenna design since the rim serves many functions. It provides the structure to keep the whole antenna rigid against bending and torsional loads. It also is the location for feed supports and mounting brackets. And as one of the first parts to be assembled, it provides the framework for fastening the petals together along their seams.

Several rim designs have been evaluated for this quasi-parabolic antenna. Three of these are shown in Fig. III-8. The first was an open box rim formed by bending the outer edge of each petal in three brake press operations. This design was not rigid enough to withstand the expected loading. The second rim design was a closed box rim formed by bending the outer petal edge in five brake-press operations. This design has proven to be capable of handling the expected loading without deforming enough to hinder performance significantly. The first corner brackets were fabricated from 0.050" aluminum which proved to be adequate although additional strength is desirable. The main problem with this second rim design is that in high volume production five brake press operations would require too much time and labor. For small volume production of 100 antennas these brake operations would be feasible.

The objective is to design a rim structure which can be mass produced at a high rate, be strong enough to keep the antenna rigid, and facilitate easy assembly. A third design for achieving this is to stamp the rim segments as single formed pieces with flanges at each end for bolting to adjoining segments. Each stamped segment would be riveted to the petal first and then the flanges or adjoining sections would be bolted together. The rim would form a jig for folding the petals in and fastening them along their seams. Some sketches and stress calculations were made for these stamped rim segments and drawings were submitted to

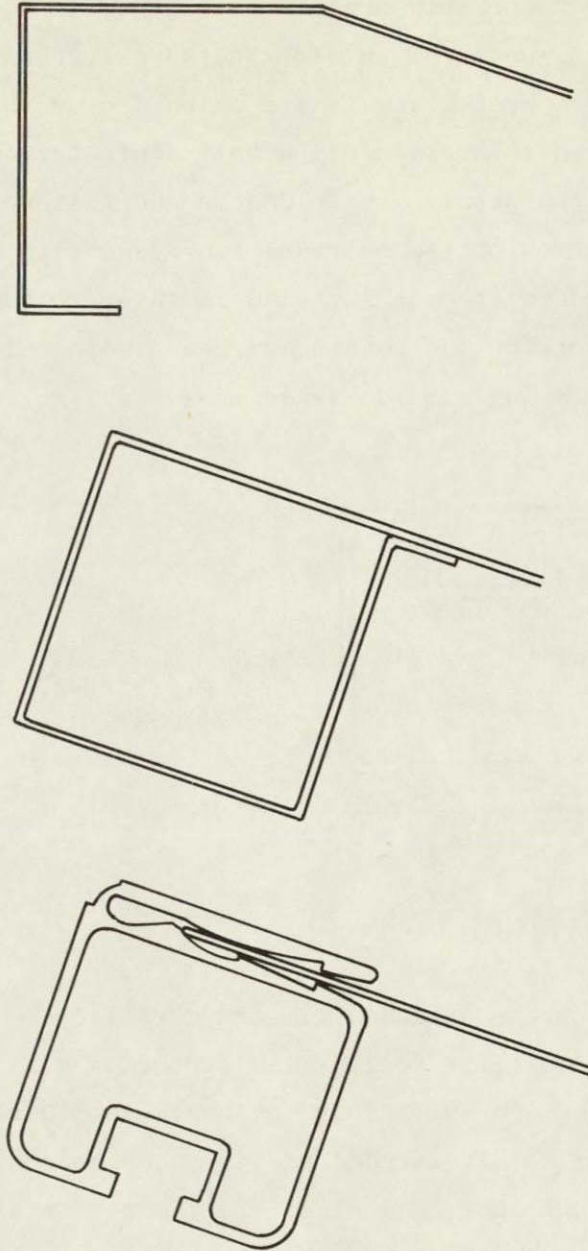


Fig. III-8. THREE RIM DESIGNS.

a metal stamping and forming company. After discussion with them, it was concluded that a single formed stamping of this design would require five operations including one annealing process and four expensive dies.

In the fourth and final rim design, it was decided to form the rim from a separate length of aluminum extrusion. Ten of these extruded segments are required per antenna; they are joined together by ten corner brackets formed in two operations on a small stamping press.

The antenna components are shown in Fig. III-2. The outside edge of the petal is slipped into a slot in the extrusion where it is held. Then the stamped corner brackets are slipped over the ends of the extrusion and bolted into place using bolt slots formed into the extrusions. Finally the petals are folded in and fastened along the seams.

A cross section of the extruded rim segment is shown in Fig. III-9. The slot is extruded in open form and is later rolled closed in the extrusion mill. Torsion and bending stresses were calculated to determine the wall thickness and outside dimensions.

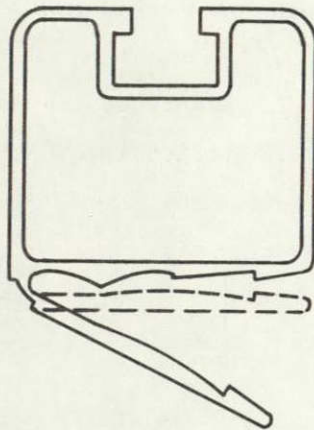


Fig. III-9. EXTRUSION
FOR RIM.

The costs for the extruded rim are as follows: the die cost is \$475, the set-up cost for rolling the slot closed is \$25, and the set-up cost for sawing the extrusions to length is \$10 plus \$0.06 per piece. The weight of the total extruded rim is 13.56 pounds. For 75 antennas the material and production cost of the rim per antenna is \$10.52, for 150 antennas the cost is \$9.10, and for 1000 or more antennas the cost is \$8.20. The dies for the extrusion were developed from our drawings by Pacific Extrusion, Inc., in Watsonville, California. Enough metal was extruded for 40 seven foot antennas.

Dies were developed for a small production run of the corner bracket stampings. This bracket will be stamped from 0.080" thick aluminum. For higher production the die cost would be approximately \$1500 for a die life of 500,000 units (50,000 antennas).

Antenna mounts have been designed which are flexible enough to be mounted on several types of surfaces. The front two mounts are made from 1 inch diameter thin wall galvanized pipe. The pipe has been bent in a V with its ends being flattened. These bolt to the under side of the extrusion and act like table legs which can be clamped to any surface by bolts or straps. The rear mount is an A-frame support hinged at the top and made from 3/4" diameter aluminum tubing.

To mount the antenna the two front legs are placed on the mounting surface and aligned in a compass direction predetermined by the latitude and longitude of the site and the satellite location above the equator. These establish the azimuth of the antenna. Elevation angle is established by the A-frame, which can be adjusted. Once the antenna is adjusted to receive the best picture from the satellite, then the bases of the legs and A-frame are permanently attached to the mounting surface. Experiments and calculations show that aiming with these mounts within the 1 db beamwidth of 2.2 degrees is not difficult.

Figure III-10 shows the third prototype and final antenna design.

We describe below a computer program designed to improve the gain from our flat petal antenna.

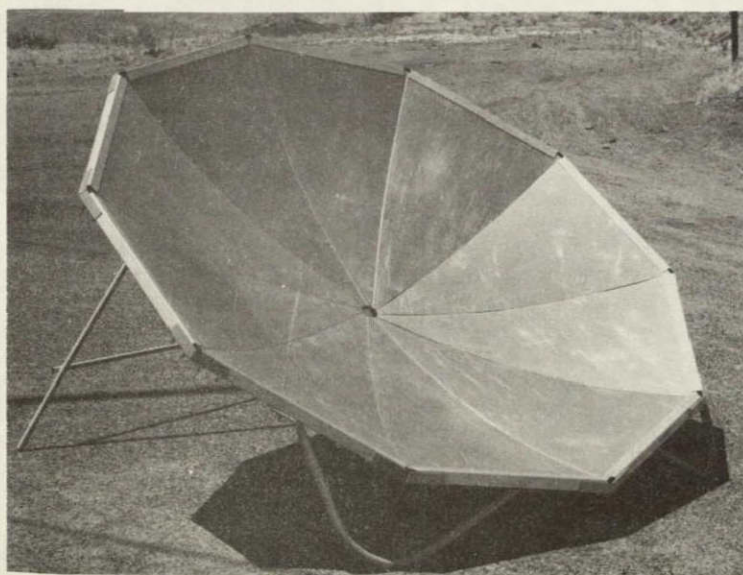


Fig. III-10. THIRD PROTOTYPE AND FINAL ANTENNA DESIGN.

The program adjusts the shape of each petal so that the signal reflected from the petal surface and collected at the feed is maximized. The program also finds the optimal feed horn pattern. The petal design differs from a true paraboloid antenna in that there is a pattern of regular antenna surface deviations. Signals reflected to the feed from different positions on the petal may arrive out of phase because a wave reflecting from the antenna surface will travel a longer distance to the feed if it strikes the petal surface near a seam between petals than if it strikes the surface near the middle of the petal. This difference in distance traveled causes the electric field vectors to add "out-of-phase" at the feed.

The computer program minimizes this phase error by adjusting the height $z(y)$ of the petal at each position to minimize the sum of the square of the phase error distances at each line $y = \text{constant}$.

The phase error distance is the difference between the distance traveled by a wave striking the section antenna surface and distance traveled by a wave striking a perfect paraboloid.

This can be described as follows. Referring to Figs. III-11 and III-12, a wave traveling from a plane normal to the axis of the antenna through the focus and reflecting from the antenna petal to the focal point travels a distance d , where d is given by:

$$d = [z_0 - Z(y)] + \left\{ [z_0 - Z(y)]^2 + x^2 + y^2 \right\}^{1/2} \quad (9)$$

where z_0 is the focal length of the antenna. If the same wave were traveling from a plane through the focus to the feed of a perfect paraboloid it would travel a distance of $2z_0$, twice the focal length.* The difference $(2z_0 - d)$, is the phase error distance.

We have developed an iteration scheme which minimizes the phase error distance over the sectioned antenna surface as follows.

* This is a geometric property based on the definition of a paraboloid.

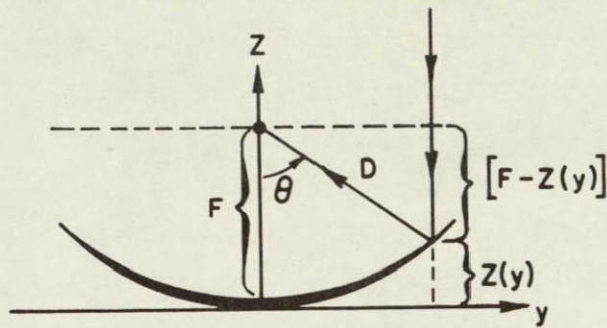


Fig. III-11. CROSS-SECTIONAL VIEW THROUGH THE ANTENNA AT PETAL CENTER-LINE.

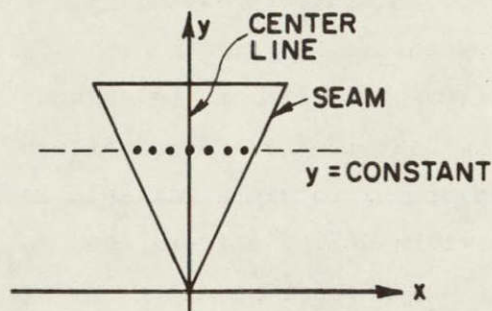


Fig. III-12. TOP VIEW OF ANTENNA PETAL.

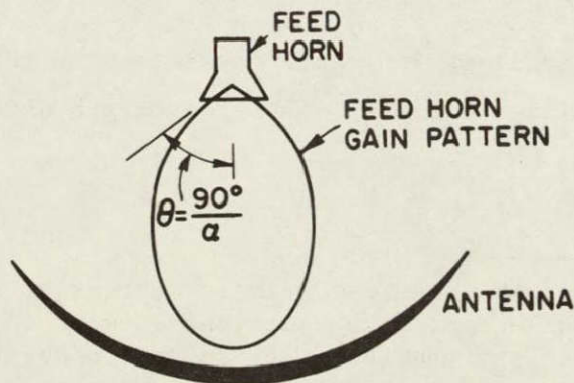


Fig. III-13. FEED HORN GAIN PATTERN.

We find $Z(y)$ such that

$$\delta^2(y) = \int_{y=0}^{r_0} \int_{x=0}^{\omega(y)} \frac{(2z_0 - d)^2 dx dy}{r_0 \omega(y)} \quad (10)$$

is a minimum and record $Z_{\min}(y)$. Where

r_0 = radius of the antenna

$\omega(y)$ = one-half the width of the section.

Having found the section height $Z_{\min}(y)$ we use a geometric transformation to find the shape of the flat petal as it must be stamped to achieve this. It is also possible to establish the tolerances on the stampings with this program.

The program calculates the gain of the antenna for different feed horn patterns,* assuming that the feed horn pattern is as $K(\alpha) \cos^2 \alpha \theta$ where K is a function of α , α is a variable ranging from 0.5 to 1.5 which affects the beam width of the pattern, and θ is an angle measured from the beam axis** of the antenna as shown in Fig. III-13.

The gain is calculated from the following integral [6]:

$$\text{Gain} = G_{\max} \left\{ \iint_A \sqrt{K} \cos \alpha \theta \cos \left[\frac{2\pi(2z_0 - d)}{\lambda} \right] dx dy \right\}^2 \quad (11)$$

where G_{\max} is the ideal maximum gain possible with this size antenna, and the integral is taken over A , the area of the antenna as projected on the x - y plane.

* Almost all microwave antennas use primary sources of radiation together with reflectors and lenses. The radiating element is spoken of as the "primary feed", the "antenna feed", or in this case the "feed horn". Its radiation pattern as an isolated unit is known as the "primary pattern" of the antenna or in this case, the "feed horn pattern."

** The line through the origin and the peak of the main beam of the feed horn pattern is referred to as the beam axis.

Some of the advantages of this program over past methods of computing gain are that (1) it treats surface variations as being regular rather than random, (2) it permits us to minimize the effect of these variations, (3) it allows us to plot a "best" shape for the flat stamping and establish manufacturing tolerance limits, (4) it permits us to find the optimal feed horn pattern, and (5) it is general enough to handle diameters, focal lengths, numbers of sections, frequencies, and feed horn patterns.

Figure III-14 shows the gain calculated for various feed horn patterns. One curve shows the unoptimized design and a comparison with the second curve for the optimized design shows the effect of minimizing the phase error losses.

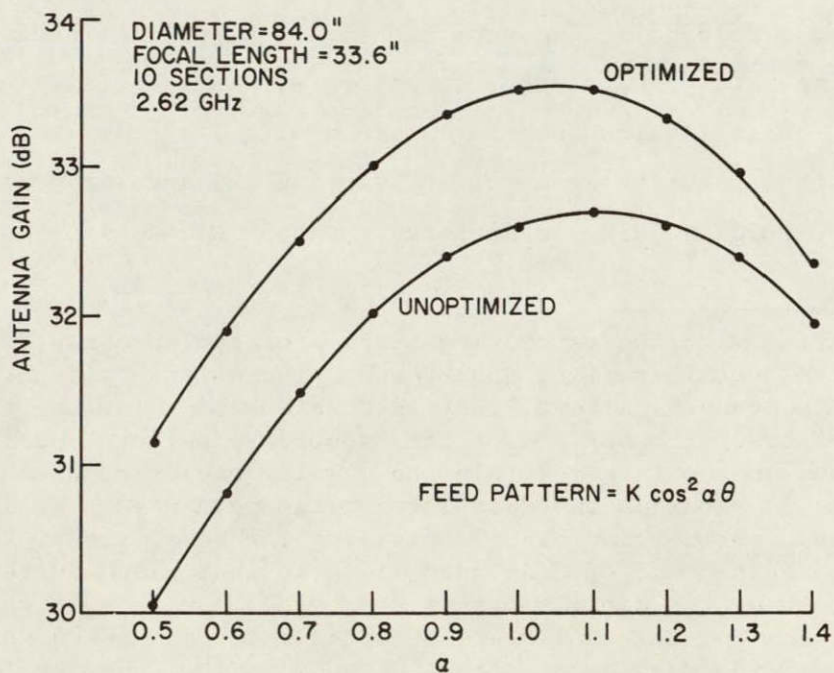


Fig. III-14. ANTENNA GAIN VS FEED HORN PATTERN.

E. Testing the Antenna: Gain Measurement Method

The gain, beam widths,* and sidelobe level** of the second prototype were measured using the test set-up shown in Fig. III-15. A photograph of the antenna during the test is shown in Fig. III-16.

A transmitting horn was cantilever-mounted from the top of a 60 foot utility pole. To measure the gain of the antenna, a signal of known strength is launched from this transmitting horn, which has been aimed along its beam axis toward the antenna. As the signal passes through free space enroute to the antenna its power is diminished in relation to the distance between the transmitting horn and the antenna. This loss in power through free space can be calculated and from this calculation we know the signal power that would be received at the position of our antenna by an isotropic antenna. An isotropic antenna, equally receptive in all directions but not physically realizable, is used as a convenient reference. Gain is defined as the ratio of the signal power received by the antenna in question to the signal power received by the antenna and we know the signal power that would be received by an isotropic antenna, therefore we can calculate the antenna gain. Initially the antenna is aimed with its beam axis pointed directly at the transmitting horn. By varying the angular position antenna and recording gain, we measured the beam widths and sidelobe

*

In combination with the reflecting surface of the antenna, the feed produces the overall radiation pattern of the antenna often referred to as the "secondary pattern" that is considerably greater in value than the others. The portion of the "secondary pattern" possessing this maximum and contained within the angular region bounded by adjacent minima is known as the main lobe or the main beam. To define beam widths, consider any plane containing the beam axis of the antenna. The half-power or 3 db beam width in that plane is the angular distance between the two directions about the beam axis in which the power radiated per unit solid angle in the main beam is one-half the peak value in the main beam. The 1 db beam width is defined correspondingly.

**

In addition to the main lobe there are subsidiary maxima in the antenna radiation pattern or secondary pattern. These are referred to as side lobes. The sidelobe level is the ratio of the power received at the sidelobe maxima to the power received at the main lobe maximum.

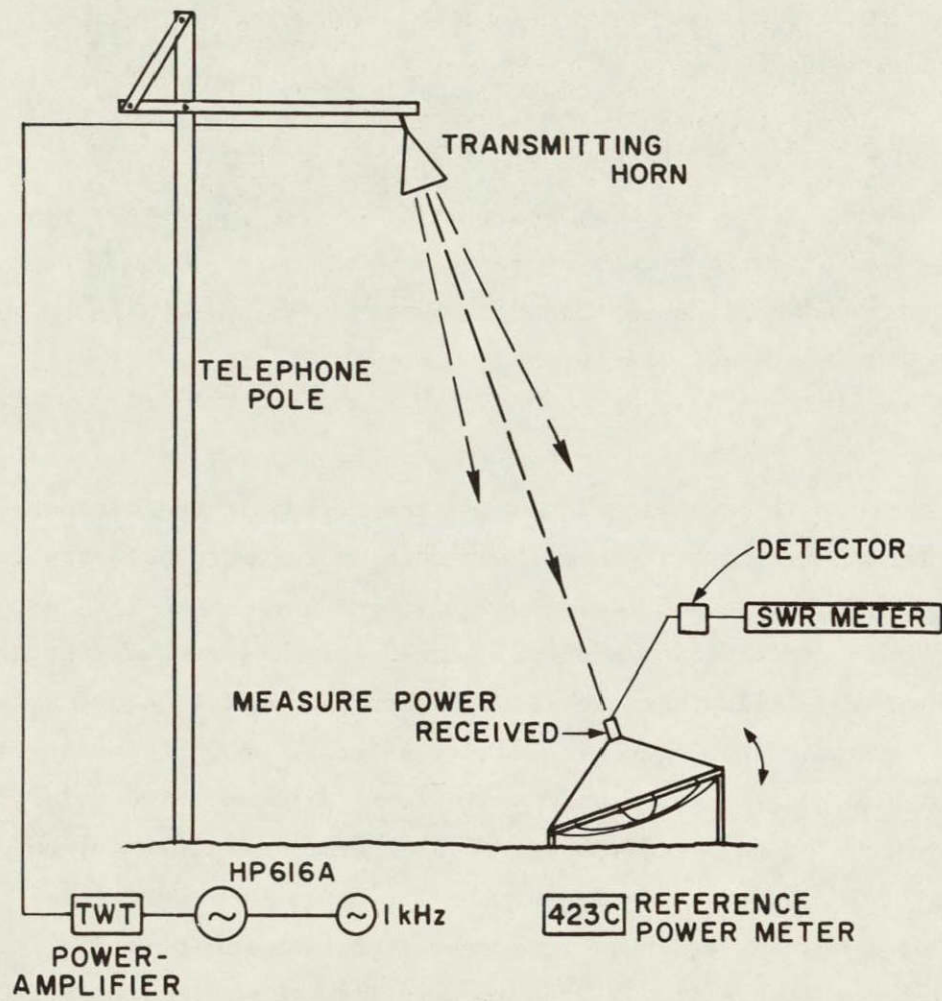


Fig. III-15. GAIN MEASUREMENT TEST SETUP.

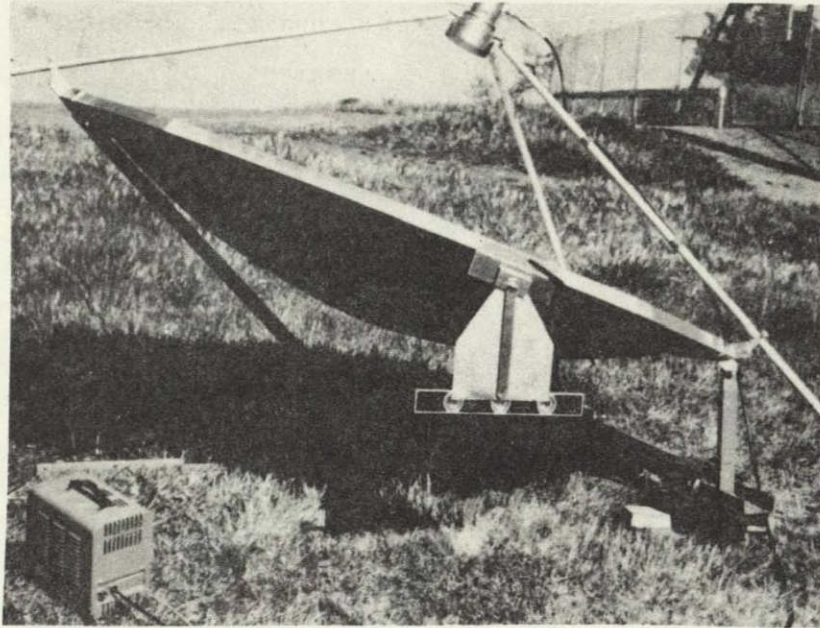


Fig. III-16. ANTENNA DURING GAIN MEASUREMENT.

levels. Due to inaccuracies in estimating losses in the cables, free space, and the transmitting horn, our gain measurement accuracy is estimated to be ± 1 db.

The gain of the antenna as calculated from the computer program was 32.4 db when illuminated by a feed horn pattern of $\cos^2 \alpha\theta$ with $\alpha = 1.1$. We take into account blockage effects, we subtract an expected loss of 0.9 db to get a gain estimate of 31.5 db. The gain as measured for the second prototype was 30.5 db which is close to the calculated value for the antenna and within the range of experimental precision. The 1 db beam width is 2.5° , the 3 db beam width is 4.4° , the first sidelobe occurs at 7.2° and is down from the main lobe by 26 db.

F. Antenna Costs and Assembly Procedure

Throughout the evolution of this antenna design, we have worked with manufacturers to assure that the design would be compatible with low-cost manufacturing methods. This consultation has helped in deciding among alternate fabrication methods for completing our final design.

The three basic components of the antenna without mounts are (1) the stamped petals, (2) the extruded rim segments, and (3) the stamped corner brackets. For costs and for fabrication of the petals and corner brackets, we have worked directly with two firms: Peninsula Metal Fabrication in Mountain View, California, and Williams Manufacturing Corporation in San Jose, California. Pacific Extrusions, Inc. in Watsonville, California, worked with us on the extrusion fabrication and costs. Quotations were requested and received from other vendors for comparison.

The costs presented in Table III-III are for the unassembled components of a seven foot antenna. This antenna design is low in cost for a wide range of production quantities.

A deployment crew will be used to install the adaptor at each site. Transportation, shipping, assembly, and installation will be the responsibility of that crew. One man can assemble the antenna in one hour; two men can assemble it in 40 minutes.

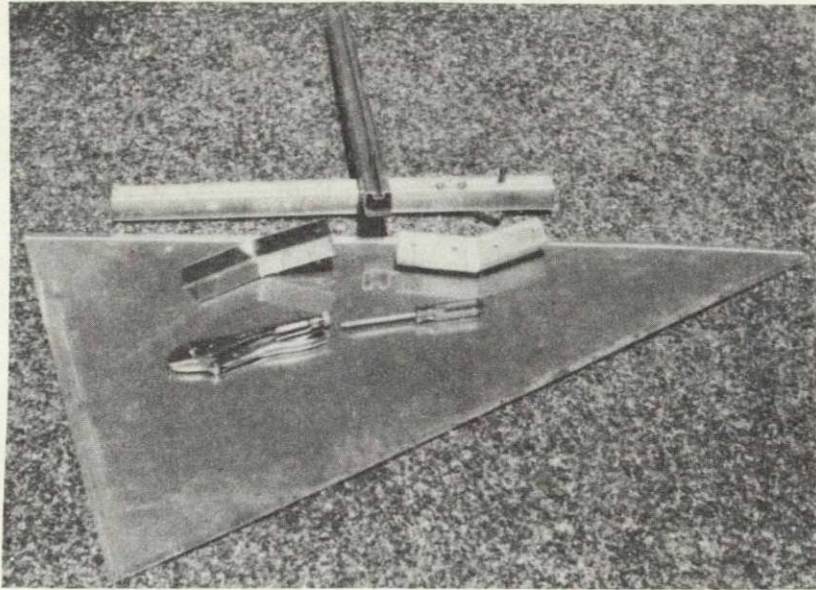
The pictures on the following pages show the assembly procedure in sequence. The tools needed are shown in the first two pictures. Also needed are a 1/2 inch open end wrench and a pop rivet gun.

First the rim structure is bolted together with corner brackets fastening the extruded segments together. Then one by one the petals are inserted into the slot in the extrusion. After the first petal is inserted then each additional petal is folded in and attached to its predecessor with pop rivets or with small nuts and bolts until the entire assembly is finished.

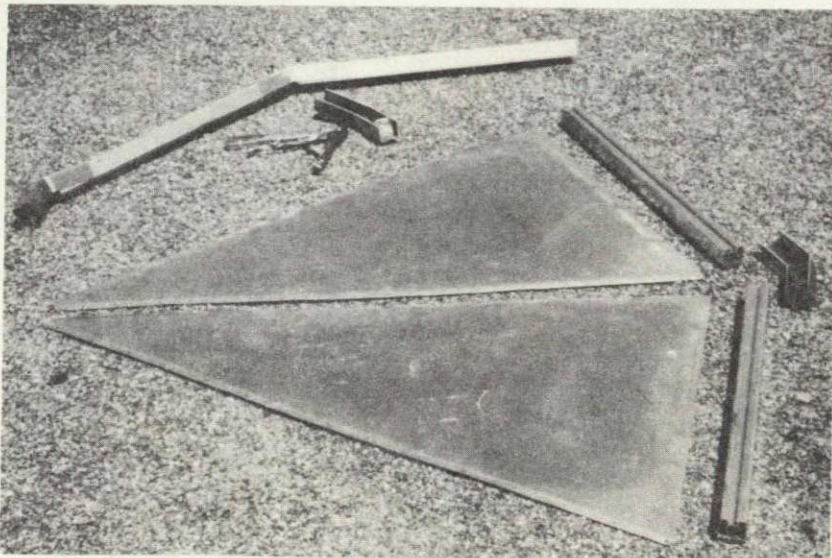
The final step is to attach the feed supports and antenna mounting brackets to the extruded rim.

Reference

Ruse, J., "Antenna Tolerance Theory - A Review," Proceedings of IEEE, April, 1966.



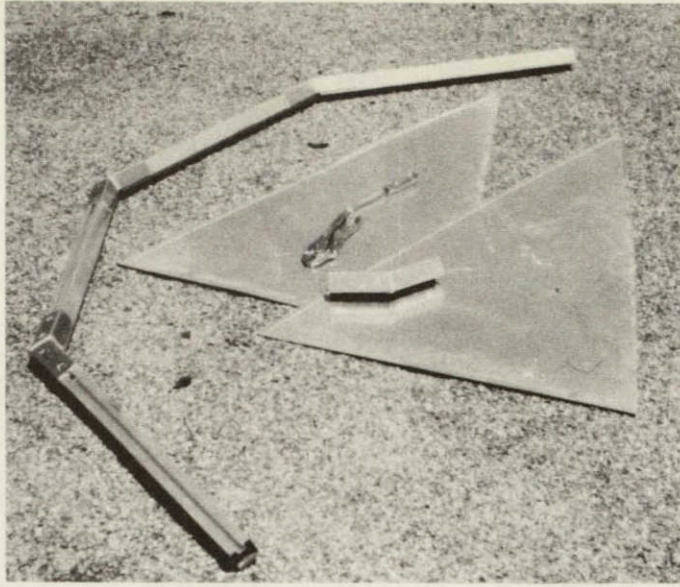
(a)



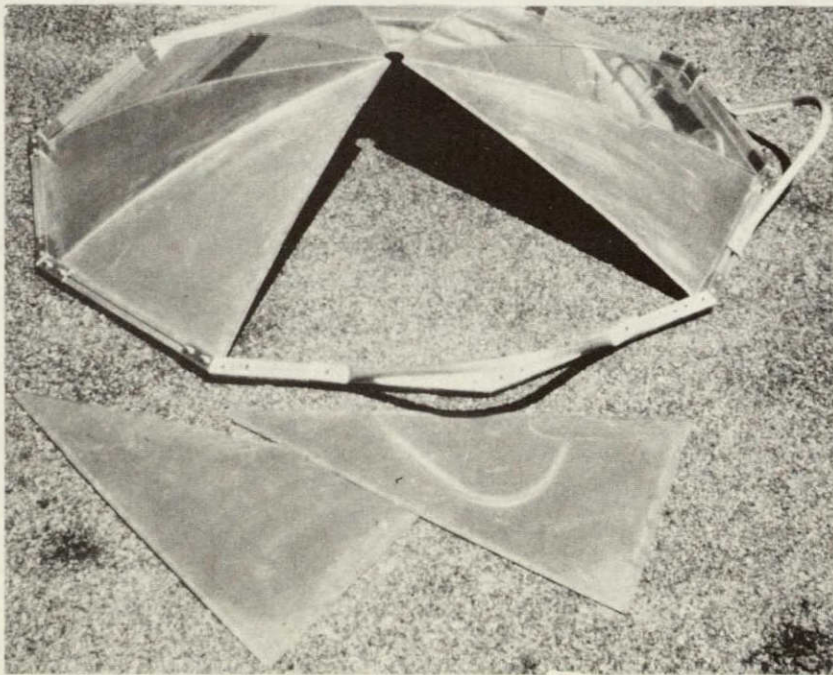
(b)

Fig. III-17. ASSEMBLY PROCEDURE.

11



(c)



(d)

Fig. III-17. CONTINUED.

Table III-III

ANTENNA COSTS AS QUOTED FROM MANUFACTURERS

- (1) Antenna Petals - quotation from Williams Manufacturing Corporation, San Jose, California

<u>Quantity</u>		<u>Price</u>
250 petals	@	\$3.11 each
1000 petals	@	2.31 each
10000 petals	@	1.84 each

plus dies and tools cost \$2100.00
includes 1 blanking die and 1 piercing die

(The minimum die life is 1.5 million stampings which is sufficient quantity for 150,000 antennas.)

- (2) Extruded Rim Segments - quotation Pacific Extrusions, Inc., Watsonville, California

<u>Quantity</u>	<u>Price</u>
500 lbs. 37 antennas	\$12.48
1000 lbs. 74 antennas	10.44
2000 lbs. 148 antennas	9.09
5000 lbs. 368 antennas	8.33
10000 + lbs. 736 antennas up	8.21
plus die cost	475.00
set-up charge for roll closed	25.00
set-up charge for sawing to length 25"	10.00 + \$0.06/pc.

(The die life is 12,000 to 15,000 lbs. No additional charge is made for die replacement or repair in quantities of 10,000 lbs. and higher.)

- (3) Stamped Corner Bracket - quotation from Williams Manufacturing Corp., San Jose, California

<u>Quantity 250</u>	<u>Quantity 1000 and 10000</u>
Tooling \$650.00	\$1485.00
Price 250 1.67 each	
1000	0.55 each
10000	0.34 each

(The minimum die life is 1.5 million stampings which is sufficient quantity for 150,000 antennas.)

Table III-IV

ANTENNA COSTS FOR VARIOUS QUANTITIES

	Quantity of Antennas			
	100	1000	10,000	100,000
(1) Petal cost per antenna				
(a) Tooling	\$21.00	\$ 2.10	\$ 0.21	\$ 0.04
(b) Material & production	23.10	18.40	17.00	17.00
(2) Extrusion cost per antenna				
(a) Tooling	5.70	1.11	0.11	0.02
(b) Material & production	10.44	8.21	8.21	7.00
(3) Corner bracket cost per antenna				
(a) Tooling	14.85	1.49	0.15	0.03
(b) Material & production	5.50	3.40	3.40	3.40
(4) Pop rivets - 100 per antenna	0.76	0.76	0.64	0.64
(5) Nuts & bolts (5/16" × 1/2") 40 per antenna	1.38	0.80	0.80	0.80
(6) Mounting brackets	6.00	6.00	3.00	3.00
TOTAL COST	\$88.73	\$42.27	\$33.52	\$31.93

IV. THE ELECTRONICS PACKAGE

This section discusses the electronics package design. The form of presentation follows the stages in the design process, rather than simply presenting the results. In this way, the important parameters and the various interdependencies between the subsystems are more clearly developed. Those stages in the design process are generally as follows.

The system parameters determine the performance of each subsystem in some particular way; we shall describe the requirements for each subsystem as derived from the system requirements presented in Section II. The possible alternatives are then presented, and a choice is made on the basis of cost, known performance, or other criteria, as appropriate. If the performance is uncertain for the application, then additional analytic and/or experimental investigations of one or more alternatives were conducted, and these results are presented.

Based on these investigations, a choice is made for use in the working model. The performance of the prototype working model is then described.

A. Development of System Requirements for the "Front End"

The antenna feed, preselector filter, mixer, local oscillator, and the first stage of the intermediate amplifier are collectively known as the front end of the receiver electronics package. The antenna feed is included because it will become an integral part of the front end. A schematic diagram is shown in Fig. IV-1. The basic operation is as follows.

Signal energy is collected by the antenna and focussed at the feed; this signal energy has an effective source impedance equal to that of free space. It is collected by the feed system and matched to mode of transmission. It then propagates to the preselector filter. This filter passes energy in a specified band and rejects energy at all other frequencies. This is done to prevent extraneous signals and noise from contaminating the desired signal, especially at the image frequency, and to prevent local oscillator radiation.

The local oscillator generates a constant signal of relatively large amplitude (compared to the desired signal) at a frequency either slightly

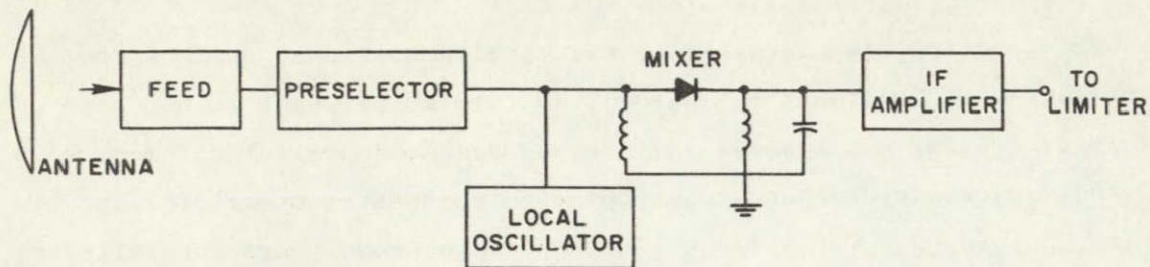


Fig. IV-1. "FRONT END" OF ADAPTOR.

higher or lower than the signal frequency; the difference is called the intermediate frequency (IF). Some method of isolating the local oscillator from the signal path is employed, in order to avoid wasting signal power in the local oscillator impedance. The large local oscillator signal causes the mixer diode to traverse its non-linear V-I characteristic, and this resulting nonlinearity provides a simple method of obtaining a frequency translation from microwaves to a much lower frequency^{*}; in this case, the IF is 120 MHz, and was chosen in consultation with the technical contract monitor.^{**} The signal received from the satellite is too weak to be detected and too high in frequency to be easily demodulated. Consequently, both amplification and frequency translation (via the mixer) are necessary. In this case, the system noise figure can be obtained with high-quality mixer diodes, and microwave pre-amplification is not necessary. Thus all of the necessary amplification can be done at the intermediate frequency. An arbitrary choice of local oscillator frequency was made at 2500 MHz, and the signal frequency at 2620 MHz. The local oscillator was chosen to be on the lower side of the signal for a specific reason, which will be discussed in the mixer section. The radio-frequency choke (RFC) and the inductor of the IF tank provide a dc return path for the diode. Some provision must be made for obtaining a short circuit at 2500 MHz on the IF side of the mixer diode, in order that the LO be able to drive the diode. The IF

* See Microwave Mixers, R.V. Pound, M.I.T. Rad. Lab. Series #16.

** The reasons for choosing this IF are developed in the mixer section.

amplifier increases the signal amplitude in order to facilitate later processing. These are the basic elements of the front end. The system noise temperature specification must be considered before the relationships between mixer configuration, performance, and local oscillator alternatives can be discussed.

System Noise Temperature Considerations

The most important electrical performance criteria which the front end must meet is the system noise temperature T_e . A performance specification has been set at 1160°K , or a noise figure of 7 dB. The overall system noise temperature is given by the following relationship:

$$T_{\text{system}} = \alpha T_a + T_o(1 - \alpha) + T_1 \quad (1)$$

where

T_a = Noise temperature of the antenna; a composite of sky and local noise temperatures;

α = Transmission coefficient from antenna feed to the mixer;

T_1 = Noise temperature of the mixer and is dependent on some of its physical properties and the noise temperature of the IF amplifier;

T_o = Physical temperature of the transmission path to the mixer.

The overall noise temperature also depends to some extent on the noise properties of the local oscillator.

If we assume that a 1000°K noise temperature (6.5 dB) is a reasonable goal for a mass-production mixer, then we have only 160°K left to meet system T_e of 1160°K . T_a ranges from 20 to 100°K , and T_o is generally 290°K . Thus the transmission coefficient α must be greater than 0.685 in order to meet the specification. This implies that the total attenuation between the mixer and the antenna must be less than 1.5 dB.* This attenuation is due to losses in the cable, if any, and the

* The attenuation is given by $10 \log \alpha$.

preselector. A preselector filter may have as little as 0.5 dB attenuation, or as much as 1.0 dB. Thus the cable attenuation is limited to at most 1 dB. Commonly available and inexpensive coaxial cable such as RG-8/A has an attenuation of 7 dB/100 feet at 2600 MHz, thus permitting a 14-foot length, at the most, between the antenna and the electronics package. This may or may not be an allowable length, depending on the installation site. Because of the large quantity of receivers needed, and the uncertainty of distances from antenna installation sites to possible mounting sites for the electronics, it was decided to mount the front end directly at the focus of the antenna. This has the advantage of eliminating microwave cable runs and the inevitable loss of signal strength, and standardizes the installation. It has the disadvantage of requiring adequate environmental protection for all the circuitry. For hot, humid countries like Brazil and India, this is a necessity regardless of indoor or outdoor installation, and so is not a serious disadvantage. The form of the feed-mounted electronics package depends on the choice of mixer configuration.

B. The Mixer

Although the diagram in Fig. IV-1 shows only one diode, there are a number of other configurations which employ 2 or 4 diodes and achieve improvements of various kinds in performance.* The balanced mixer, using two diodes, can improve mixer noise performance because cancellation of local oscillator noise is possible.** It can improve front end performance by reducing local oscillator radiation out the signal port. The disadvantage is that two diodes are needed, and the microwave mixer diode is one of the most expensive components in the electronics package. The question of whether local oscillator noise will cause a degradation of system noise performance is more serious than the local oscillator radiation problem; the preselector filter can be used to help with that. The potential problem of local oscillator noise turned out to not be

* See for example, Pound, Microwave Mixers, Chapter 6, and "Broadband Double Balanced Mixer/Modulators," by R. B. Mouw and S. M. Fukuchi, Part I, Microwave Journal, Vol. 12, No. 3, pp. 131-4.

** See Microwave Mixers, by R. V. Pound, MIT Rad Lab Series, #16.

serious, but it was not until both single and balanced mixers were tested that it was certain. There are a number of different possible physical realizations of the mixer, and the major alternatives are now discussed.

The two major realizations for balanced mixers are in stripline* and waveguide. Single diode mixers can also be realized in stripline, waveguide, or coaxially, and so there is no problem to convert to a single mixer. Designs for both waveguide and stripline mixers (and associated circuitry, as applicable) were begun and proceeded until it became clear that there are significant disadvantages to stripline mixers for this application, in comparison to a waveguide configuration. The first is that stripline substrates are expensive, and the material is available only in the U.S. and some European countries, and not in South America. The maximum size substrate necessary for a hybrid coupler, mixer, and a coupled-bar filter for the local oscillator is estimated at $15 \times 15 \times 0.318$ cm, and two boards are needed for each assembly. The price quotes for large quantities of various substrates are given in Table IV-I. The substrate materials listed are of good quality; less expensive materials could be used, but the likelihood of greater variations in overall performance would increase. A stripline mixer could require at least two connectors, and this is an additional expense.

Table IV-I
STRIPLINE SUBSTRATE MATERIAL PRICES (1969)

Material	Stock Sheet size	Cost/Sheet	Cost/Mixer
Rexolite, 1 oz. Cu. (Brand-Rex Co.)	.125" \times 2' \times 3'	\$41.75	\$3.48
Polyguide GF 165 1 oz. Cu. (Electronized Chemicals)	to size	-	2.00
Polyguide GF 265	to size	-	3.50

* Stripline is a generic term for strip transmission line, in which a narrow flat strip of a conductor is sandwiched between two dielectrics with ground planes on either side

In contrast, a waveguide mixer does not need any connectors, and can be die-cast or sand-cast from aluminum which is readily available. Further, the mixer structure could be part of an integral feed and housing for the electronic circuit boards. If die-cast, this structure does not need any additional machining after casting.* The cost for aluminum is \$1.04/kilogram in Brazil (1969); it is not likely that more than two kilograms would be needed for such a housing, and so the materials cost is about \$2.00. Consequently, we pursued the waveguide mixer design. The General Electric Co. is presently engaged in a study similar to this one (under contract NAS 3-11520), with emphasis on a receiver system for the United States, and they are actively pursuing the stripline realization. In conversations with G. E.** we agreed not to duplicate our efforts by having each group consider both waveguide and stripline designs.

The Prototype Waveguide Mixer

The configuration chosen for the prototype mixer is similar to the Varian Orthomode mixer, except that it is realized in circular waveguide, as shown in Fig. IV-2. Circular waveguide was chosen instead of rectangular or square waveguide because it is easier to effect the conversion from circular to linear polarization with less phase compensation vanes and stubs in the feed, since the feed will be a conical horn. These problems are discussed more fully in the section on future work.

In the orthomode mixer, the local oscillator signal is injected with its E-field perpendicular to the axis of the diodes. Energy is coupled to the structure and a match is obtained with the tuning screw. The local oscillator signal excites both diodes, causing them to conduct simultaneously. Since they are connected in opposite polarity to the IF port, the noise voltages, now proportional to the diode currents, cancel out. The E-field of the signal energy must be aligned with the axis of

* In an article by A. F. Harvey, "Mechanical Design and Manufacture of Microwave Structures," PGMTT, October, 1959, p. 418, it is stated that the surface roughness for die-cast surfaces is half the roughness for ordinary machined parts.

** December, 1968, with John Dysinger and R. Hesselbacher, at Stanford.

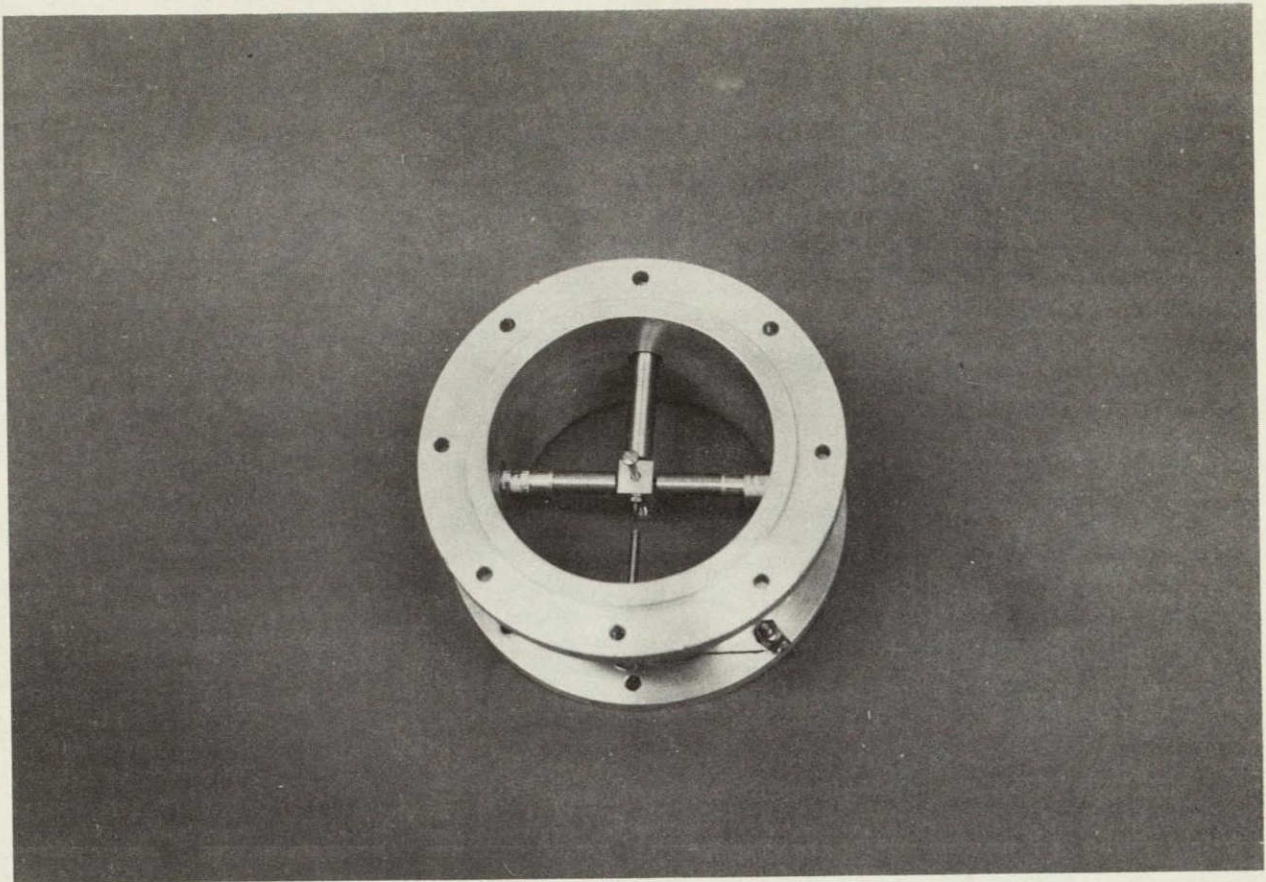


Fig. IV-2. BALANCED MIXER IN CIRCULAR WAVEGUIDE.

the diodes, and so we are limited in our choice of allowable mode to the TE_{11} . This mode is also the dominant TE mode, and therefore we can guarantee that no other mode can propagate by making the waveguide small enough in diameter. It will be to our advantage to make it smaller than is normally done in practice for the following reasons.

It has been shown that the optimum source impedance seen by the mixer diodes at the image frequency for best conversion loss is an open circuit;* we may incorporate this requirement into our design in the following way. We choose to operate the mixer with the LO at a frequency

* P. D. Strum, "Some Aspects of Mixer Crystal Performance," Proc. IRE, Vol. 41, p. 882, July 1953.

less than that of the signal frequency. The image frequency is now less than the LO, by the amount of the IF. As the cutoff frequency is approached, the wave impedance of the TE_{11} mode increases rapidly; if the image frequency is only slightly above cutoff, the source impedance seen by the mixer diodes will tend toward an open circuit, as required. The success of this technique depends on having a large intermediate frequency, since the signal frequency should not be too near cutoff, or the waveguide will have to be excessively long.* Specification of the waveguide diameter thus depends on the choice of intermediate frequency.

Intermediate Frequency

The choice of IF depends primarily on rf signal bandwidth, the upper limit at which amplification can be easily obtained, and the local oscillator configuration. With a 25 MHz rf bandwidth, the IF should be at least 60 MHz, in order to avoid difficulties in obtaining good phase and amplitude characteristics. From the standpoint of the image termination goal, the IF should be as large as possible. Inexpensive, epoxy-encapsulated rf transistors are available in Brazil with f_t 's in excess of 1000 MHz, and so good amplification is possible to 200 MHz. The local oscillator configuration becomes important if a crystal oscillator-multiplier scheme is employed. Care must be taken to avoid generating spurious responses of large amplitude anywhere near the IF passband. These problems can be avoided if the crystal oscillator frequency is chosen to be above the IF. Otherwise, some additional precautions must be observed. These particular problems will be discussed further in the following section on the local oscillator.

The actual choice of IF was made in consultation with the contract monitor. Initial calculations showed that a satisfactory ratio of signal frequency wave impedance to image-frequency impedance could be obtained with an IF greater than 100 MHz; the contract monitor advised that

*The guide wavelength increases as the cutoff frequency is approached.

NASA has standard test equipment for IF systems at 120 MHz, and so 120 MHz was chosen. The diameter of the waveguide may now be calculated

Waveguide Diameter

The signal frequency is 2620 MHz, the local oscillator is 2500 MHz, and the image frequency is 2380 MHz. The diameter corresponding to a cutoff frequency of 2380 MHz in the TE_{11} mode is 7.38 cm (2.90 inches),* the actual cutoff frequency can be somewhat lower, since a perfect open circuit is not required, and the guide wavelength at the signal frequency will not be quite as long. A diameter of 3 inches (7.60 cm) was chosen to simplify construction, since 3-inch tubing is a standard size, and it was originally thought that tubing or pipe could be used for the mixer. The new cutoff frequency is 2310 MHz.

Noise Performance of Mixer Diodes

The effective noise figure F'_{mixer} of a mixer diode (and its effective noise temperature T_1) depends on its conversion loss L , its own physical properties as expressed by its noise temperature ratio t_m , and the noise factor F'_{if} of the IF amplifier, and is given by

$$F'_{\text{mixer}} = 10 \log L + 10 \log (t_m + F'_{\text{if}} - 1) \text{ dB} \quad (2)$$

when the variables are expressed as numerical ratios.** The effective noise temperature T_1 can be found from the relationship

$$F' = 10 \log (T_1/290 + 1) \quad (3)$$

* The diameter in cm is given by $\text{DIA} = 17.6/f_c$, when f_c is in GHz. This is derived from the well-known relationship $\lambda_{c,11}/a = 3.41$, where λ_c is the cutoff wavelength and a is the radius of the waveguide.

** H. C. Torrey and C. A. Whitmer, Crystal Rectifiers, MIT Rad Lab Series, #15, p. 30

The effects of local oscillator AM noise have usually been accounted for by increasing the value of the noise temperature parameter t_m

In order to guarantee a system noise figure of 7 dB, the receiver should be capable of achieving 6.5 dB noise figures. In order to guarantee a 6.5 dB noise figure in mass-production, the mixer diode should be capable of 6.0 dB noise figures in laboratory conditions. In order to achieve such low noise figures, it is necessary that each factor in Eq. (2) be minimized. The conversion loss L depends on the various conditions of impedance match between the mixer diode, the signal impedance, the image impedance, and the IF amplifier impedance. Conversion losses in the neighborhood of 4 dB are obtainable by proper impedance matching to a good diode. IF amplifiers using field-effect transistors (FET's) can provide noise figures of 1.6 dB in mass-production, which will be adequate. The noise temperature ratio t_m depends on the conversion loss to a slight extent and the intrinsic diode temperature ratio t_d , and is essentially a function of diode choice. Good Schottky Barrier diodes exhibit t_d 's of 0.85, and good point-contact diodes such as 1N21G have t_d 's of 1.2. Using a 1.6 dB noise figure IF Amplifier and a 4 dB conversion loss for both cases, the resulting mixer noise figures are 5.33 dB and 5.97 dB, thus the Schottky Barrier diode offers better performance than the point contact diode. However, the average performance of all diodes produced by either method is worse than 6 dB, and so some kind of testing and sorting would be necessary regardless of which type is chosen. Presently the SB diode costs \$2.25 more than the point-contact diode, because production is not as completely automated as it is in the point contact operations. However, the SB diode has two other features which make it attractive for this application.*

*The following material is taken from several references

"Comparative Analysis of Point-Contact and Schottky Barrier Diodes," Robert E. Bayless, et. al, given at the Microwave Exposition, New York, N.Y., June 7, 1967, the authors are with Sylvania.

"Performance Characteristics of Philco-Ford Microwave Schottky Barrier Diodes," R. T. Wright and S. T. Smola, Microelectronics Application Report #300, July 1968

First, the SB diode is more resistant to burnout from transients than the point-contact diode, because the rectifying junction is larger and therefore the thermal energy absorbed by the junction is dissipated more quickly. The junction is larger because it is formed by depositing a metal contact directly on the semiconductor, instead of using a cat's whisker to form a pressure contact over a much smaller area. Consequently, the SB diode should be more reliable, both electrically and mechanically, and thus should reduce downtime and replacement costs.

Second, the variation of dc parameters with temperature is substantially less with SB diodes than with point contact diodes. The essential result is that the noise figure is not as severely degraded at higher operating temperatures. Sylvania reports a 0.5 dB degradation for a point-contact diode at 60°C, while an SB diode shows no degradation until 120°C. While this last point may be minor, it is a factor in assessing the overall reliability of the system. The enhanced reliability of the Schottky Barrier diode makes it more desirable for this application, and worth the extra cost.

Performance of the Balanced Mixer

A waveguide balanced mixer as shown in Fig IV-2 was constructed. Several additional waveguide accessories were needed to properly test the balanced mixer, they included two waveguide-to-coax transitions with adjustable end-plates, and several lengths of 3-inch diameter waveguide for use as spacers. The drawings are given in Appendix F. The LO signal source was coupled through a 2500 MHz bandpass filter which effectively prevents the signal energy from being absorbed by the LO source impedance. (This experimental filter is a prototype which is described in detail in the local oscillator section.) Using Philco-Ford L8200C and HPA 1N2553 Schottky Barrier diodes, a HP 616A signal generator for the LO, and a 3 dB noise figure IF amplifier, mixer noise figures better than 7 dB were consistently obtained. A 1.6 dB noise figure IF amplifier was eventually designed, and mixer noise figures of 6 dB or less were then obtained.

By the time of the tests, a breadboard transistorized local oscillator was available, and similar noise figures were observed.

Proper matching of the signal to the diode was primarily by the adjustments on the waveguide-to-coax transition, good noise figures could be obtained over a wide range of spacing of the rear wall of the mixer cavity from the diode plane. This is an important consideration for the overall layout of the mixer-feed housing. Using the transition to achieve the proper impedance match is permissible to demonstrate that the mixer works well, but it will be necessary to eventually incorporate proper matching structures into the waveguide. This problem is discussed in detail in a subsequent section.

The Single Diode Mixer

The balanced mixer was converted into a single-diode mixer and the capability of performing critical adjustments of the diode position in the waveguide was incorporated. A section view of the single diode mixer is shown in Fig IV-3. The concentric sliding diode holder was used to provide a fixed path length from the diode to the quarter-wave coaxial line, which acts as a short circuit for the local oscillator signal at 2500 MHz. The entire assembly slides in and out to adjust the impedance match of the diode to the waveguide. By fixing the path length to the short circuit, we eliminated any variations which would have required recalculation or remeasurement when the prototype was constructed. This single diode mixer exhibited noise figures less than 6.5 dB when driven by the LC oscillator-multiplier breadboard at 1 to 2 milliwatts and used with a 1.5 dB noise figure IF amplifier. Changes in the rear wall spacing were easily compensated for by moving the diode in or out of the waveguide. The support rod which is perpendicular to the diode assembly was originally a tuning screw which matched the local oscillator signal to the diode. It was experimentally determined that the mixer worked best when this screw was shorted to the diode support structure.

Some experiments were performed to determine the best position for the local oscillator probe. The probe is always oriented the same way as shown in the section view, we varied the insertion depth into the waveguide and the relative spacing of the probe from the plane of the

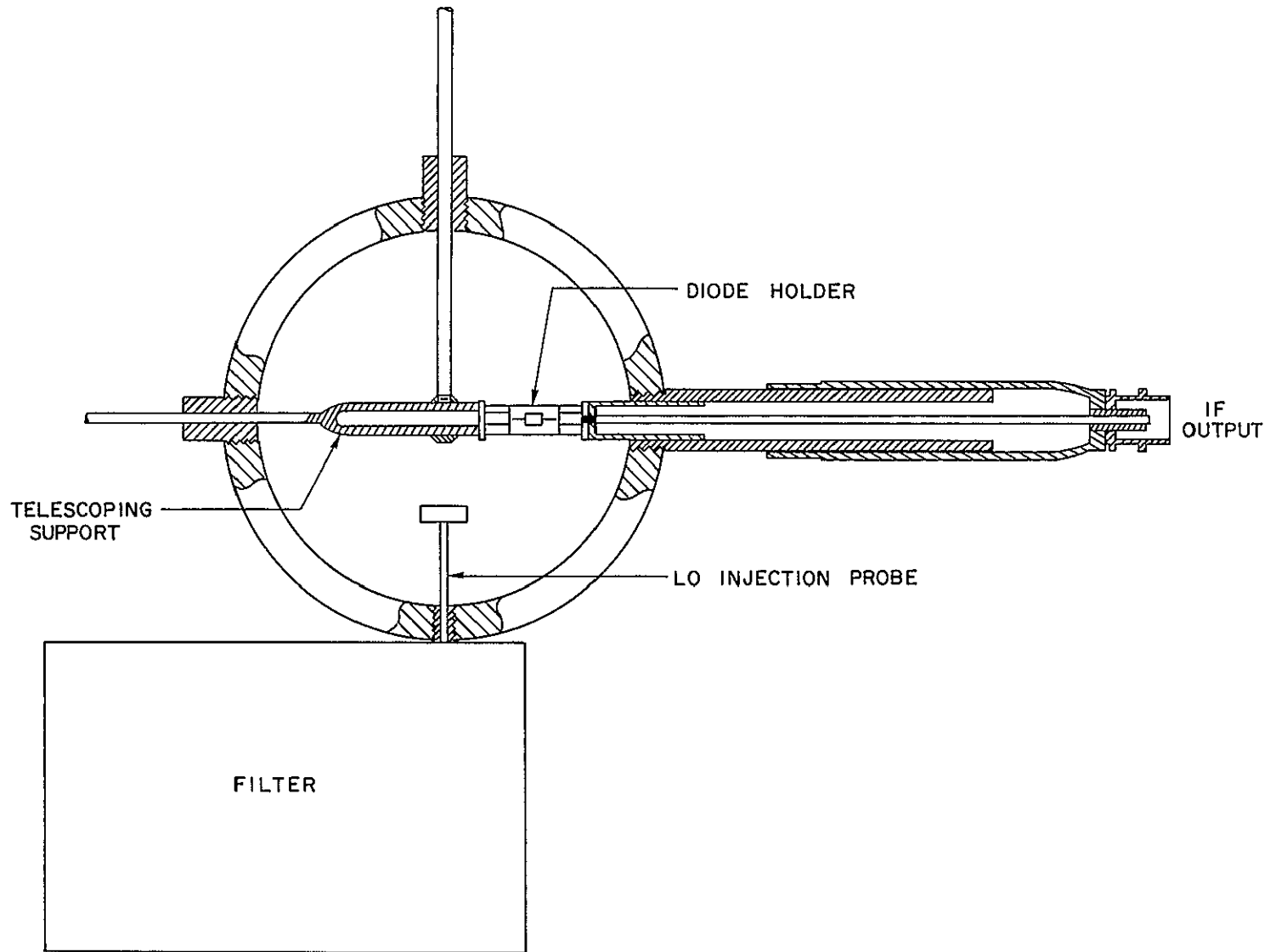


Fig IV-3 SINGLE-DIODE MIXER IN CIRCULAR WAVEGUIDE

diode structure as far as 6 cm. The best performance is obtained when the probe is in the plane of the diode support structure.

Since the noise figures obtained with the transistorized local oscillator were adequate, the single diode mixer using a Schottky Barrier diode was selected for the working model

C. Preselector Filter

For this design, image rejection is achieved by operating with a waveguide diameter which is close to cutoff at the image. Further rejection of other signals is obtained because the diode mounting structure is essentially a tuned circuit, as are any matching structures which are needed. Therefore the only serious problem is with local oscillator radiation. The amount of this radiation has not been measured, so the importance of the problem is as yet unknown. However, it is felt that some effort should be spent in reducing it, simply on the basis of reducing spectrum pollution. We may take advantage of the mixer configuration in designing a preselector filter, or a local oscillator trap, by noting that the local oscillator signal is essentially vertically polarized, there is some horizontal component from the diode mounting structure, but it should be minor. By positioning a stub in a vertical plane somewhere in the mouth of the feed, it should be possible to provide a short-circuit reflector to the local oscillator signal, while the stub will be electrically invisible to the desired signal because of their orthogonality. This method has not yet been tried, but is reserved for future work.

D. The Local Oscillator

The local oscillator (LO) must supply a reference signal stable in both frequency and amplitude with a power level of one milliwatt. This LO signal must be coupled to the mixer in a manner which does not permit any received signal power to dissipate across the source impedance of the LO. For frequencies up to 3000 MHz, there are several basic ways of generating the desired power level. It may be done directly with a microwave transistor capable of oscillating directly at 2500 MHz in a

cavity, or with a transit-time vacuum tube oscillator such as a klystron in a cavity. It may also be done indirectly, by using a lower-frequency oscillator and a frequency-multiplying technique. A step-recovery diode (SRD) may be used to generate a series of signals which are harmonically related to a fundamental driving signal. In 1968, this indirect method was the least expensive and most reliable method available for supplying the LO signal. In 1967, the parts cost of the oscillator-SRD multiplier was estimated at \$10.* In contrast, the cost estimate for single quantities of microwave transistors was in the range of \$100. The klystron-cavity oscillator is not quite as expensive, but has the disadvantage of requiring a high-voltage power supply and in general is not as reliable as a solid-state device. Consequently, it was decided at that time to pursue the design of the oscillator-SRD multiplier. This technique is useful to about 6000 MHz, for low-cost designs. Above that frequency, Gunn oscillators are preferable, depending on the stability requirements. A modulation method which significantly reduces the FM noise and stability requirements is proposed in a following section.

The cost for microwave transistors capable of adequate power generation at 2500 MHz such as the 2N5386 has dropped substantially in the past two years, and can now be obtained at prices which make its use quite competitive with the indirect methods. A brief discussion of the gross parameters of the direct transistor oscillator will therefore be discussed in addition to the details of the indirect method.

Basic Operation of the Local Oscillator Multiplier

The basic operation of the indirect method is as follows. The low-frequency transistor oscillator generates a signal at a fundamental frequency such that 2500 MHz is an integral multiple N of that fundamental.

The output of this oscillator is amplified to a sufficiently high level, such as .100- 200 watt. This signal is applied to a step-recovery diode through an appropriate impedance matching network. The

* ASCEND Study, p 3-49

step-recovery diode is a two-terminal P-I-N junction which is capable of switching from the low impedance (when forward-biased) to a high impedance (when reverse-biased). As the driving signal reverses polarity and begins to reverse-bias the diode, current flows in the reverse direction until the minority carriers are swept out, at which point the junction abruptly switches to the high-impedance state. Typical switching times are less than 1 nanosecond. Thus during the negative half cycle, a sharp pulse is produced across the diode. The spectral density of this very fast risetime pulse is rich in harmonics, and a resonant filter is used to select the desired harmonic. This filter should have a narrow passband at 2500 MHz and should behave as an open circuit elsewhere.

The major variables to be specified are the multiplication factor N , and thus the frequency of the driving source for the step-recovery diode multiplier, the type of step-recovery diode, the type of oscillator-driver, and the type of filter for the SRD output.

The important performance constraints concern frequency stability, noise from incidental FM on the LO signal, ease of fabrication and adjustment, and the relation to other subsystem requirements, such as spurious response control, harmonic rejection, and discriminator linearity. The design of the local oscillator begins with a determination of the multiplication factor N .

Multiplication Factor N

The choice of N depends on the efficiency of the SRD multiplier and the filter, the intermediate frequency of the system (120 MHz \pm 15 MHz), and the upper limit in driver frequency for easy fabrication and tune-up. A description of the alternative configurations available is needed to clarify these relationships.

The two basic oscillator types are crystal-controlled and LC (inductor-capacitor) controlled. The crystal-controlled type has several alternatives, as shown in the diagram in Fig. IV-4. The configuration in Fig. IV-4a uses the basic LC oscillator and a buffer-amplifier stage for isolation and to obtain sufficient power for the SRD. Fig. IV-4b uses a crystal oscillator and a buffer amplifier and multiplies

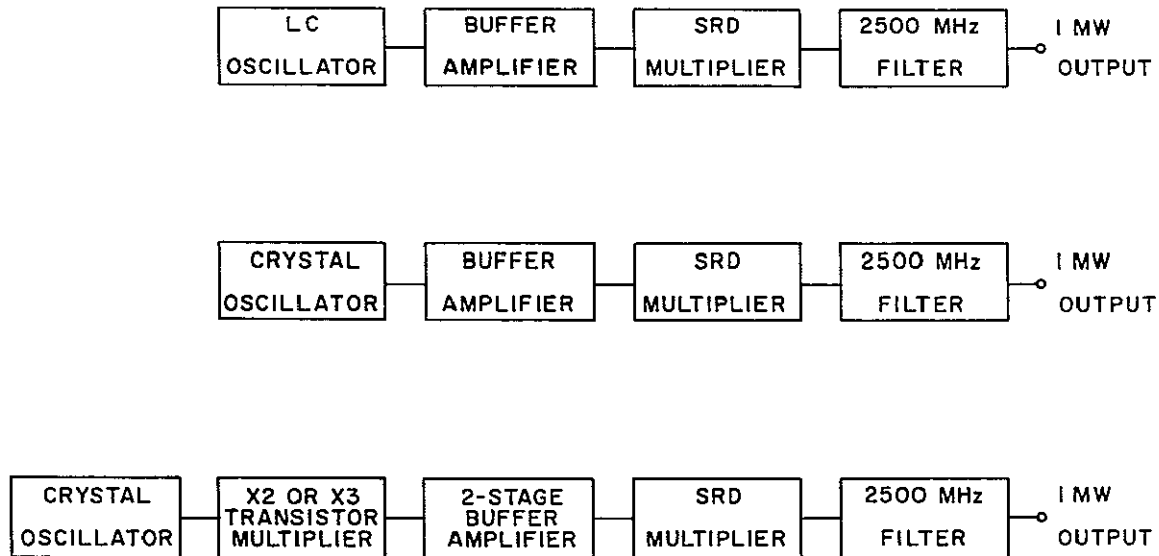


Fig IV-4 THREE LOCAL OSCILLATOR CONFIGURATIONS

the crystal frequency directly to 2500 MHz. Figure IV-4c uses a lower-frequency crystal oscillator and an intermediate transistor multiplier stage to reach the SRD driving frequency. The remainder of the circuitry for the driver-amplifier, SRD, and filter is the same as for the other cases.

The lower limit on N is determined by the highest driver frequency at which 100-200 milliwatts (mw) of power may be obtained economically and without excess tuning difficulties. The 2N3866 transistor costs \$0.80 in large quantities, is capable of 500 mw output as an oscillator to over 500 MHz, and 200 mw as an amplifier easily to 350 MHz. Beyond that frequency, tuning becomes more critical because components are becoming smaller in value and parasitic and stray inductances and capacitances become more of a problem. We thus chose 350 MHz as the upper limit on drive frequency, and the lower limit on N becomes 7.

Efficiency is inversely proportional to N , but since 100 multipliers are available, this is not the most significant parameter in finding the upper limit. The intermediate frequency is centered at 120 MHz, it is important to avoid generating high-powered signals (~1 mw) at any frequency within 25 MHz of the IF amplifier band edge, even if these high-powered signals are located in other subsystem compartments and are attenuated by 50 dB or more. This is because the desired signal

level is at -82 to -84 dBm at the IF amplifier input, and the IF amplifier and limiter will have 90 dB of gain in the bandpass. Any spurious response within ± 40 MHz of the IF center frequency with a power level greater than -50 dBm could cause limiting on that signal, and thus reduce the gain available for the desired signal. This reduction in effective sensitivity is not acceptable, and so great care must be taken to adequately attenuate spurious signals near the IF bandpass, or eliminate them completely. Thus the lower drive frequency is arbitrarily chosen at 167 MHz, and the upper limit on N is 15.

The spurious signal problem is quite severe if the lower-frequency crystal oscillator configuration of Fig. IV-4c is employed. The range of available crystal frequencies is quite limited, because none of the harmonics should fall within the IF passband for all the reasons cited previously. Thus no crystal frequency below 70 MHz is permitted, and none above 80 MHz should be allowed. Since there are likely to be incidental AM signals on the 2500 MHz local oscillator signal due to the 70-80 MHz crystal fundamental leaking through and modulating the SRD, the LO filter must have a much narrower passband to prevent these signals from reaching the mixer. These problems would be much worse if the 70-80 MHz crystal oscillator signal were to be multiplied directly to 2500 MHz, since the power level would be so much higher. However, multiplication at low power levels to a higher driver frequency is possible.

We have selected a drive frequency of 250 MHz, with $N = 10$. An LC oscillator power amplifier is quite simple to fabricate at this frequency, and an 83.333 MHz crystal oscillator (with a X3 transistor multiplier) can be substituted without redesigning the SRD circuitry if the stability of a crystal oscillator is required.

Frequency Stability and Noise

Stability requirements for the oscillator may be arbitrarily divided into two categories: long-term and short-term stability. Long-term stability refers to changes in frequency which occur over a period greater than 0.1 second.* This variation is called drift, and occurs

* There is no industry standard, and so there is a range from 0.1 to 10 seconds in which one can find both definitions applied.

because of temperature changes in components and changes due to aging. The magnitude of this drift must be limited in order to prevent the translated signal at IF from shifting out of the bandpass of the IF amplifier. A severe degradation of picture quality would occur if too much drift were permitted.

Short-term stability refers to the small changes in frequency which occur in less than 0.1 second. These variations are due primarily to thermal noise present in all components. The magnitude of these variations are of concern because they are transferred directly to the intermediate frequency via the mixer. At this point, the variations are indistinguishable from the frequency-modulated signal, and consequently behave as a noise contribution. For variations whose frequency is greater than some arbitrary value, such as 30 Hz, these variations are termed incidental FM noise. These variations are multiplied directly in the SRD multiplier and so the fundamental oscillator noise must be 1/N as great as the specified limit.

The long-term stability and noise requirements are now derived, and the capabilities of crystal and IC oscillators are examined.

The nominal IF noise bandwidth is 31.5 MHz, the 3-dB bandwidth is 30 MHz, and the signal bandwidth by Carson's rule is 25.2 MHz. Time and temperature variations will result in a bandwidth shift of at most 0.5 MHz. The 3-dB bandwidth is larger than the signal bandwidth because the phase linearity of the IF filter begins to degrade rapidly at the band edges, in order to avoid distortion, the signal must not approach closer than 1 MHz from the band edges. Also, the discriminator is optimized for best linearity at 120 MHz, and deviations will affect the linearity. We shall therefore specify the long-term stability at ± 1 MHz. The fractional long-term stability (or fractional frequency variation) is given by

$$S_{lt} = \frac{\Delta f}{f_o} \triangleq \frac{10}{f_o} \times 10^{-4} \quad (4)$$

where f_o is in Gigahertz. This expression is graphed in Fig. IV-5. At 2.5 GHz, the required stability is 4×10^{-4} .

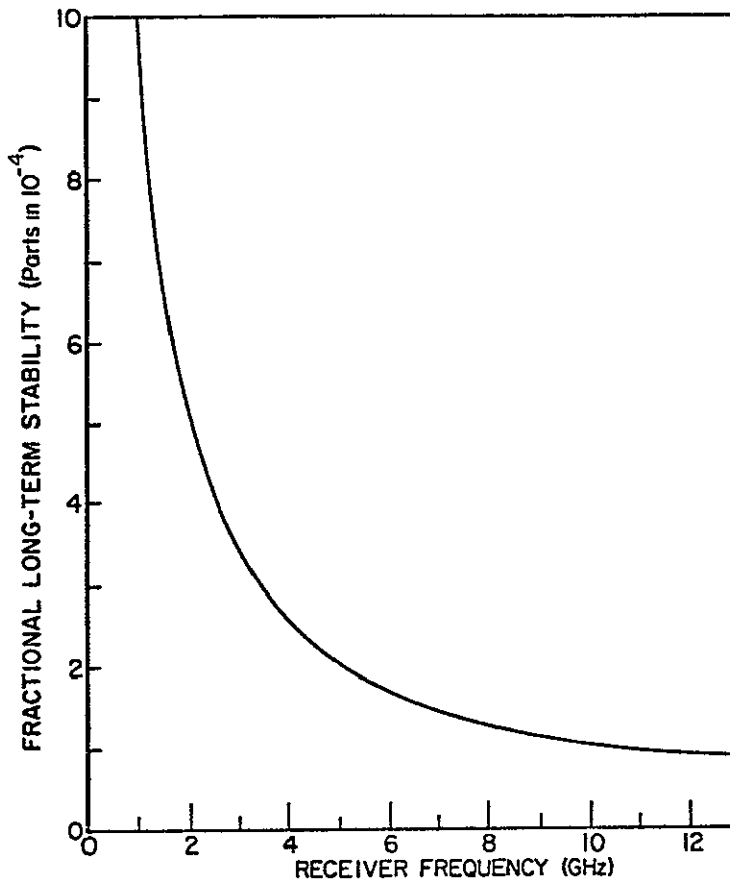


Fig IV-5 FRACTIONAL LONG-TERM STABILITY VS FREQUENCY.

The short-term stability of an oscillator may be specified by a quantity called the deviation density γ . It is defined as the root-mean square frequency deviation of an FM signal measured in a given bandwidth.* It is expressed as

$$\gamma = \frac{\Delta f_{\text{rms}}}{\sqrt{bw}} \text{ Hz}/\sqrt{\text{Hz}} \quad (5)$$

* This deviation density is essentially the square root of the power spectral density, and thus the units are derived from the units of watts/Hertz. The square root is commonly expressed as volts/ $\sqrt{\text{Hz}}$. The use of volts/ $\sqrt{\text{Hz}}$ would require a conversion factor which depends on the equipment used to measure the deviation density. This equipment calibration factor can be suppressed by simply defining the density in terms of the deviation which produces the voltage.

The relative noise contribution of the local oscillator can be assessed by comparing the square of its deviation density to that of the information-bearing signal density. This can be seen by considering the discriminator function. The ideal discriminator has a linear frequency-to-voltage transfer characteristic. The discriminator thus recovers the amplitude variations from the frequency variations in the desired signal. The amplitude of the recovered AM signal is proportional to the deviation of the FM signal. Thus the amplitude of a noise-like signal relative to the desired signal can be determined by comparing the deviation densities. This density is not constant, but depends on the baseband modulating frequencies.

Deviation densities can be measured with a discriminator (with a known transfer function) and a tunable narrowband filter which can tune across the modulating frequencies of interest.

The deviation density of a television video signal is a complex function of the video signals in the baseband range of 30 Hz to 4.2 MHz. We shall make some simplifying assumptions about the spectra which shall introduce some error but will not be serious enough to affect the overall result. The assumptions are that the baseband spectrum of the television video signal is uniform in amplitude, and that there is a frequency component at every one-Hertz interval in the range from 30 Hz to 4.2 MHz. Thus the modulating signal is a set of uniform-amplitude sinusoids. The rms frequency deviation for the wideband FM signal produced by this AM spectrum is simply the rms value of the peak deviation. Thus

$$\begin{aligned}
 \Delta f_{\text{rms}} &= 0.707 (\beta) (f_m) \\
 &= 0.707 (2) (4.2 \text{ MHz}) \\
 &= 5.95 \times 10^6
 \end{aligned}
 \tag{6}$$

Since we have assumed a frequency component at every one-Hertz interval in the baseband, the signal deviation density is given by

$$\begin{aligned} \gamma_s &= \frac{5.95 \times 10^6}{\sqrt{4.2 \times 10^6}} \\ &= 2.91 \times 10^3 \text{ Hz}/\sqrt{\text{Hz}} \end{aligned} \quad (7)$$

The rms signal-to-noise ratio specified for this adaptor is 41.00 dB. In order that this SNR is not degraded by more than 0.5 dB, the noise density from the local oscillator must be at least 10 dB lower than the ambient thermal quadrature noise from the front end. Thus

$$\text{SNR}_{\text{fm noise}} = 10 \log \frac{\gamma_s^2}{\gamma_N^2} \geq 51 \text{ dB} \quad (8)$$

Thus the deviation density of the local oscillator must be less than

$$\gamma_N \leq 8.2 \text{ Hz}/\sqrt{\text{Hz}} \quad (9)$$

at every frequency in the video spectrum of the baseband television signal.

Stability Properties of LC and Crystal Oscillators

The basic oscillator circuit is shown in Fig. IV-6. A crystal controlled oscillator employs a thin slice of quartz in the feedback path $I(\omega)$, while an inductor-capacitor (LC) oscillator uses some combination of L's and C's to achieve the 180° phase shift needed to produce the total 360° and cause oscillation. The crystal is cut in such a way that it is mechanically resonant in a fundamental mode for frequencies up to 20 MHz.

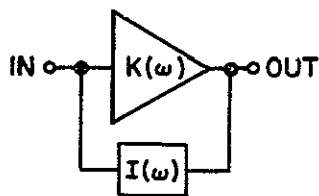


Fig. IV-6 BASIC OSCILLATOR CIRCUIT.

Quartz crystals are used extensively because the crystal can have a very low thermal coefficient of expansion, depending on how the crystal is cut, they do not exhibit much long-term drift, when compared to the present requirement of $\pm 4 \times 10^{-4}$. Stabilities of less than $\pm 1 \times 10^{-5}$ over a 10 to 50°C range are easily obtained. Because the vibrational and mechanical losses are very low, the resonant frequency is very well-defined and the quartz resonator has a high Q. This and other factors make it possible for a crystal oscillator to provide very good short-term stabilities and very low incidental FM noise.

Much larger frequency variations are exhibited by LC oscillators because of the larger temperature coefficients for metal inductors and some capacitors. Over the 10 to 50°C range, a fractional stability of $\pm 5 \times 10^{-3}$ could be expected. A fine tuning adjustment is not appropriate because of the location of the electronics package. Thus some form of compensation is necessary. The reduction of variation is less than an order of magnitude, and so satisfactory compensation should be straightforward for LC oscillators, possibly by using capacitors with negative temperature coefficients. The possibility of using voltage-variable capacitor (reverse-biased diode) is also attractive because of the potential for providing a multi-channel capability by tuning the local oscillator.

The short-term or incidental noise properties of LC oscillators are generally much worse than crystal oscillators. We are interested in the magnitude of variations which occur at 30 Hz and more, since this is the lower limit of the video television signal at baseband. A graph of incidental FM noise density for LC and crystal oscillators is shown in Fig. IV-7. This graph shows a range of FM noise and is based on a sampling of commercial microwave sources at 2.5 GHz.* At a modulation frequency of 30 Hz, the LC oscillator noise exceeds the $8.2 \text{ Hz}/\sqrt{\text{Hz}}$ limit, and the crystal oscillator noise is much less than the limit. On the

*The curves are drawn to show the range of available noise densities as given in the published specifications of Applied Technology, Inc., California Microwave, and Frequency Systems, Inc. Our own measurements of a 190 MHz LC oscillator gives comparable results.

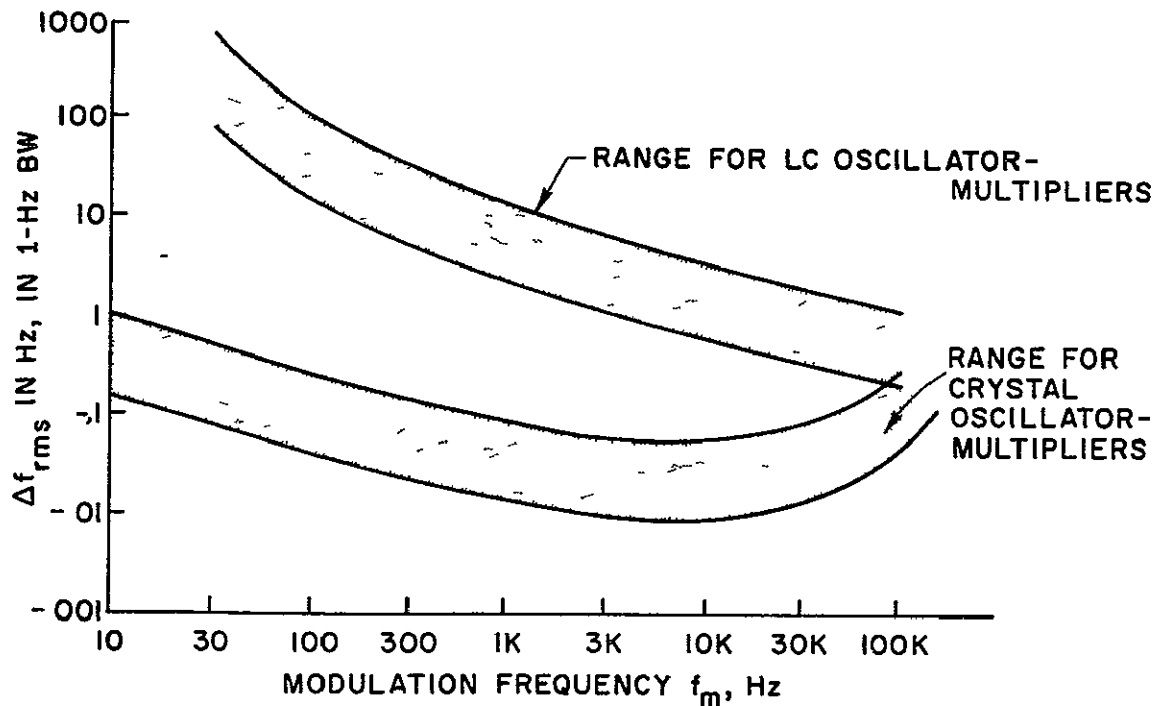


Fig. IV-7 FM NOISE DENSITY VS APPARENT MODULATION FREQUENCY FOR VARIOUS OSCILLATORS

basis of stability and noise, the crystal oscillator is superior. However, there are a number of other factors which had to be taken into account before a decision was made.

It is neither necessary nor desirable to have the baseband video television signal occupy the same precise spectral location (30 Hz to 4.2 MHz) in the adaptor system as it does where it is generated, or where it will eventually be used. It is not necessary since this baseband signal will be translated to a particular channel (2-5) in order to guarantee that no modification need be made to any television set with which it is used. It is not being used in any way at baseband in the adaptor. It is undesirable to have to demodulate an FM signal with modulation components as low as 30 Hz, since the slight nonlinearity in the discriminator will produce intermodulation distortion products at these low frequencies and degrade the signal quality by affecting the synchronization and other low-frequency components. If the composite video signal generated by the television camera and equipment were shifted up the spectrum 10 to 100 KHz, these intermodulation problems

could be minimized to a great extent. Many of the intermodulation products would now fall into this guard band. A maximum increase of 1.2 MHz in FM bandwidth would result, since the highest modulating frequency at the central transmitter would be 4.3 MHz. Further study and measurements would be needed to determine the best guard band size. But by incorporating such a guardband, the FM noise from LC oscillators is no longer a problem, and the choice of oscillator type must be determined by the remaining factors of circuit complexity and spurious signal generation.

Circuit Complexity

Block diagrams of the LC and crystal circuits needed to generate 100 mw in the range of 160 to 350 MHz are shown in Fig IV-4. The LC oscillator can be made to operate at exactly the fundamental frequency desired. This provides an important advantage over the crystal oscillator, in that it (1) reduces circuit complexity, and (2) gives a good measure of control over spurious signal generation, since the fundamental can operate anywhere in this 167-350 MHz range. The LC oscillator can generate 10 milliwatts of output power and maintain adequate noise performance. Consequently only one additional amplifier stage is needed to provide the 100 milliwatt power level for the SRD multiplier. One stage is desirable to serve as a buffer and to provide some isolation of the frequency-determining stage from load variations further along the signal path.

In contrast, the crystal itself is limited in fundamental operating frequency to 20 MHz. Odd-order harmonic mode operation is possible to the 11th harmonic, but circuit adjustments are somewhat more critical as the order increases. Fifth-order crystals are commonly used to 100 MHz, and 7th order crystals are only slightly more expensive. From a circuit complexity standpoint, a 167 MHz crystal and a power amplifier driving a X15 SRD multiplier would be the best choice for a crystal oscillator. However, at the beginning of this study, 7th order crystals were thought to be special order products, expensive and not available on a mass-production basis. Croven Ltd of Canada has recently quoted us a \$1.50 price for a 10,000/month

delivery rate for a year (this is the way we have estimated all component costs) for crystals in the 145-170 MHz range. U. S. manufacturers have quoted \$1.00 for 5th overtone crystals up to 100 MHz. Use of the latter crystals would necessitate a X2 or X3 transistor multiplier, followed by a 2-stage power amplifier to obtain the desired 100 mw.

Thus the IC oscillator has a reasonable advantage in terms of circuit complexity over 5th harmonic crystal oscillators, and if the guardband is used in the baseband spectrum, it would be the logical choice. This was the original conclusion, and is also the final recommendation. However, a crystal oscillator-SRD multiplier was built in order to make a more accurate comparison of the relative importance of each of the three performance factors of stability, noise, circuit complexity and ease of adjustment. The crystal oscillator design went through numerous iterations before satisfactory performance was achieved, and the significant result is that circuit complexity, control of spurious responses, and ease of adjustment are the most important performance constraints in the design of a mass-producible microwave adaptor. If the guardband cannot be employed and an IC oscillator cannot be used, the design for a crystal oscillator is available. But before any large scale production of adaptors is begun, the possibility of using a 167 MHz-X5 multiplier should be investigated.

Delay Line Oscillator

The possibility of using a two-stage delay line oscillator was also extensively investigated. The feedback path is simply a length of transmission line and the oscillation frequency is the inverse of the loop propagation delay time. The object of the investigation was to determine if it was possible to fabricate an oscillator which would require no tuning whatsoever. The initial estimates of receiver frequency stability and allowable frequency drift were somewhat less restrictive early in the study, and the initial results of the investigation were quite encouraging. However, the problem of temperature compensation still remained, and two transistors were needed for the oscillator circuitry, exclusive of any buffering stage. As the stability requirements were tightened and crystal oscillator work was begun, this oscillator

was set aside. In view of the possibility of providing multiple channels by tuning the local oscillator, the single-transistor oscillator is more desirable at the present time. The details of the delay line oscillator analysis are given in Appendix D

LC Oscillator Design

The design of an LC oscillator involves a mixture of analysis and experimentation, especially at 250 MHz, because stray capacities and component lead inductances increase the model complexity. The best solution is to eliminate strays as much as possible by making a good layout in which leads are as short as possible and capacitive effects are minimized

Of the 24 variations available for LC oscillators, we have selected the one in Fig IV-8, because the capacitors C_1 and C_2 complement the device capacities, and C_2 could easily be replaced by a voltage-variable tuning capacitor (isolated from the collector by a large-valued coupling capacitor) A tee-network (the dual of this pi-network) was also extensively investigated and was used in the 2 62 GHz wideband FM test generator, the circuit diagram is given in Appendix G If we neglect the feedback parameter y_{12} of the device, the model for this pi-network oscillator circuit is as shown in Fig. IV-9

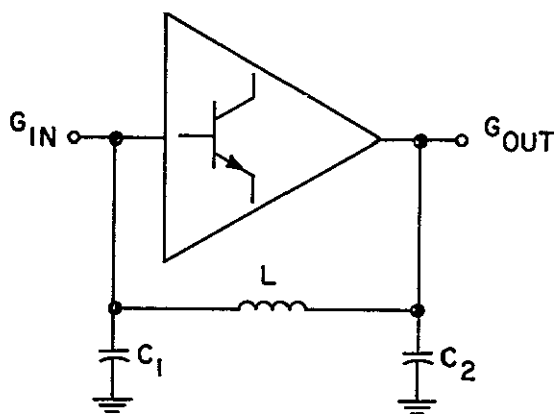


Fig. IV-8. TYPICAL LC OSCILLATOR.

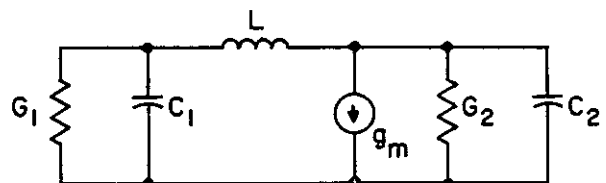


Fig IV-9. EQUIVALENT CIRCUIT OF LC OSCILLATOR

The various circuit elements are grouped as follows

- C_1 is the sum of the input capacity and any tuning capacity
- G_1 is the sum of the input admittance and the bias network admittance
- L is the feedback inductor
- g_m is the forward current gain
- G_2 is the sum of the output admittance and the load admittance
- C_2 is the output capacity and any tuning capacity

Setting the determinant for this network equal to zero and simplifying the result, we have

$$s^3 LC_1 C_2 + s^2 L(C_1 G_2 + C_2 G_1) + s(LG_1 G_2 + C_1 + C_2) + G_1 + G_2 + g_m = 0 \quad (10)$$

Equating imaginary (odd-order) terms to zero, the frequency of oscillation is

$$\omega = \left(\frac{LG_1 G_2 + C_1 + C_2}{LC_1 C_2} \right)^{1/2} \quad (11)$$

For the magnitude of the parameters involved, the effects of circuit damping can be ignored and the oscillation frequency is essentially given by

$$\omega = \left(\frac{C_1 + C_2}{LC_1 C_2} \right)^{1/2} \quad (12)$$

Substituting this value into Eq. (10), we find the condition for oscillation

$$g_m \geq \frac{C_1}{C_2} \left[G_2 + \frac{G_1}{(C_1/C_2)^2} \right] \quad (13)$$

This is the minimum g_m for which oscillation will commence, conversely, there is a specific relationship between the capacities and the admittances which requires the least g_m for oscillation, it is given by

$$\frac{C_1}{C_2} = \left(\frac{G_1}{G_2} \right)^{1/2} \quad (14)$$

The ratio $(C_1 + C_2)/L$ should be as large as possible to minimize the effects of transistor parameter variations, after incorporating the effect of Eq (14), the resonant frequency is given by

$$\omega = \left[\frac{1}{LC_2} \cdot \frac{\sqrt{G_1} + \sqrt{G_2}}{\sqrt{G_1}} \right]^{1/2} \quad (15)$$

and C_2 and L may be determined to suit the $(C_1 + C_2)/L$ ratio requirement.

The type of transistor used depends on the power required and the oscillation frequency, for 10 mw power levels, the Brazilian PE3002 and the 2N3563 are adequate and inexpensive For a 100 mw level, a 2N3866 or its lower voltage equivalent, the 2N4427 should be used

A 250 MHz power oscillator was constructed with a 2N3866 as a breadboard, a photograph of it is shown in the next section in Fig IV-14 Satisfactory operation was achieved, but the SRD matching circuitry naturally affected the oscillation frequency Therefore a lower powered oscillator with a buffer amplifier should be used. 15 volts has been chosen as the power supply voltage, and so the buffer transistor should be a 2N4427 A typical circuit diagram for the LC oscillator is shown in Fig IV-10

Crystal Oscillator Design

The important parameters in overtone oscillator design are crystal drive level and circuit arrangement One of the simplest ways to convert an LC oscillator into a crystal-controlled oscillator is to

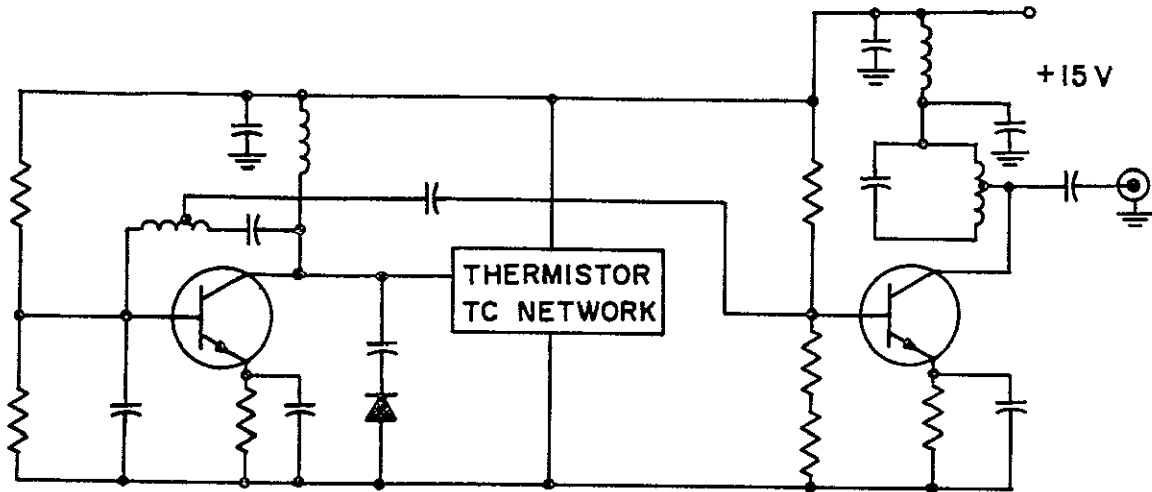


Fig. IV-10. TYPICAL LC OSCILLATOR CIRCUIT.

add the crystal in series with the LC feedback network. The crystal behaves as series resonant circuit, slightly inductive. This has been done for the low-power oscillator as shown in the complete local oscillator schematic in Fig. IV-11. Viewing the emitter as the reference point, an LC pi-network connects the collector to the base, through chassis ground and back through the crystal. In this way, the drive level to the crystal can be controlled. This is important for noise and stability.

Multiplier and Buffer Amplifiers

The multiplier transistor is biased as an amplifier with a collector tank circuit which is tuned to the third harmonic of the driving signal. For more efficient con multiplier conversion gain, an "idler" circuit at $2f_{in}$ could be connected from the base to ground. The present conversion gain is about 4 dB, with the idler, it could increase by 3 dB or more. Before such a change is made, the crystal oscillator should be buffered with another stage of amplification. Thus in the present local oscillator schematic, the multiplier should become the buffer and the AMP 1 stage should become the multiplier.

The amplifier design is reasonably straightforward, since these are narrowband tuned amplifier stages. Proper care must be taken in impedance matching, power supply decoupling, and circuit layout to prevent oscillations.

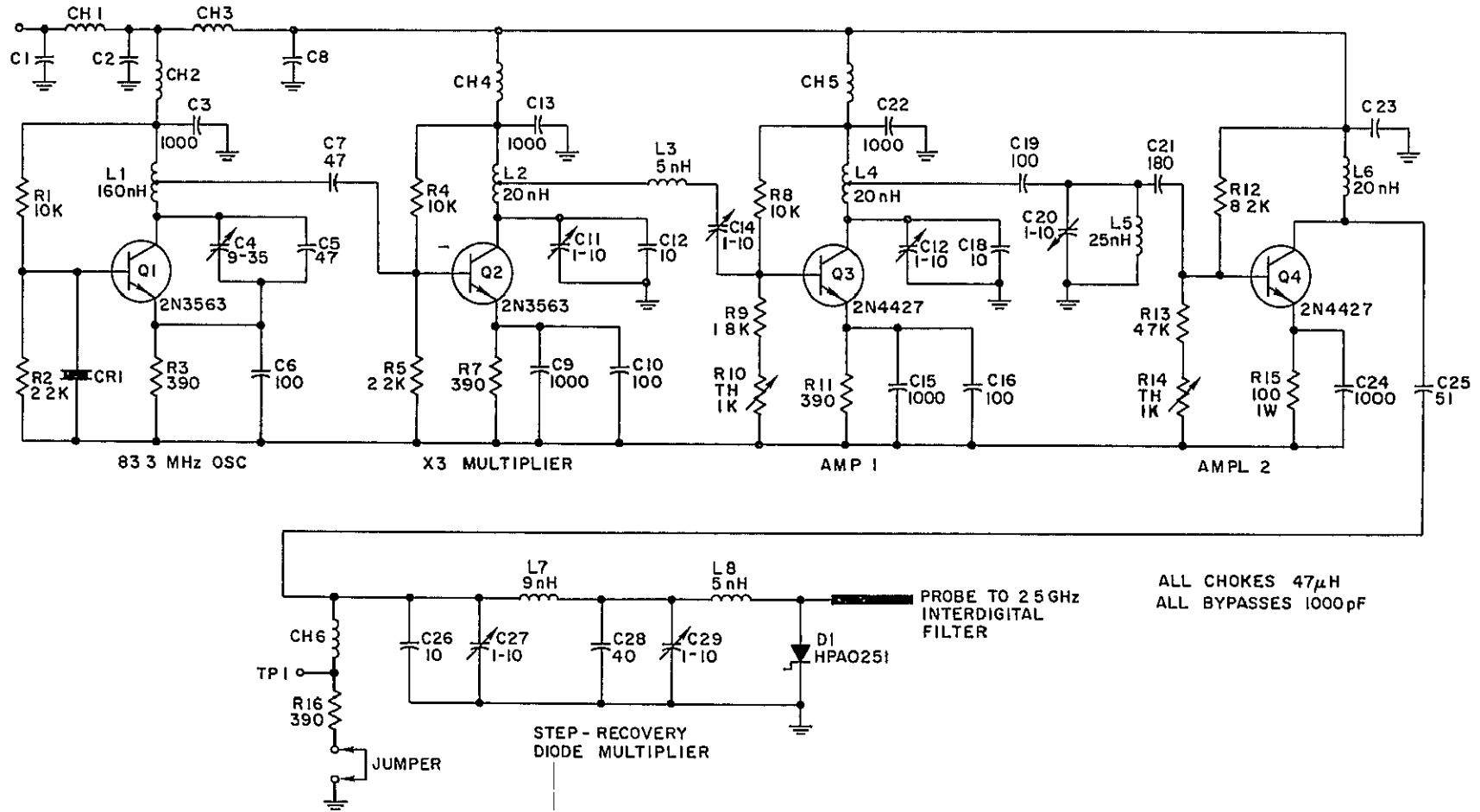


Fig IV-11 COMPLETE LOCAL OSCILLATOR CIRCUITRY

Microwave Transistor Oscillator

The design of the microwave transistor oscillator can be approached in a fashion similar to that of the lower frequency IC oscillator, since the principles are the same. However, another approach can be used, because of the difficulty in determining the exact values of the parameters in the model in Fig. IV-9. Essentially, one must construct a feedback circuit (if the device is not already potentially unstable) which renders a negative output impedance in the frequency range of interest. This condition can be conveniently checked with an S-parameter measurement system. Then one must supply a conjugate reactance to tune out the reactive component of the output impedance at the desired frequency of oscillation. The load admittance must not be larger than the absolute value of the output admittance in order to sustain oscillations. The problem of temperature compensation appears to be somewhat more difficult at the microwave frequency because of the small size of component parameters, and the small variations needed for compensation.

The Step Recovery Diode Multiplier

The SRD multiplier design is reasonably straightforward and one can proceed using the methods outlined in the Hewlett-Packard Application Note 920. The circuit diagram appears in Fig. IV-12.

The choice of multiplication factor N was initially made arbitrarily at $N = 10$, and thus the fundamental drive frequency for the SRD is 250 MHz. This choice gives a reasonable compromise between

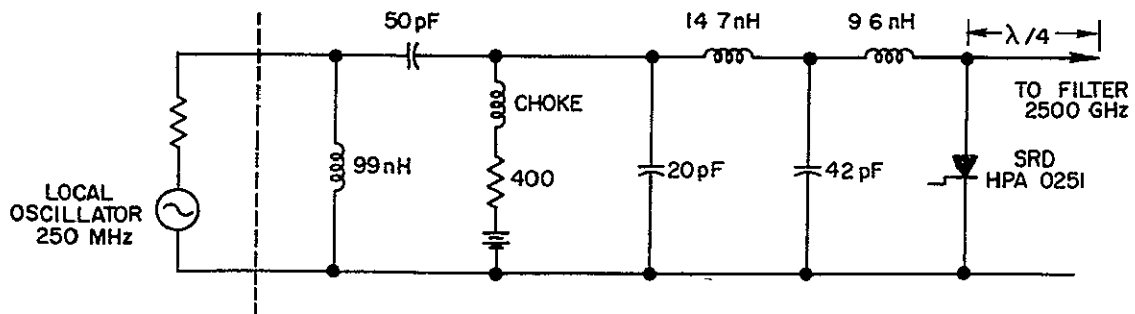


Fig. IV-12. STEP-RECOVERY DIODE MULTIPLIER CIRCUIT.

drive oscillator circuitry and SRD multiplication efficiency. All experimental work has been done with the HPA 0251 diode which comes in a top-hat package. The output power level required is 1-2 mw at 2500 MHz. However, a summary of the calculations of the circuit parameters given in Table IV-II indicates that almost any diode will work in this application, and so the least expensive one, the HPA 0112, should be used. The only critical circuit element is the resonating capacitor C_T . This capacitor must be of good quality in order to pass energy at 2500 MHz effectively. A dipped mica or group of micas should be adequate. Experience has shown that the diode must be driven with at least 50 mw in order to obtain good sharp transition pulses, allowing a safety margin for aging and for simplification of tune-up, we specify a 100 mw minimum drive level.

An experimental multiplier was built, using the HPA 0251 diode, an interdigital filter, and a 250 MHz LC oscillator. A photograph of this LO appears in the following section on the filter in Fig IV-14. A clean, stable signal of up to 3 mw can be obtained with little difficulty in tune-up, once the correct range of component value is installed. Obtaining a correct impedance match, correct resonance for the pulse forming network, and correct filter impedance will require three adjustments, and although they are iterative, they are not critical.

The Local Oscillator Filter

The local oscillator filter serves three functions

- (1) It acts as a resonant circuit at 2500 MHz and thus concentrates the energy of the SRD pulse at the 10th harmonic,
- (2) It acts as an open circuit outside of the passband, and thus prevents signal power in the mixer from being dissipated in the output impedance of the SRD,
- (3) It attenuates the other harmonics and any other spurious signals which may be present in the local oscillator

Table IV-II

STEP-RECOVERY DIODE MULTIPLIER CIRCUIT PARAMETERS

<u>Diode Type (HPA)</u>	<u>0112</u>	<u>0151</u>	<u>0251</u>
Reverse Bias Capacity C_{VR} , pf	1 7	0.85	0.95
Transition Time $t_t \leq \frac{1}{f_o} = 400$ psec	175	90	100
Lifetime $\tau \gg \frac{1}{2\pi f_{IN}} = 636$ nsec	50	20	20
Pulsewidth $t_p = 300$ psec [200 psec < t_p < 400 psec]			
Driving Inductance $L_{(max)} \cong \left(\frac{t_p}{\pi}\right)^2 \frac{1}{C_{VR}}$ nh	5 4	10.7	9.6
Resonating Capacitor $C_T \cong \frac{C_{VR}}{(2f_{IN} t_p)^2}$ pf	75	38	42
Input Resistance R_{IN} to Pulse-Forming Forming Network $R_{IN} = \omega_{IN} L \Omega$	8.5	16 8	15.1
Matching Network $L_M, C_M, R_S = 50 \Omega$			
$L_M = \frac{\sqrt{R_S R_{IN}} - R_{IN}^2}{\omega_{IN}}$ nh	12	15	14
$C_M = \frac{Q^2}{(1 + Q^2)\omega_{IN}^2} \frac{1}{L_M}$ pf, $Q = \omega_{IN} L_M / R_{IN}$	28	18	19
z_o of Resonant Filter			
$z_o > \sqrt{L/C_{VR}}$ Ω	56.5	112	100
High Pass Network			
$L_{HP} = 95$ nh			
$C_{HP} = 35$ pf			

The important constraints on the filter concern the allowable insertion loss, the desired stop band attenuation, the ease of fabrication and adjustment, and its size. Development of these constraints and evaluation of various alternatives leads to a specification of the filter type, the number of poles, the bandwidth, the surge impedance, and various methods for fabricating the filter.

The in-band insertion loss should be as low as possible, a 1-dB maximum specification is a reasonable design goal for a mass-producible adaptor. The stopband attenuation should be at least 50 dB for the nearest harmonic or spurious signal and 30 dB at the microwave signal frequency of 2620 MHz. The 30 dB attenuation means that less than 0.1% of the signal power could be dissipated in the local oscillator source impedance, and this should be adequate. The 50 dB attenuation of adjacent harmonics is necessary because they act as interfering signals to the desired signal. They are translated to IF just like the desired signal. They are at a much higher power level than the desired signal, and could drive the IF amplifier into saturation, in spite of their being outside the passband of the IF filter. (The gain of the IF amplifier is not zero for a large portion of the spectrum.) The bandwidth of the local oscillator filter is thus related to the fundamental drive frequency for the SRD multiplier and to the choice of oscillator--either crystal or LC.

If a crystal oscillator in the range of 70-80 MHz is used, then the passband should be narrower in order to guarantee the required rejection. This is necessary even if the X2 or X3 transistor multiplier is used, because there will be appreciable feedthrough of the fundamental (and second harmonic) of the crystal in addition to the 9th and 11th harmonic of the high-powered 250 MHz signal.

To achieve the required rejection with a minimum number of poles, the filter bandwidth must be narrow, but in order to obtain a reasonably low insertion loss at narrow bandwidth, the resonator Q must be very high.* This could require polished filter elements and

*The resonator Q is given by $Q = q_{\min} (f_o/f_3 \text{ dB})$

critical adjustments, which is not desirable for a mass-production design. Thus some compromise must be made.

A Chebyshev filter response will be assumed, because this response has the fastest rate of attenuation with frequency in the stopband. A two-pole 1 dB ripple Chebyshev filter would require a 3-dB bandwidth of 23.6 MHz, which is too narrow to achieve without great care, the minimum resonator Q is 250. A three-pole 1 dB ripple Chebyshev filter with 30 dB stopband attenuation at the lowest frequency of the FM signal (2607.5 MHz) has a 3-dB bandwidth of 97 MHz.* The minimum resonator Q is 112.5, which is much easier to obtain. The attenuation at the 9th and 11th harmonics (2250 and 2750 MHz) is slightly over 50 dB. Thus we are trading potentially higher manufacturing costs for another pole and therefore an additional adjustment, but it will be shown subsequently that only one of the adjustments (of three) is actually needed for alignment of this filter.

Types of Filters

At 2500 MHz, there are three different ways of realizing a filter: coupled waveguide cavities, stripline resonators, and interdigital resonators. The waveguide filter is rejected because of its size and the fact that it is not as convenient to couple the signal in and out of it as it is with the interdigital filter. Stripline filters are feasible, if the entire local oscillator is built on a high-quality dielectric,** but the high cost of dielectric material has eliminated this choice (see Mixer section). Interdigital filters are very attractive because of their comparatively small size, and the large selection of coupling methods which can be employed with them, since propagation is TEM. An interdigital filter consists of a series of resonant rods ($\approx \lambda/4$ in length at band center)-spaced between ground planes like fingers, as shown in Fig IV-13. The rods are alternately grounded on either side of the cavity.

* These figures are taken from the attenuation tables on p. 193 and 194 of the Reference Data for Radio Engineers Handbook.

** Several stripline filters were built to find out more about insertion loss, adjustment difficulties, and general performance. See Quarterly Report #3.

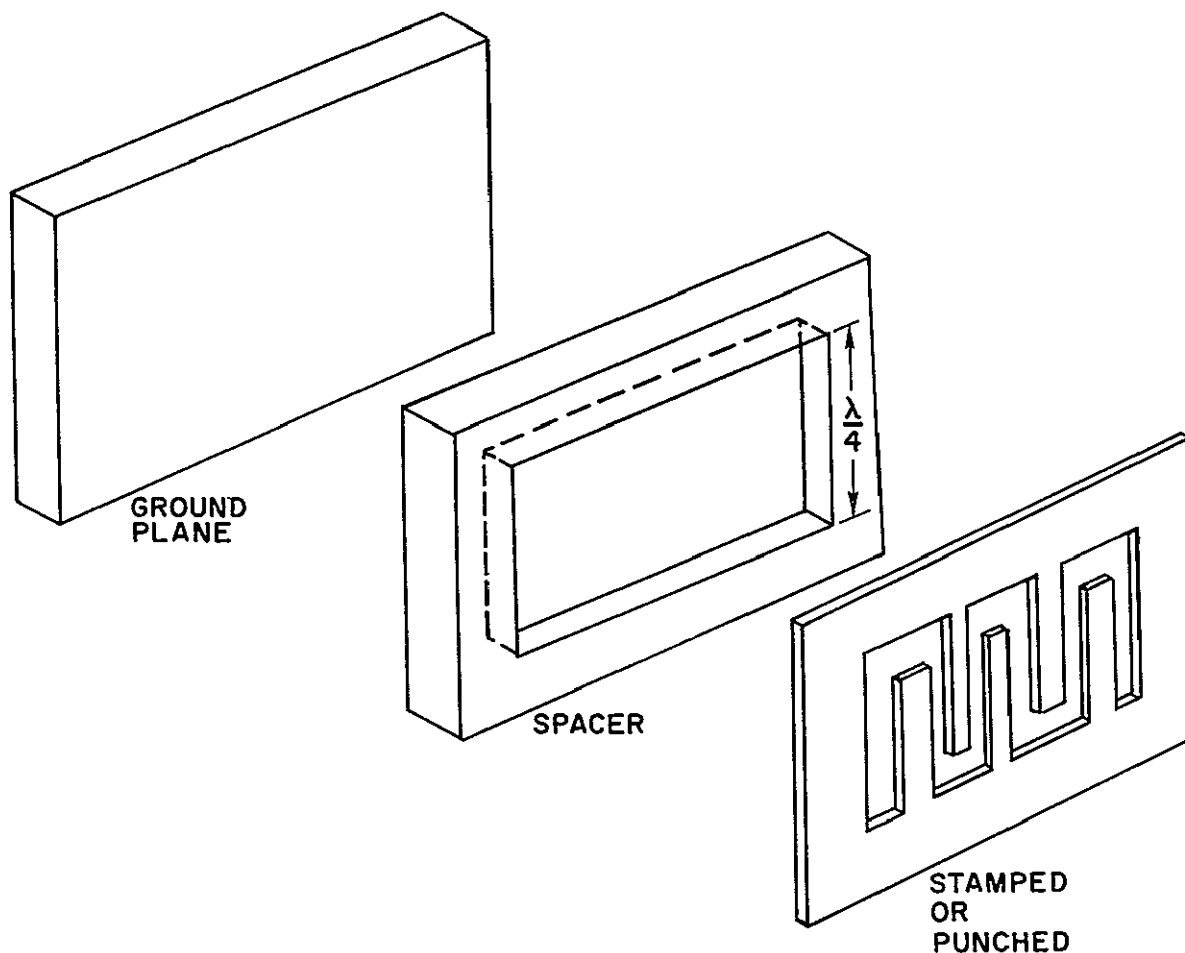


Fig IV-13. INTERDIGITAL FILTER STRUCTURE REALIZED BY A SANDWICH CONSTRUCTION TECHNIQUE. (Mating spacer and ground plane not shown)

The design of this filter depends on a determination of the appropriate self- and mutual capacities, as specified from the desired low-pass equivalent prototype response Getsinger* has derived curves for the capacities of rectangular rods, and Pyle** has used Getsinger's results to generate curves which specify the rod width and spacing directly as a function of percent bandwidth One may use round rods

* William J Getsinger, "Coupled Rectangular Bars Between Parallel Plates," MTT-10, January 1962, p 65-72

** John R. Pyle, "Design Curves for Interdigital Band-Pass Filters," MTT-12, September 1964, p 559-566

(variable diameter) as well, and design charts are available, but there is no real difference between the two types, and no clear advantage to one or the other. Pyle's charts are for a rod thickness-to-ground plane spacing ratio of 0.2, and a rod thickness of 0.0625 inch, but the given dimensions may be scaled for any desired rod thickness. The choice of rod thickness is a key parameter in determining the sensitivity of the filter response to variations in dimensions. Sensitivity is of primary concern for two reasons. The first concerns manufacturability and the second concerns alignment.

Sensitivity

The filter should be easy to manufacture and should need little or no attention for alignment, its realization should therefore not require any precision machining or skilled labor. The techniques available are stamping and die-casting. The tolerances commonly observed with these processes are ± 0.005 inch nominal and ± 0.002 inch at best. The latter tolerance often does require machining. The most significant change in response occurs when the length of the rod changes.* A first-order sensitivity analysis and experimental verification indicate that the effects of such dimensional variations can be reduced to an acceptable level. This is possible because the tolerance is ± 0.005 inch regardless of the overall dimensions involved, so the percent variation decreases with increasing size. We thus make the rods sufficiently large to obtain a sufficiently small variation in the filter response. The result is that once the proper length has been determined, only one of the rods needs to be tuned to obtain the desired impedance level for correct operation of the step-recovery diode. If the input impedance were not a significant parameter, then no adjustment would be needed to obtain a satisfactory response. A very brief synopsis of the most important sensitivity calculation is given, along with the results of the experimental testing.

* The changes in finger width and spacing cause changes in the bandwidth. Worst-case sensitivity calculations indicate that the bandwidth change is about 10%, or 10 MHz, if all fingers were oversize by 0.004 inch. This is not serious. Changes due to variations in ground-plane spacing are even more negligible.

The diagram in Fig. IV-14 shows a cutaway view of one of the rods. The end capacity consists of a parallel-plate capacity C_p and

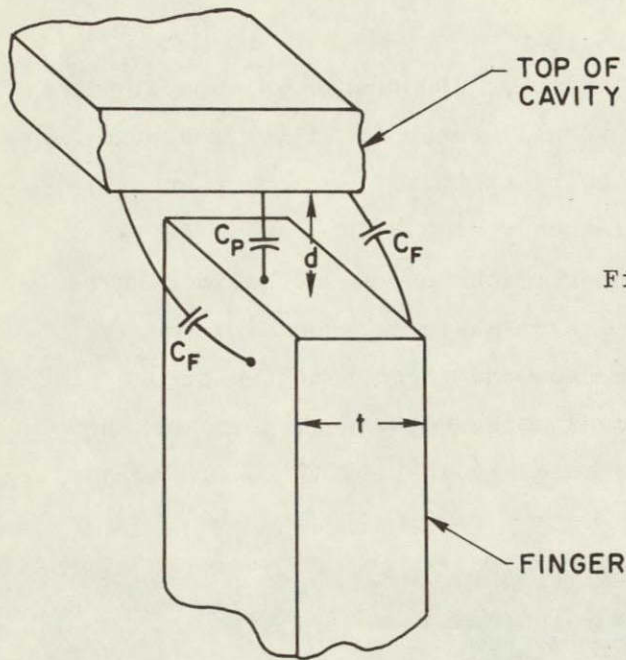


Fig. IV-14. CUTAWAY VIEW OF A FILTER ROD WITH CAPACITIES.

a fringing capacity C_f . The total capacity C_t is a constant for a particular center frequency and bandpass response. If a thicker rod is used, the spacing d must be increased in order to compensate for the larger area, which would have provided too much capacity if the old spacing were maintained. This will decrease the change in capacity caused by a small change in the spacing; to show this, consider the following:

$$C_p = \epsilon \frac{A}{d} \quad (16)$$

The partial derivative of C_p with respect to the spacing d is

$$\frac{\partial C_p}{\partial d} = -\epsilon \frac{A}{d^2} = -\frac{C_p}{d} \quad (17)$$

The total change in capacity ΔC_p is

$$\Delta C_p = \frac{\partial C_p}{\partial d} \Delta d = -C_p \frac{\Delta d}{d} \quad (18)$$

Since the spacing d is larger than before, the change in capacity is smaller, for a given Δd , and the overall change in filter response should be smaller. Extensive tests bear out this first-order analysis. A three-pole filter with a center frequency at 3.8 GHz* and a 100 MHz bandpass was constructed using a finger thickness of 0.0625 inch. The fingers on either side are fabricated from a single sheet in order to guarantee a good low resistance path from the fingers to the ground planes, and to insure proper relative spacing between fingers, as shown in the experimental local oscillator assembly in Fig. IV-15. Each half-

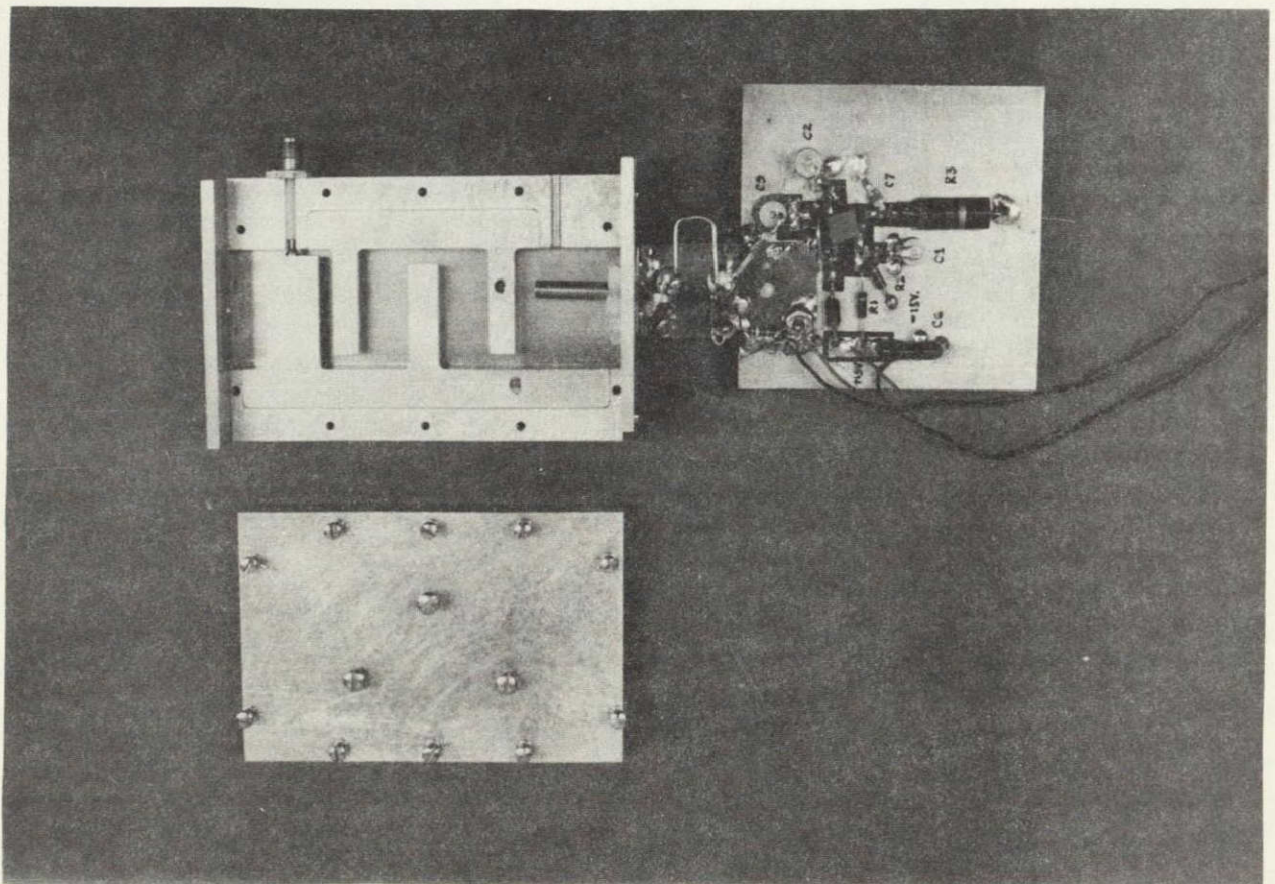


Fig. IV-15. EXPERIMENTAL LOCAL OSCILLATOR ASSEMBLY.

section is firmly clamped between the two ground planes with the finger bases on a recessed ledge. The finger lengths were shortened in 0.001 to 0.002 inch decrements, and the overall bandpass response was measured. Bandpass shape was examined without adjusting any of the tuning screws, and then the screws were adjusted to obtain the best bandpass shape and to determine the change in center frequency. The measurements indicate a 7.8 MHz/mil rate of change of center frequency with length, and an allowable variation of ± 0.001 inch in length for good bandpass response shape, as shown in Fig. IV-16. The working model specifications had been determined by this time, and a three-pole 100 MHz bandpass filter was constructed at a 2.5 GHz center frequency, with a finger thickness of 0.125 inch. The finger lengths were decreased in one-mil steps using a milling machine, and the filter response was examined. The results, as shown in Fig. IV-17, indicate that random variations of ± 0.003 inch cause a 0.5 dB degradation of insertion loss (to 1 dB, the specified limit), and a ± 0.004 inch variation could be tolerated.

Fabrication Methods

The interdigital structures could be realized by punching the spaces between the fingers out of a single sheet of 0.125 inch aluminum, as shown in Fig. IV-13. This punched piece could be sandwiched between two sheets of metal with spacers. Since a two-stage punching process can provide ± 0.002 inch tolerances, this method would require absolutely no machining to guarantee the required dimensions.

Die-casting is also feasible for this filter because the surface roughness available is less than half that which normally results from machining parts, and our experience has shown that machined filter fingers have excellent Q's. The insertion loss of the experimental filter shown in Fig. IV-15 is 0.4 dB, which is very good. The entire filter could be die-cast in two pieces if it were cut in half in a plane perpendicular to the ground plane. There would be some angle of drag ($1-2^\circ$) along the filter fingers, but this could be compensated for in the design, probably experimentally.

One could also die-cast the same structure as the punched piece, including the spacers. This piece could be inserted into a

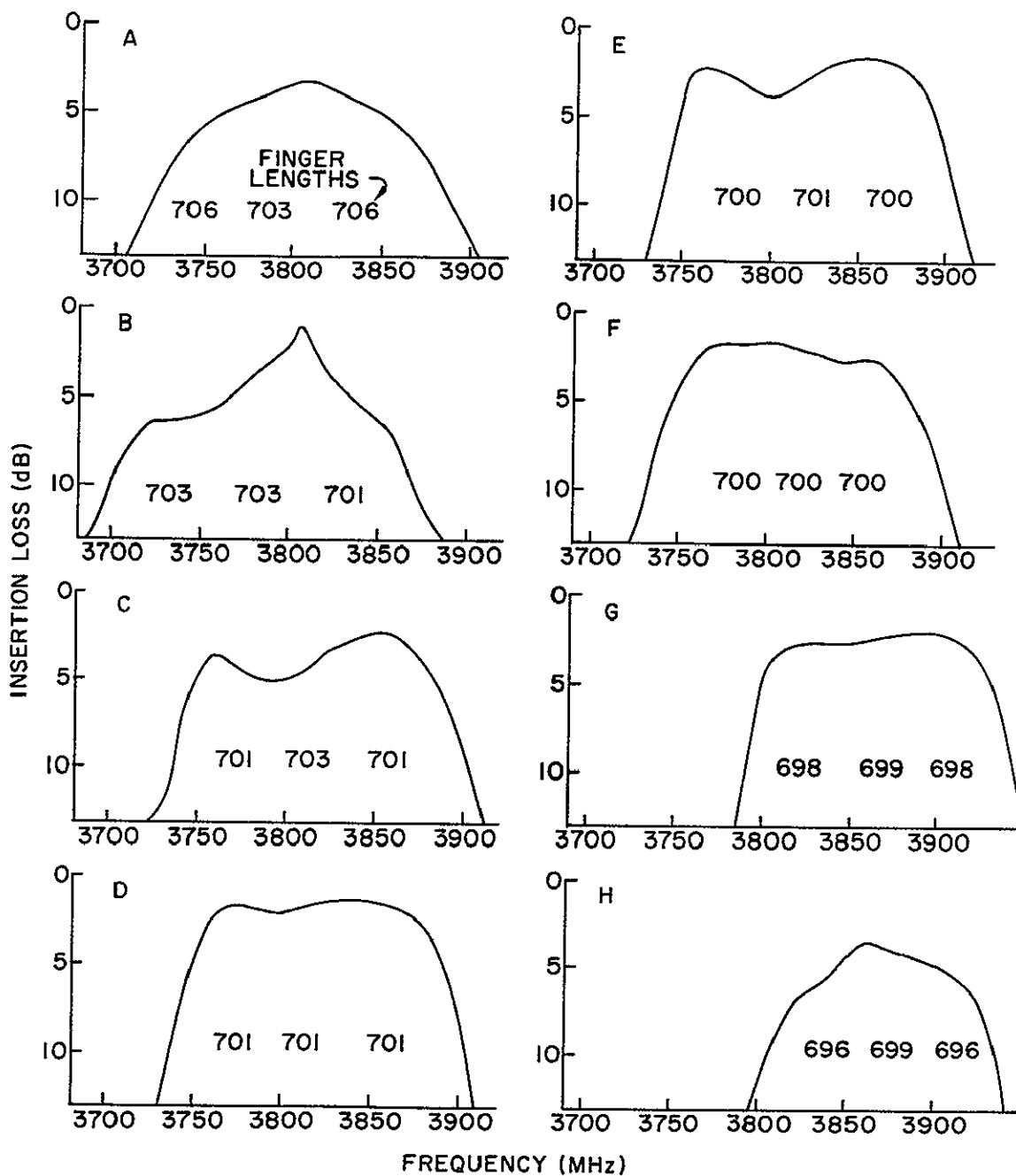


Fig. IV-16. 3.8 GHz FILTER RESPONSE AS A FUNCTION OF ROD LENGTH.

bathtub-like housing and sealed with a top ground plane. This method was selected over the other method because of its simplicity and because the other method did not lend itself to total integration of the mixer-feed-housing assembly. Photographs and drawing of the first prototype for this die-cast filter are given in paragraph K of this section.

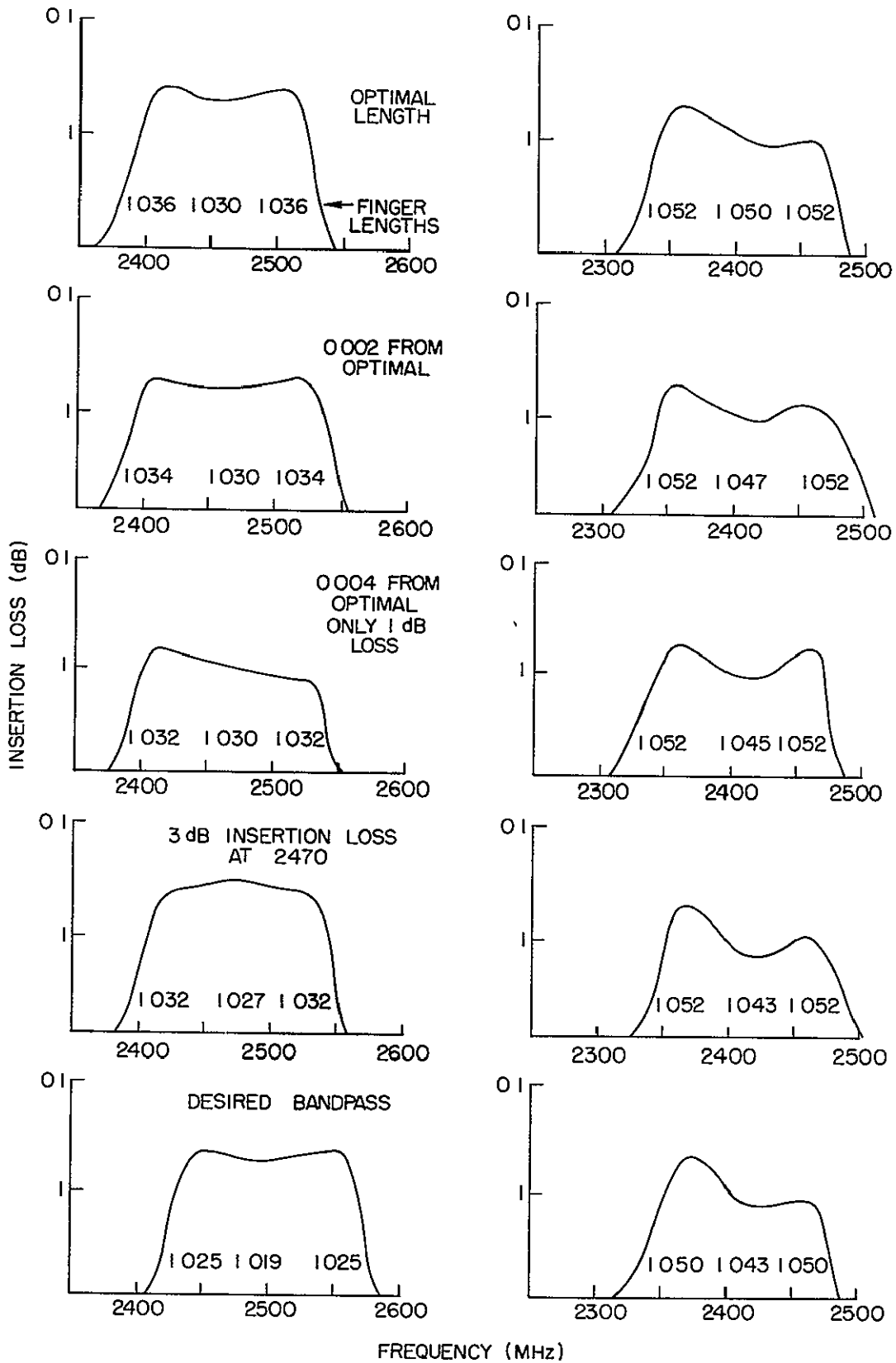


Fig. IV-17. 2.5 GHz FILTER RESPONSE AS A FUNCTION OF ROD LENGTH

E. The IF Amplifier

Requirements and Alternatives Noise Figure, Bandwidth, Phase, and Gain

The first stage of the IF amplifier must have a very low noise figure, less than 2 dB, in order that as little extra thermal noise be added to the signal as possible. The gain of this stage should also be as high as possible to minimize the noise contributions of the following stage. Field-effect transistors (FETs) exhibit much lower noise figures than bipolar transistors because there are only majority carriers flowing through the semiconductor and there is never any transition from a majority to a minority carrier to generate additional shot noise, except for gate leakage. Blaser* has shown that, when shot noise is neglected, the noise figure is given by

$$NF = 10 \log \left(1 + \frac{1}{g_{fs} R_s} \right) \quad (19)$$

where g_{fs} is the forward transconductance and R_s is the source resistance. The 3N159 FET has an advertized noise figure of 2.5 dB typical at 200 MHz, but in our breadboard, 10 FETs exhibited an average noise figure of 1.6 dB, with no adjustments to the circuit. Although FET technology in developing nations is in its infancy, the ability to achieve a 7 dB system noise figure depends on having a low-noise preamplifier stage, and low-noise FETs are cheaper than low-noise transistors. Therefore the 3N159 is selected for the first stage, even if it has to be imported. The large-quantity price quote is \$1.15 each.

Bandwidth and Phase

The IF amplifier should limit the frequency range of amplification to include the desired signal bandwidth (and as much additional bandwidth as deemed necessary by other constraints) in order to limit

* L. Blaser and J. S. MacDougall, Applications of the silicon planar field effect transistor, Fairchild Application Bulletin, Dec 1964

the thermal noise contribution ($N_o = kT_e BW_{if}$) The noise bandwidth BW_{if} is always greater than the 3-dB bandwidth, since it is an equivalent bandwidth obtained by integration of the noise contribution from all frequencies in the passband * As the number of poles in the filter increases, the noise bandwidth approaches the 3-dB bandwidth For example, the noise bandwidth of a 3-pole Butterworth filter is 1.047 times its 3-dB bandwidth. One could equate the 3-dB bandwidth of the filter to the signal bandwidth (25.2 MHz) if a linear-phase filter were used in the IF amplifier. Linear phase response is necessary over the signal bandwidth in order to prevent delay distortion of the FM signal Any phase nonlinearity causes a change in the group delay which results in different frequency components arriving at the output at different times, thus causing distortion Such filters can be obtained in a multistage IF by synchronously tuning the interstage matching networks But 4 or 5 stages of double-tuned circuits means 8-10 adjustments, and this is not desirable for mass-production The alternative is to use a filter of the desired number of poles as one of the interstage networks and use broadband matching networks which require no tuning for the remaining interstage networks Even so, the alignment of most linear-phase filters is also extremely tedious, and is not recommended for a mass-production system However, a new realization of linear-phase filters has been presented by Lerner** which could be significantly less difficult to align. Unfortunately, we have not had time to properly evaluate this filter design, but we are familiar enough to recommend further consideration The great attraction of the Lerner filter is that each resonator can be tuned to a predetermined series resonance frequency independently on a Q meter or bridge, and then is installed in the circuit, as shown in Fig IV-18 Only minor readjustments should be necessary

* $BW_N = \int_0^{\infty} |H(j\omega)|^2 df$, where $H(j\omega)$ is the Fourier transform of the network's impulse response

** Robert M Lerner, "Bandpass Filters with Linear Phase," Proc IEEE, March 1964, p 249-268

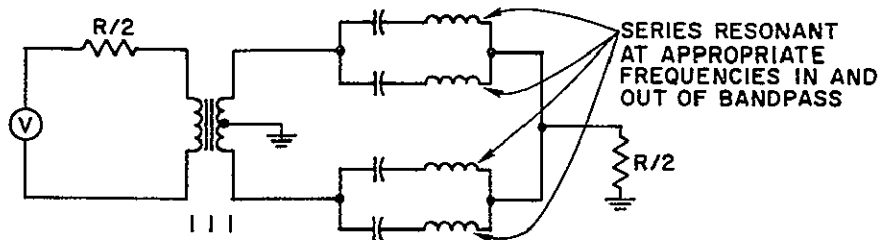


Fig. IV-18. LERNER FILTER CIRCUIT.

In case the Lerner filter is not appropriate, the following alternative can be used. It is possible to trade alignment difficulty for greater 3-dB (and therefore noise) bandwidth by using a 30 MHz Butterworth filter which has a small nonlinearity in its phase response over the range of RF signal bandwidth. Exact calculations of the delay distortion are difficult to make, because the spectrum of the wideband FM signal is not constant. We think that the distortion will be negligible. The real penalty paid in this tradeoff is for the increased antenna diameter necessary to collect sufficient signal power to maintain the 15 dB carrier-to-noise ratio. This has already been accounted for in the system parameter determination, and a 30 MHz filter will be used in the working model, until a better alternative is definitely available.

Gain and Interstage Matching

The IF amplifier and limiter increase the amplitude of the wideband FM signal to a magnitude at which (1) amplitude saturation (limiting) can be easily obtained, and (2) there is sufficient signal strength to obtain a useable signal from the discriminator. Limiters can be designed to operate at output levels ranging between -10 dBm and +10 dBm. 0 dBm (1 mw) to 10 dBm is an acceptable range in which to operate the discriminator. The output power from the mixer at 120 MHz will be approximately -82 dBm,* the limiter should be 5-10 dB into

* Assuming a 4 dB conversion loss and a -78 dBm signal level at the mixer input.

limiting, and so approximately 90 dB gain is needed from the IF amplifier and limiter. The limiter chosen for this application has approximately 30 dB gain, and so the IF amplifier must supply 60 dB.

Although the maximum available gain (MAG) for many transistors is in excess of 25 dB, this gain generally cannot be attained in a multi-stage IF amplifier without the use of neutralization, and even then system stability is extremely critical. But neutralization of each stage is time-consuming and is therefore undesirable for this mass-producible design. The required degree of stability can be achieved by mismatching either the load or source impedance, or both, for a given stage. Single-stage gains of 12-15 dB are possible at 120 MHz, thus 5 stages will be needed.

This mismatching technique can be easily implemented by using wideband toroidal transformers which give transformations of $N^2:1$ where N is an integer*. While this method does not allow as precise a control of the mismatch ratio as one might like, it is not serious because some kind of RLC feedback is also needed to provide a uniform amplitude versus frequency response. The amount of feedback can be varied to suit the stability needs as well as to provide the amplitude smoothing.

Preamplifier and Filter Design

Obtaining the desired low noise figure with the first stage is a matter of providing the proper impedance mismatch between the source impedance of the mixer diode and the FET input impedance. There is an optimum source impedance for best noise figure, and it is very unlikely that the transformed load impedance seen by the mixer diode will be the conjugate of the mixer diode source impedance, one accepts the mismatch in power transfer in order to get the low noise figure.

This impedance matching network should have a low insertion loss, and therefore the number of resonators should be kept to a minimum. Thus the filter cannot be placed at the input. A simple self-resonant inductor can be used as an autotransformer to obtain the desired impedance mismatch, as shown in the complete schematic in Fig. IV-19. The coil has 8 turns wound in a 0.5 inch diameter and 1 inch in length. The

* Ruthroff, C. L., "Some Broadband Transformers," Proc. IRE, August 1959

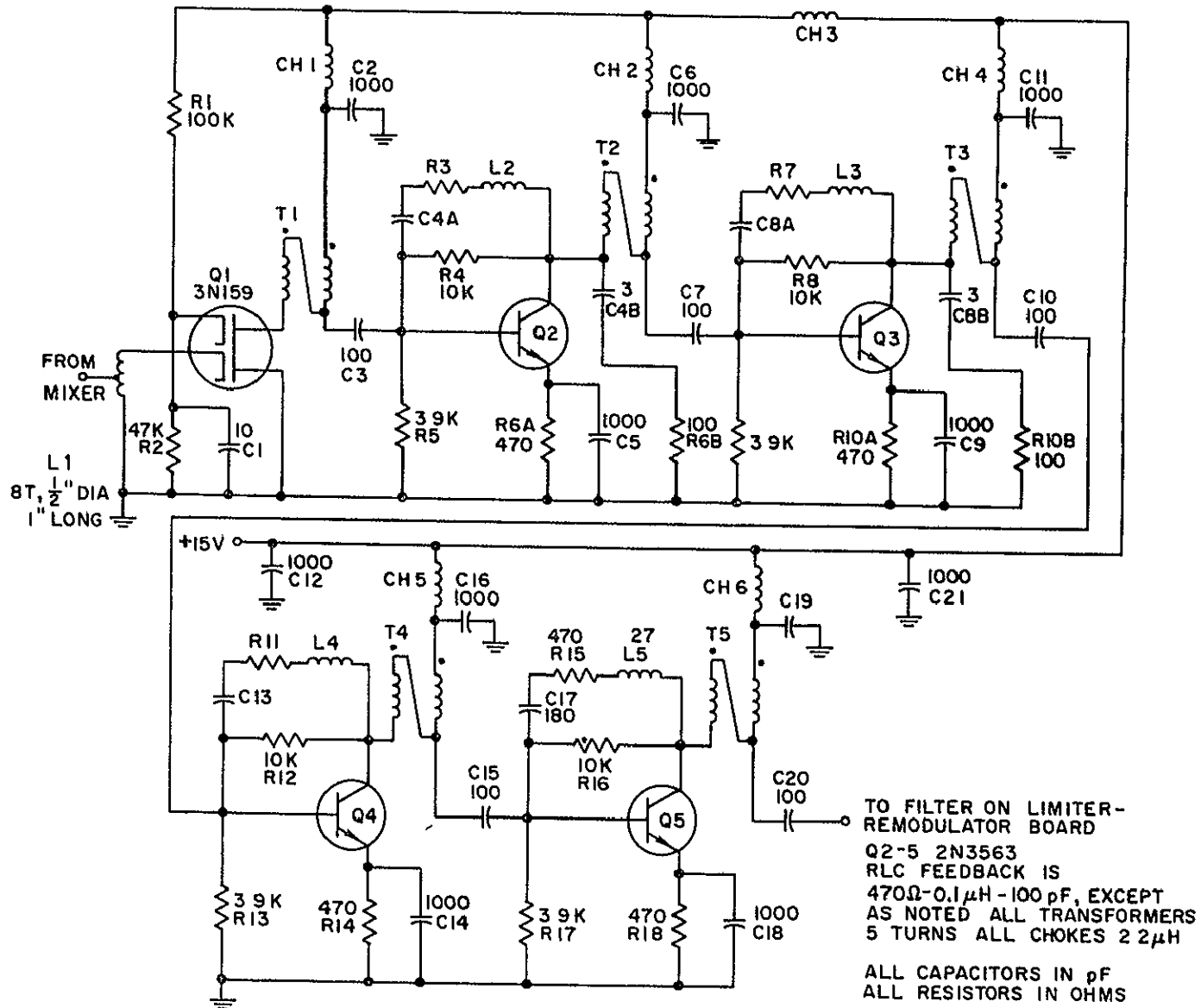


Fig IV-19 COMPLETE IF AMPLIFIER CIRCUITRY

diode input is tapped three turns from the bottom, and the hot end connects to the FET input. This tap position is experimentally determined

The FET is biased for operation at maximum transconductance g_{fs} ($V_{G1-S} = 0$ v, $V_{G2-S} = 4$ v) and the present impedance matching circuitry provides about 15 dB gain. This minimizes the noise figure and the effects of noise contributions from the successive stages. A 100-ohm resistor in the drain serves as current limiting protection for the FET because the required bias conditions do not permit the use of a source resistor for stability protection.

Ordinarily, the IF filter should follow the first stage in order to limit the noise power passed along to each stage and to prevent spurious signals from producing intermodulation distortion or causing saturation in successive stages. This was not recognized as a vital requirement until after assembly and testing of the IF module for the working model. It was originally decided to place the filter on the Signal Processor circuit board where a number of other adjustments were known to be necessary, and thus leave the IF module completely free of adjustments. The filter can easily be repositioned when the IF circuit board is laid out again, to account for other changes. A three-pole filter response was selected as a reasonable compromise between alignment difficulty and stop-band rejection.

Filter element values are given in Table IV-III for both linear phase and Butterworth response, assuming 50 ohm terminations. One of the difficulties with this filter design is that large values of inductance are hard to obtain at 120 MHz because of distributed capacity.

Table IV-III

120 MHz FILTER ELEMENT VALUES

Element (ohms, pf, nh)	R_1	C_1	L_1	C_2	L_2	C_3	L_3	R_3
Linear Phase	50	35.8	49.1	6.8	259	234	7.5	50
Butterworth	50	106	16.6	3.3	531	105	16.6	50

These element values are calculated from the formulas in the Reference Data for Radio Engineers, p. 217. The 3-dB points are at 106 and 136 MHz.

Amplifier Design

There are a large number of inexpensive transistors suitable for this application, we have used a Brazilian-made device, the PE3002, by Philco-Ford of Brazil, in a breadboard, and the 2N3563 in the working model IF amplifier. Both devices are epoxy-encapsulated, cost about \$0.25 in large quantities, and have f_t 's of over 1000 MHz. Good forward current gain is obtained when the emitter current is greater than 5 ma, we use 7.5 ma.

Since this equipment must function over a wide temperature range, bias stability is very important. The worst parameter variation in silicon devices with regard to bias stability occurs with the base-emitter junction voltage. The effects of this $-0.002 \text{ v}/^\circ\text{C}$ variation can be made negligible by using an emitter resistor for dc degeneration, this resistor must be bypassed in order to avoid ac degeneration. A simplified expression for the fractional change in collector current is given by

$$\frac{\Delta I_c}{I_c} \approx \frac{\Delta V_{be}}{I_e R_e} \quad (20)$$

where

V_{be} is the change in the junction potential

R_e is the emitter resistance

I_e is the emitter current

For a 60°C range, the change in V_{be} is 0.12 volt, the fractional change in collector current can be kept to as small a percent as desired by choosing R_e . The only restriction is that this emitter drop be less than 5 volts, if a 15 volt power supply is used, in order to maintain the collector-emitter voltage at 10 volts. A 3.5 volt drop is used in this design, giving a collector current variation of 3.3% with temperature. Thus the effect of variations in current gain with temperature will be the only change over which we have no control in the present

design It was originally thought that the problem of too much gain at low frequencies (<90 MHz) could be reduced by using a small emitter bypass capacitor. S-parameter measurements of the 2N3563 were taken with a 470 ohm emitter resistor and different values of bypass capacitor. This device exhibits a negative input impedance for bypass capacities of less than 500 pf, and is thus potentially unstable. Since the toroidal transformers do not allow adjustment of the mismatch, which could swamp out the negative input impedance, the emitter resistors must be bypassed with 1000 pf. For this case the input and output impedances are

$$Z_{in} \cong 30 - j30 \text{ ohms}$$

$$Z_{out} \cong 400 - j100 \text{ ohms}$$

The degree of stability and the stage gain depend on the transformer impedance matching properties.

The broadband transformers are proposed because they are not critical in their construction and need no adjustment after installation. After deciding on the integer transformation ratio N , the transformer is constructed by twisting N wires together and then winding them on the toroid. Very close coupling is achieved over a wide frequency range. The transformer is connected by taking the end of one wire on one side of the toroid and connecting it to another wire on the other end of the toroid. Thus these transformers can be thought of as very closely coupled autotransformers. S-parameter measurements of the impedance transformation were made on bifilar transformers for various loads and various number of turns, using toroidal cores made by Sieferit and Micrometals. There is a considerable difference in transformation ratio between the two core types under equal conditions of 5 and 7 turns and 499 ohm loads, over a 100-150 MHz range. The Sieferit cores have a near-ideal ratio of 4:1 in transforming the 499 ohm metal film resistor to 120 ohms, with some inductive component. The Micrometals cores have a 6:1 ratio and a smaller capacitive component. Little difference was noted in actual performance in the breadboard 3-stage amplifier, the higher ratio of the

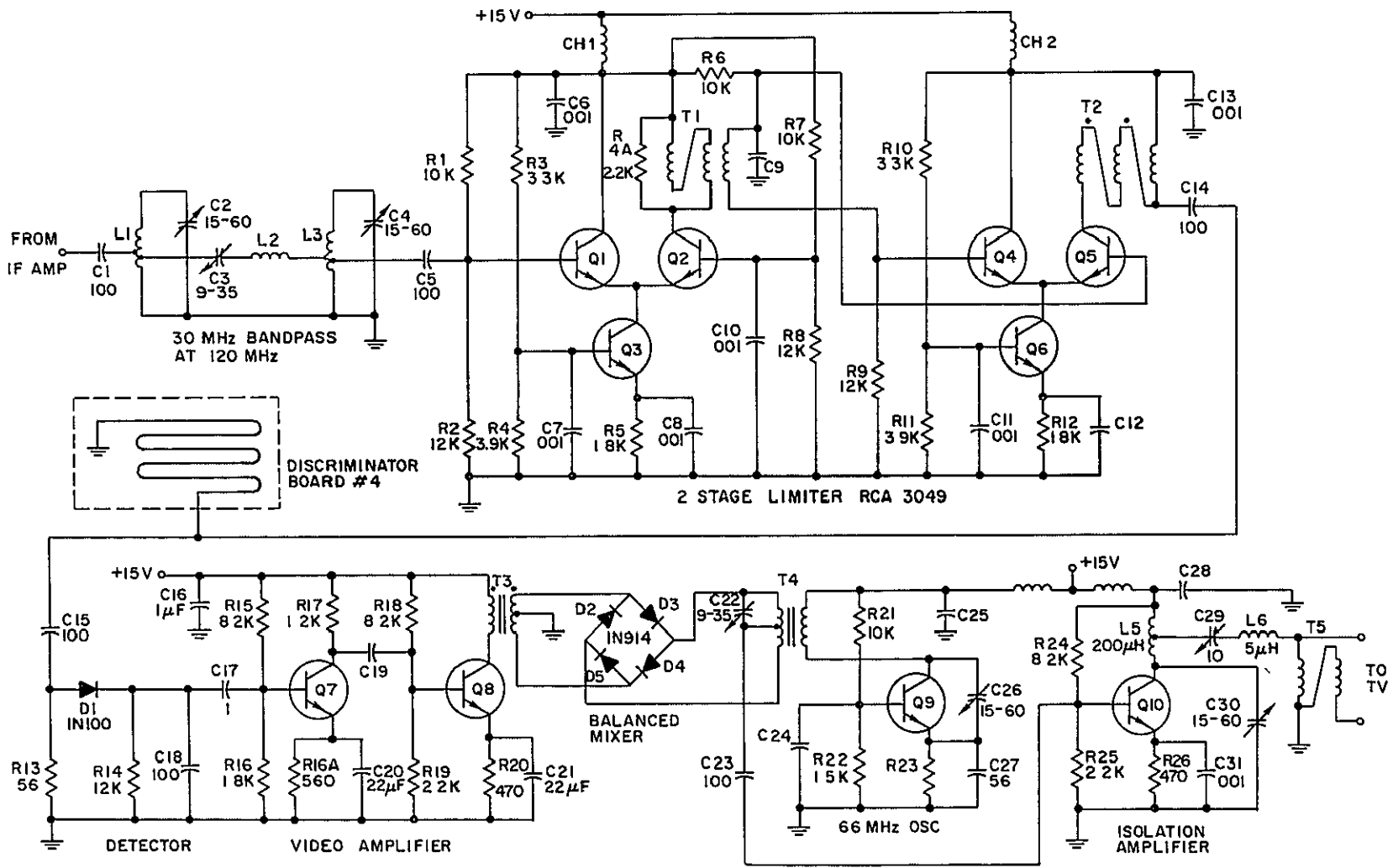
Micrometals cores allowed a better impedance match and thus increased the gain by about 2 dB. This increase is offset by the use of collector-base RLC feedback. The Micrometals cores are used in the working model IF

It was found that in spite of the very poor transformation ratios of the transformers at lower frequencies, the mismatch was not enough to appreciably reduce the overall gain. The transistor properties are varying rapidly and the current gain increases with decreasing frequency. The net result is that the broadband coupling gives a high gain from 50 to 150 MHz. RLC collector-base feedback has been used to reduce the gain at the lower frequencies slightly and to smooth out the variations over the range. The values of R, L, and C were experimentally determined to be 470 ohms, 0.10 to 0.24 uh, and 100 pf. The low-frequency response could not be appreciably reduced by selective emitter bypassing as mentioned, or by reducing the number of turns on the transformer, since coupling at the higher frequencies was also affected. The resulting net average gain per stage for the bipolar transistors is 12 dB

The layout of the IF amplifier is the most critical layout in the receiver design. It is discussed in detail in the section on the working model.

F The Limiter

The purpose of the limiter is to remove in-phase noise components which cause variations in the amplitude of the FM signal. This is necessary in order to realize the FM improvement in the signal-to-noise ratio at the discriminator output. The limiter must also maintain good phase response (have low AM-PM conversion) over at least a 5 dB range of amplitude variation at the input, since this is the maximum margin for the carrier-to-noise ratio over detector threshold. This last requirement eliminates the use of simple saturated amplifiers. These requirements are best met by using a pair of transistors in an arrangement which varies the gain inversely with the instantaneous amplitude variations, in a certain region of amplifier gain. The limiter circuitry is shown in Fig. IV-20 as part of the signal processor circuitry.



ALL CHOKES 2 2μH
 ALL BYPASS CAPACITORS 1000 pF, EXCEPT AS NOTED

Fig IV-20 SIGNAL PROCESSOR CIRCUITRY FILTER, LIMITER, DISCRIMINATOR, AND REMODULATOR

Limiter operation is accomplished as follows. The signal is coupled from the emitter of Q_1 (an emitter-follower circuit) across the constant-current source impedance of Q_3 to the emitter of Q_2 , a common base amplifier. As the signal level increases, the average emitter current in Q_1 increases, but since the pair is supplied by a constant current source, the emitter current in Q_2 must decrease. This decreases the gain of Q_2 , since forward current gain is directly proportional to emitter current. By experimentation and design, one can achieve a bias condition in which an increase in signal level at Q_1 can cause the exact decrease in gain in Q_2 , resulting in no change in output level. Beyond a certain signal level, the emitter current in Q_2 becomes sufficiently cut off to overcompensate, and the output can decrease with increasing signal level.

This circuit could be realized with discrete transistors, but the price of the CA3049 integrated circuit is just about the same as the price for the 6 transistors. Use of the integrated circuit provides a slight advantage with regard to temperature variations, since all the integrated devices experience the same temperature changes, and thus thermal differentials are eliminated. In addition to these basic performance factors, the limiter is responsible for guaranteeing that the FM threshold is no more than 10 or 11 dB, threshold measurements have not yet been made, but conversations with other limiter users* indicate that no difficulty should be experienced with this type of limiter.

G. The Discriminator

The discriminator together with the detector converts the wideband FM signal back into the baseband television signal. It should have as large a sensitivity as possible while maintaining a specified maximum distortion of less than 3%. It should have as few components as possible, and should require no adjustments after assembly.

* J. Hesler of General Electric and M. Sites of Stanford University

A transmission line, short-circuited at one end and connected in parallel with the output of the limiter and the detector diode, provides the least expensive method of obtaining a frequency discriminator. The transfer function for this discriminator is given by

$$\frac{E_L}{E_{IN}} = K_1 \left[1 + K_2^2 \cot^2 \left(\frac{2\pi l}{c} f_1 \right) \right]^{-1/2} \quad (21)$$

where

K_1 = discriminator efficiency factor

$K_2 = Z_o / Z_o'$

Z_o = output impedance and load impedance

Z_o' = characteristic impedance of transmission line

l = line length

c = velocity of propagation in the transmission line

f_1 = frequency of the FM signal.

The derivation of the optimum line length, characteristic impedance, and linearity are given in Appendix H. That analysis shows that the best results will be achieved when the line length is $(3/8) \lambda$ at 120 MHz and when the ratio of output impedance to line impedance is $2\sqrt{2}$. For this choice the calculations show less than 2% distortion for a ± 12.5 MHz deviation.

Two versions of the discriminator have been assembled and tested. First, breadboard models were made with three pieces of 50-ohm coax all connected in parallel to simulate a 16-ohm line, satisfactory results were obtained. For actual manufacture, a stripline realization of the transmission line appears to be the most economical. This can be made on almost any dielectric board material and can easily be given the low impedance required for best linearity. A version was made on a fiber-glass laminate with a dielectric constant $\epsilon_r = 5.4$. The strip width of 0.25 inch gives a characteristic impedance of 17 ohms, which is

needed for a 50-ohm output impedance. This is done so that individual circuits can all be measured with 50-ohm test equipment. The line is simply folded back and forth on the board in order to get it all onto a 4" x 4" board. A graph of the output voltage versus input frequency is given in Fig IV-21, the linearity is adequate.

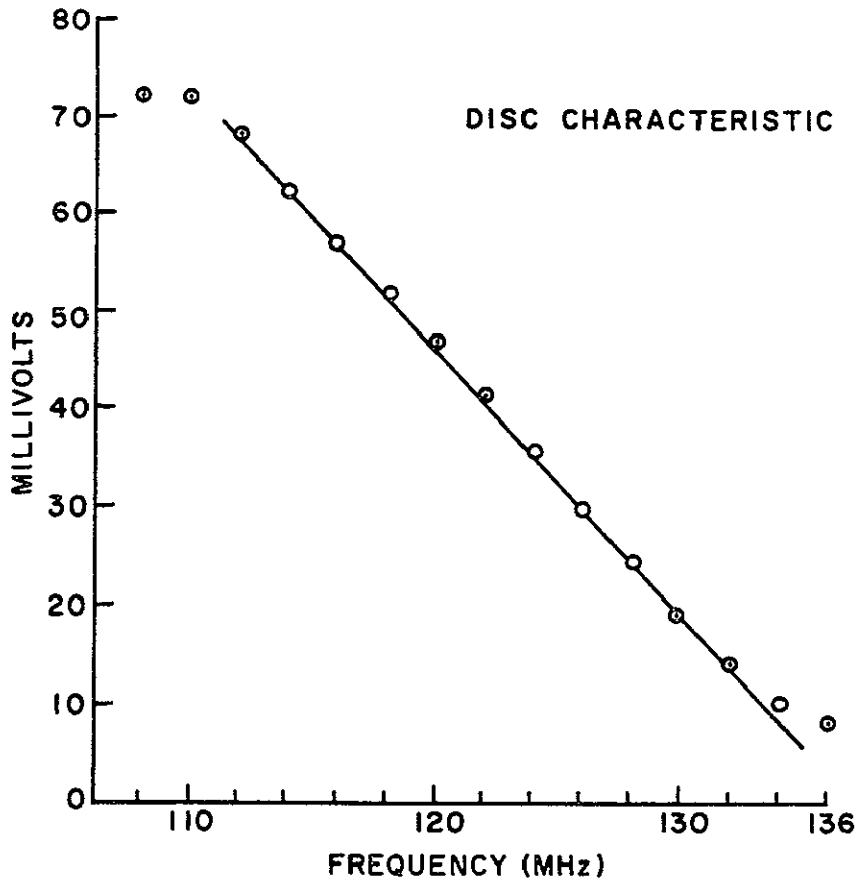


Fig. IV-21. MEASURED DISCRIMINATOR RESPONSE.

H. The Detector

The discriminator changes the 120 MHz FM signal into a 120 MHz AM signal. The detector shifts the signal down to baseband and filters the rf but not the video signal. The detector circuit uses a 1N100 germanium diode which has a higher detector efficiency and is slightly cheaper than a silicon diode. Tested with the discriminator, this detector gave a sensitivity of 2.6 mv/MHz for a 0 dBm input level.

I The Remodulator

The remodulator amplifies the baseband video signal and then must shift it to a convenient channel location, such as Channel 2 through 5. If the baseband signal is simply the ordinary video signals as taken directly from the TV camera, then the remodulator must be similar to a vestigial-sideband modulator. But if the baseband signal is already a vestigial-sideband signal which has been shifted back down to baseband with a 100 KHz guardband, then the remodulator need only be a balanced mixer. This is slightly easier to build, since the lower sideband need not be attenuated appreciably. The shifting carrier at 75.9 MHz (for Channel 5) must be reduced considerably in the output in order to prevent it from activating the AGC in the television and reducing the gain of the desired signal. A balanced mixer does this. We have assumed the vestigial side band type of video modulating signal, and a balanced mixer is shown in Fig IV-20 is used in the Signal Processor circuitry. A buffer amplifier is used at the output to drive the balun.

J The Power Supply and Voltage Regulator

The power supply itself consists of a fuse, switch, a transformer, a diode quad rectifier, and a filter. It is designed to be mounted by the television set, because it is felt that the twin line which is used to bring the television signal from the adaptor could also be used to carry the dc power to the adaptor. The schematic diagram is shown in Fig IV-22. The voltage regulator uses a junction field effect transistor (similar to Motorola MPF 103) to supply a constant current to a transistor whose emitter voltage is stabilized by a zener diode. An increase in the supply voltage tends to cause an increase in the output voltage across the series regulating transistor, this increased output voltage tends to cause Q_2 to conduct more current, but since both Q_2 and Q_3 are being supplied by a constant-current source Q_1 , the base drive for the regulator transistor Q_3 decreases, which reduces the output voltage. This type of regulator will work well over temperature because of the constant current properties of junction FETs.

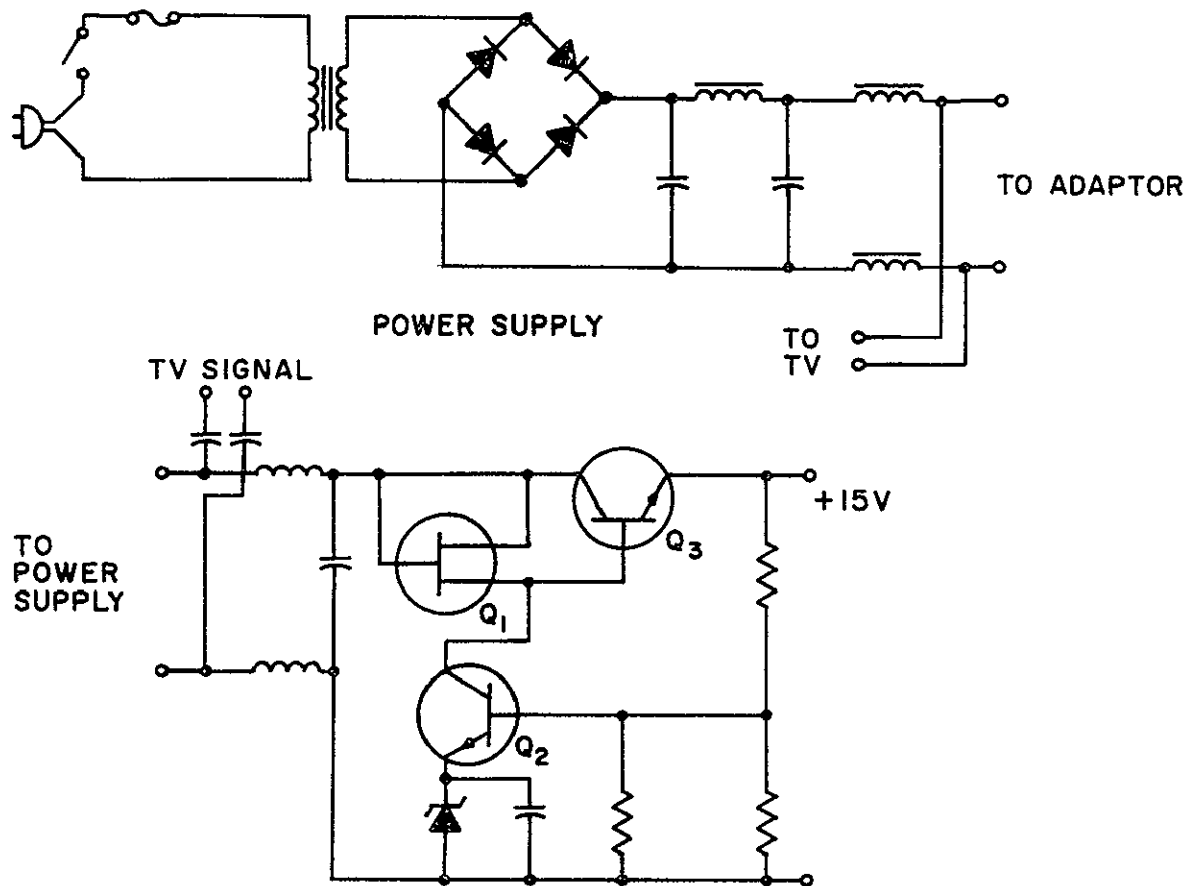


Fig. IV-22. POWER SUPPLY AND VOLTAGE REGULATOR SCHEMATIC

K The Working Model Layout and Performance

The problem in laying out the receiver functions is essentially to determine how to arrange things so that the entire receiver body can be die-cast and will require no machining, that interconnections for signal paths are short, other necessary functions are easily achieved, and assembly and final tune-up adjustments are as simple as possible. The present configuration shown in Fig. IV-23 is a machined version of a die-castable realization of the feed, mixer, local oscillator filter, and a compartment for the electronic circuitry. A discussion of the allocation of the circuits on the boards and the layout of the boards is given in a following section. This present arrangement of modules has evolved through three iterations, as the factors important to a simple regulation became clearer in the design process. The basic

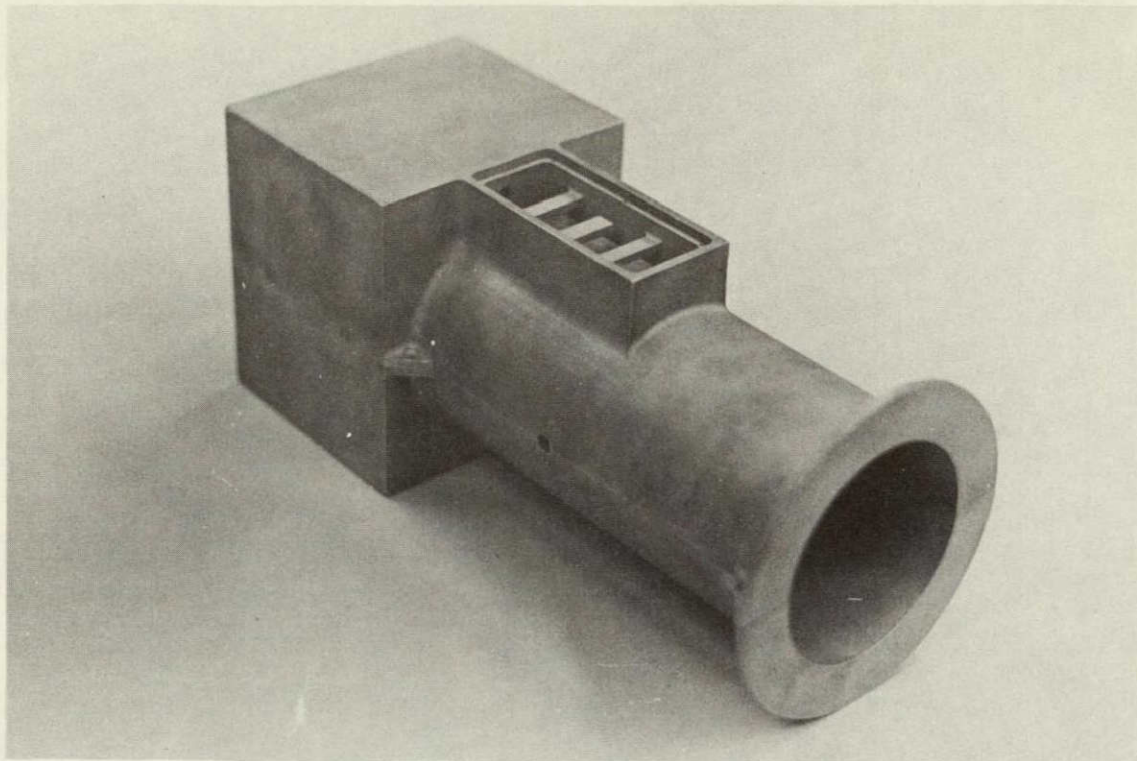


Fig. IV-23. THE DIE-CASTABLE MIXER-FEED HOUSING.

concept has proved quite adequate, and we anticipate that only minor changes and additional details need to be incorporated. These additions and changes will be given as part of this description, rather than in a separate section. A brief sketch of other arrangements is given in an appendix.

Front End Considerations

The model shown disassembled in Fig. IV-24 is designed to be die-cast; if a smaller quantity were needed than is necessary to justify die casting, the housing could be sand-cast. The wall thickness would increase by 50% everywhere, but very few other changes would be necessary.

The mixer-feed housing is split into two pieces, rather than cast as a single piece with a top cover for the filter and circuit compartments, for two reasons:

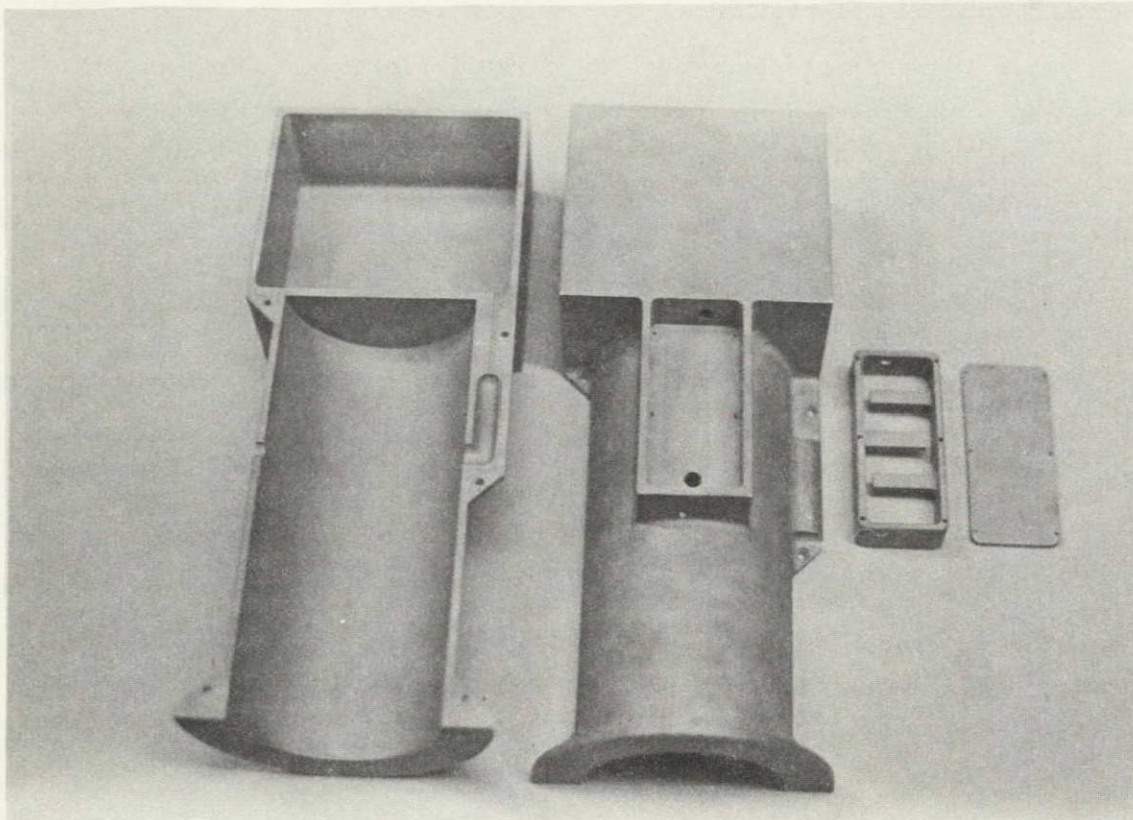


Fig. IV-24. DISASSEMBLED MIXER-FEED HOUSING.

- (1) The E-field of the signal will be in the direction of the line of separation. This is arbitrary but convenient, because the diode and its mounting structure are easily installed in notches by clamping the two halves of the casting together. Thus no machining is needed in the casting for screw threads or other fastening techniques, which might be needed if the circular cavity were cast as one piece.
- (2) The IF output lead is conveniently brought from the mixer diode to the IF amplifier along a channel which is cast in the edge of the housing. A quarter-wave coaxial choke fits into a small hollow at the mixer output and provides a good short-circuit path for the 2500 MHz local oscillator signal.

A more complicated interconnection scheme would be required if the housing were cast as a single piece.

Circuit Board Compartment

It is desirable to mount the circuit boards as shown in Fig. IV-25 because this method minimizes the overall length of the mixer-feed casting and does not contribute any more to the blockage beyond what is already there from the mixer-feed cavity. The mixer-feed housing should not be any longer than necessary in order to minimize loading of the feed support arms. The circuit boards could be mounted in a different plane with very little increase in length; such an alternative is considered in an appendix, in which the circuit boards are installed from the rear, toward the mixer-feed cavity.

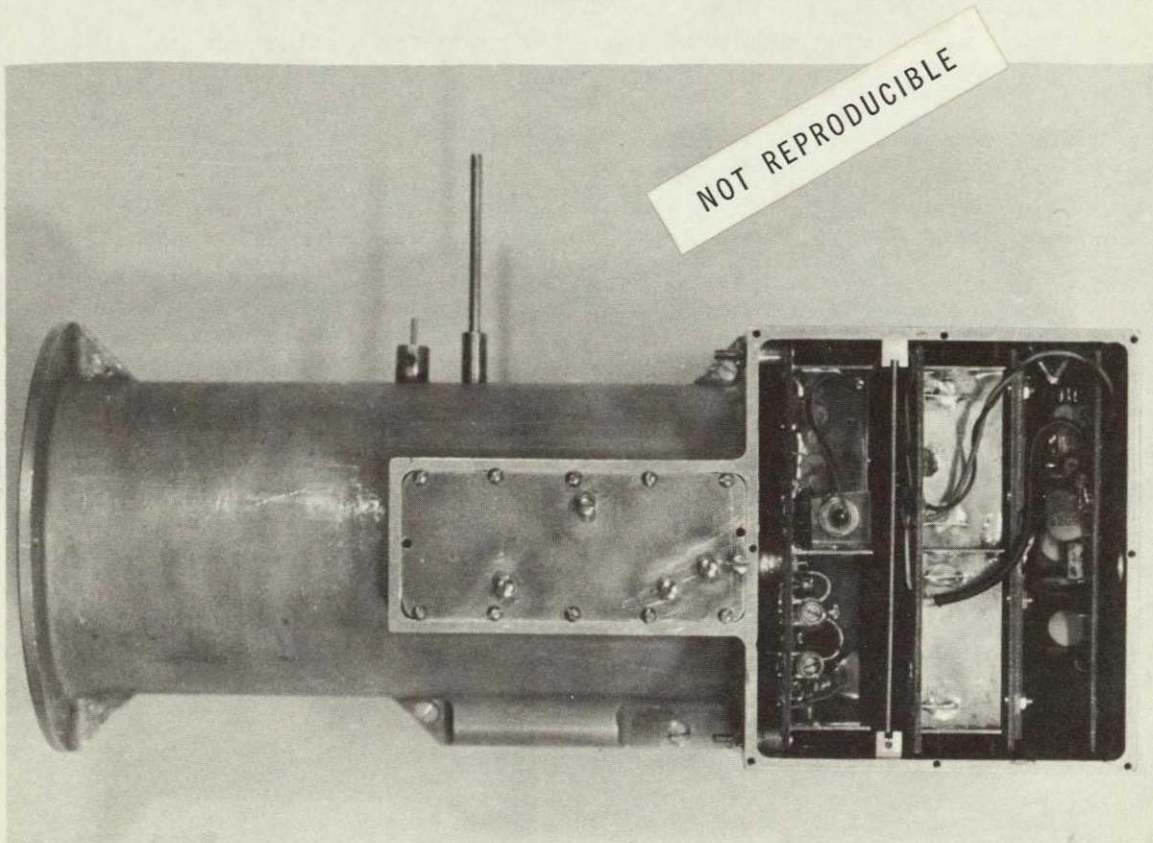


Fig. IV-25. MIXER-FEED HOUSING WITH CIRCUIT BOARDS INSTALLED.

Vertical webs can be cast in the electronics compartment to provide isolation from one board to another; this is accomplished at present with brass plates which slide in slotted aluminum channels,

which in turn are screwed to the box walls, as shown in the photograph in Fig. IV-25. The top cover of the electronics compartment has been removed to facilitate installation and removal of the various circuit boards. At present, all other boards must be removed in order to remove or install the Local oscillator board, because the probe from the SRD multiplier must be inserted through a hole in the wall between the filter cavity and the electronics compartment. This problem can be eliminated by leaving a slot in the wall where this hole is located so that the probe can be installed in a vertical direction. The cover for the filter will have a shoulder which will come down into the slot and clamp the insulated probe firmly in place. The filter fingers are die-cast on a supporting ring which is inserted into the filter cavity. This piece will also have the slot cast into it for the probe. This insert method was chosen (see Filter section) instead of the other method in which the fingers and ground plane were to be cast with a separation line through the ground plane for the following reasons. The plane of separation in the filter casting must align with the plane of separation in the mixer-feed cavity casting; this means that the filter would have to be mounted at the seam. But the local oscillator signal must be injected into the mixer cavity perpendicular to the plane of separation, and so there would be a difficult interconnection problem in bringing the local oscillator output from the filter a quarter of the way around the mixer cavity. Thus the insert method was selected. Mechanical drawings of the mixer-feed housing and the filter insert are given in Figs. IV-26 and 27.

Front End Performance

Good noise figures (6 dB or better) have been consistently obtained with this prototype mixer-feed and the first engineering model local oscillator. The 1.6 dB breadboard IF amplifier was used in a standard noise figure measurement setup using both a Hewlett-Packard 341A Noise Figure meter and an AIL hot and cold source. The automatic test system of Hewlett-Packard which employs a gas-discharge noise source has given 6 dB readings which are corroborated by insertion of a known attenuation between the noise source and the perfect transformer.

120

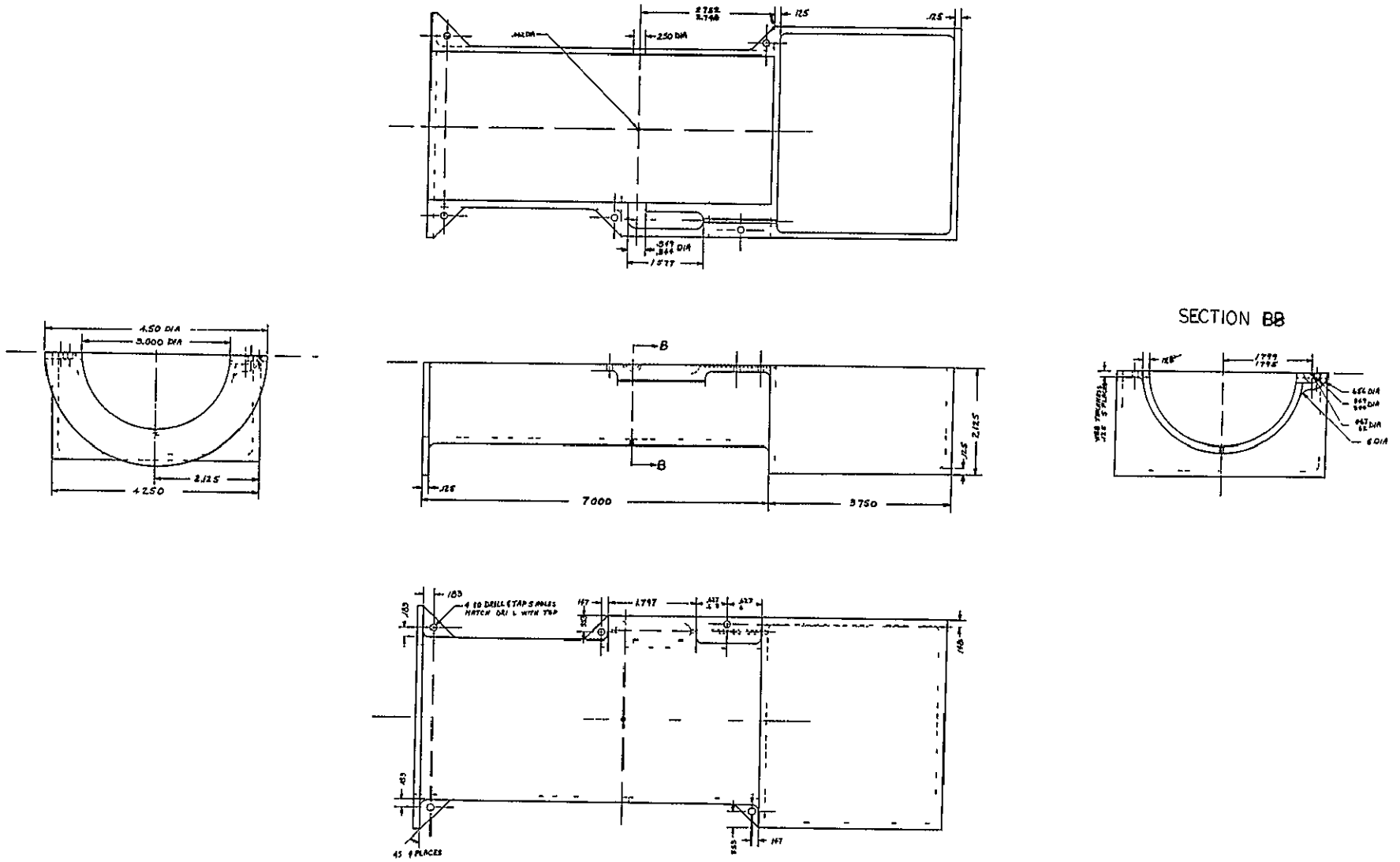


Fig IV-26 CONTINUED.

No 53 DRILL, 6 HOLES
MATCH DRILL
WITH TOP & COVER

125 DIA
NOMINAL

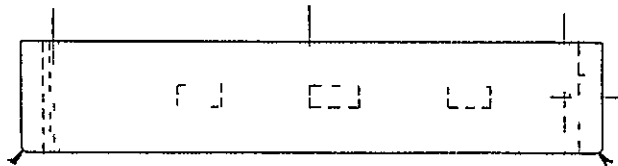
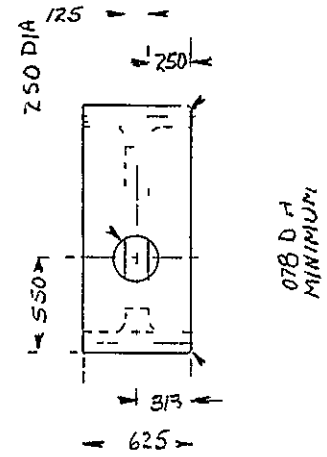
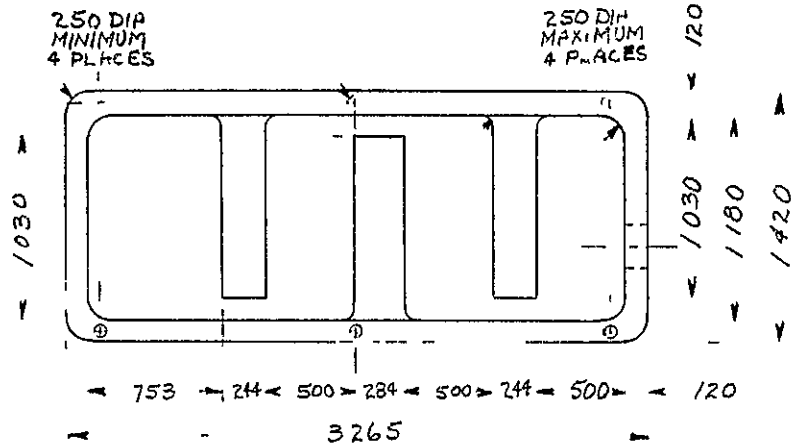


Fig. IV-27 MECHANICAL DRAWING OF FILTER INSERT

(The reading is correct if it drops by the amount of the known attenuation.) An AIL Hot/Cold Noise Source #7004 was rented to further substantiate these measurements. Before this noise source failed, noise figures of 6.5 dB or better were observed by the Y-factor method.*

Experiments with metallic and non-metallic gaskets between the two halves of the mixer-feed housing indicate that slightly more consistent operation is obtained with the metal gasket, but there is no difference in noise figure. Use of the non-metallic gasket (Myiar type) required more care in tightening the screws which joined the two halves, 0.5 dB variations in noise figure were observed if the screws were not tightened enough, but 6 dB was easily obtained.

A coax-to-waveguide transition designed to match to a perfect waveguide load** is used to couple the signal or noise source into the mixer cavity. Thus the source impedance seen looking from the mixer structure out of the feed and into the transition is essentially that of a perfect waveguide load, by reciprocity. A short matching stub (.85 inches) located 90 inches in front of the diode support structure projects into the cavity from the line of separation and is used to effect a match between the diode and the source impedance. To complete the design of the front end, we must match the waveguide to free space at 2620 MHz. Obtaining this match is a simple matter, now that the mixer is appropriately matched to a source impedance which is the same as the wave impedance. It can be done by using the coax-to-waveguide transition again, as adjusted for a perfect waveguide load, and a short piece of waveguide, and a slotted line. The position of another stub can be found which will match this waveguide to free space, locating a stub in the waveguide of the mixer cavity will then effect the desired match.

* AIL Instruction Booklet, the Y-factor method measures the difference in IF noise power as a function of two different input termination temperatures, both of which are known.

** The design and construction of this transition is discussed in Appendix F.

Good noise figures have been obtained, but at present, the adjustment of the local oscillator (crystal-controlled version) and the interdigital filter is critical. This is due to the fact that there is considerable 83 MHz fundamental feedthrough, either as modulating sidebands or directly which must be eliminated by careful adjustment. These difficulties would be completely eliminated if the 250 MHz LC oscillator or a 167 MHz crystal oscillator-multiplier were used instead. We know this, because when the mixer is driven by a HP-616 signal generator, very little problems are encountered in the tuning for noise figure. These problems will be rectified with the second engineering model.

Circuit Allocation and Circuit Board Arrangement

Allocation of the various circuits to different boards depends on two factors: interference and available space. The approximate shape of the circuit boards is already determined by the choice of orientation and the use of a complete compartment box.

The local oscillator is contained on one circuit board because it is necessary to isolate the high level signals which it generates from the other circuits. This isolation will be maintained by casting vertical webs, as mentioned earlier. The same concepts of elimination of potential interfering signals by isolation is applied to the rest of the circuits and their resulting layouts.

The layout of the crystal-controlled local oscillator board is shown in Fig IV-28. The voltage regulator was included on this board because it was not certain if there would be room on the other boards. But it is possible to include the regulator on the Signal Processor board, and it is also more desirable to do so from an interconnection viewpoint, to locate the regulator near the point of entrance of the power leads. Another layout for the crystal controlled local oscillator will be prepared to incorporate the changes found necessary with the first LO board. The component markings on this layout are out of date and do not agree with the labels in the schematic.

There is 90 dB of gain from the input of the IF amplifier to the limiter output, therefore, it is necessary to provide a great deal of isolation between these two points in order to prevent loop oscillation.

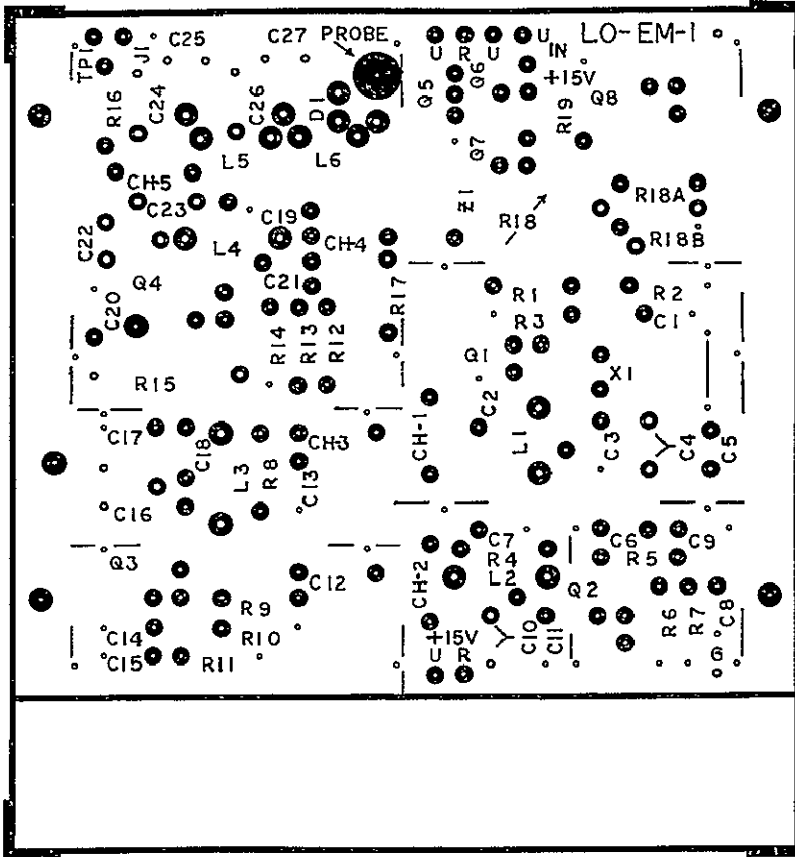


Fig. IV-28 CRYSTAL CONTROLLED LOCAL OSCILLATOR BOARD LAYOUT

This can be done by separating the IF-limiter chain at some point and putting the circuits on separate boards, in separate compartments. If the IF-limiter circuitry cannot all fit on one board, then isolation is obtained automatically. To obtain adequate isolation on the board from one circuit to another and to facilitate making connections to other boards, the circuits may be arranged so that the signal path flows in a U around the board down one side and vertically up the other. Isolation between the two vertical halves can then be obtained by casting an additional vertical web in the middle of each major dividing web with a slot just wide enough to slip the circuit board down into, as shown in Fig IV-29, thus forming two compartments for one board. In this case, the entire IF-limiter chain could be put on one board, if there is sufficient room.

In the present allocation of circuits, there are five working IF stages on the IF board, and room for two more stages, the filter, limiter, and detector are on the signal processor board, along with the remodulator and the voltage regulator. An additional web for the signal processor board should also be used to obtain isolation between the remodulator circuitry and the IF-limiter circuitry. The discriminator is contained on a separate pair of circuit boards.

The sketch in Fig IV-29 also contains the interconnection routing plan and the changes planned for the second version of the mixer-feed housing. Since the local oscillator board need not contain the voltage regulator, its size can be reduced and the channel from the mixer diode can be extended all the way to the IF amplifier board position. The signal routing is shown for the case in which the limiter is on the IF amplifier board. The dotted-lines show an interconnection scheme for the case where the limiter is located on the signal processor board.

The layout for the first engineering model IF amplifier is shown in Fig. IV-30. Two more stages than actually needed are included, it was not expected that the limiter would have as much gain as it does, and so the two stages were included here as a precaution in case more gain was needed. In future work, this layout will be changed to include the IF filter between the first and second stages and to incorporate other circuit changes.

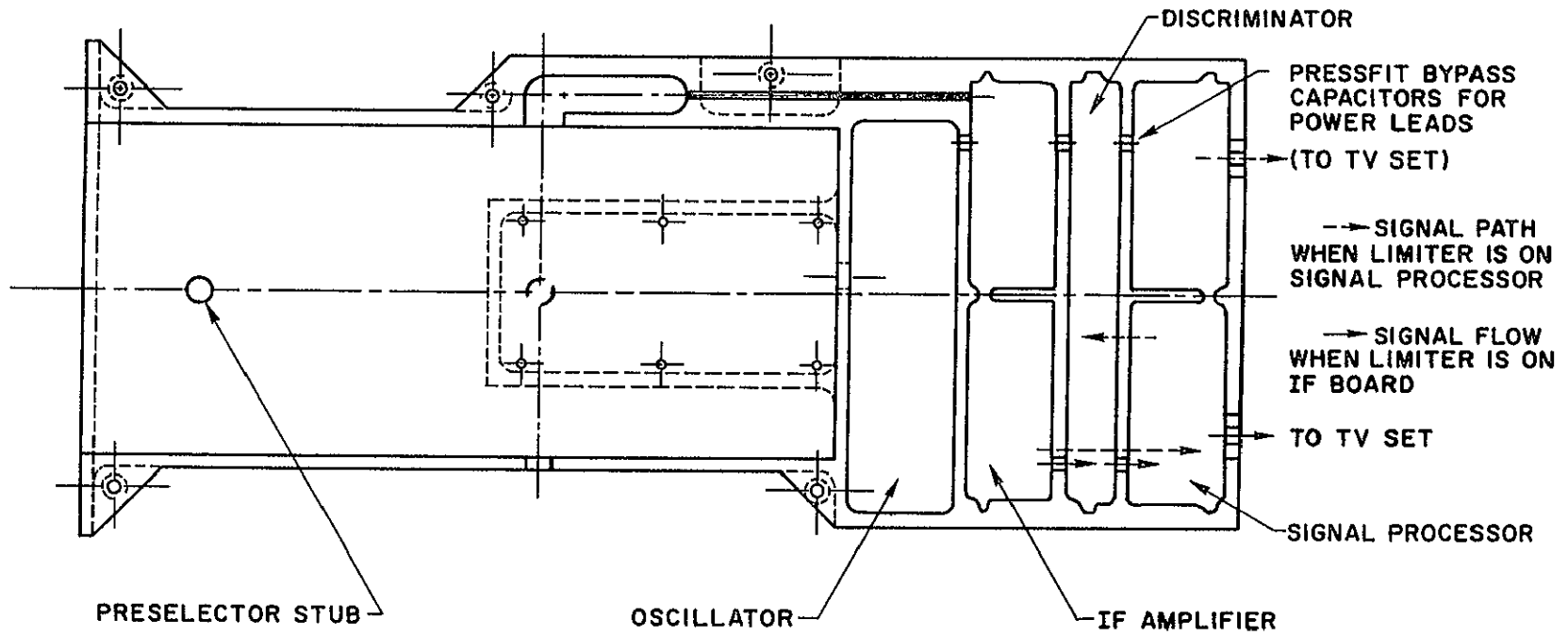
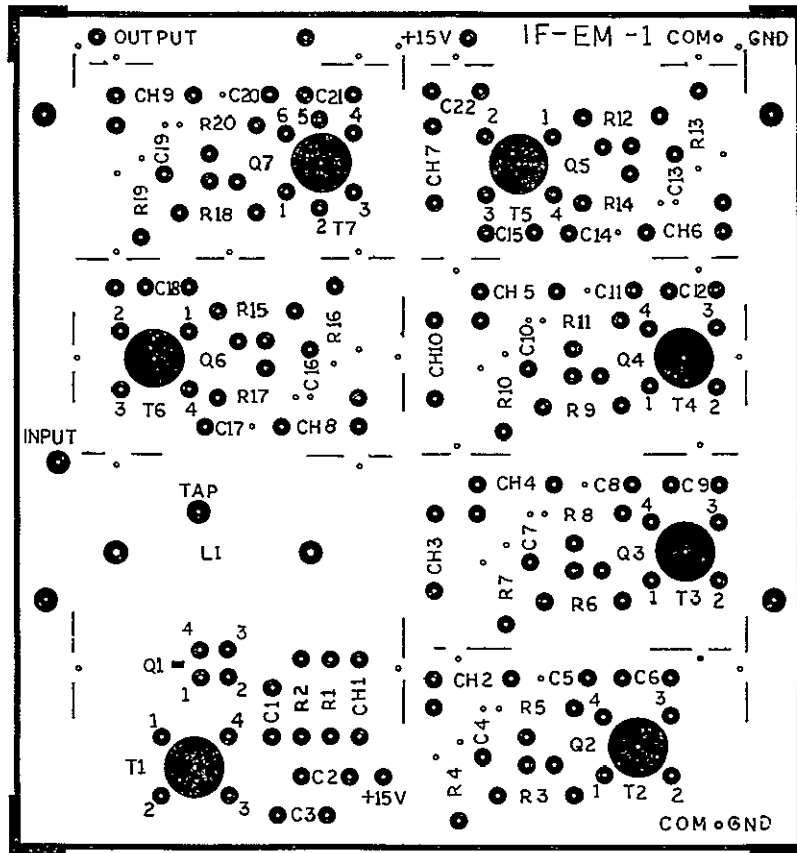


Fig IV-29 SKETCH OF PROPOSED CHANGES IN LAYOUT OF MIXER-FEED HOUSING.



GROUND PLANE COMPONENT SIDE

Fig. IV-30 IF AMPLIFIER LAYOUT

Experience has shown that it is advisable to shield the first and sometimes the second stage, even though there may be only one more stage in the same compartment, just to provide a constant electrical environment from the designer's bench to the installation. This helps to prevent interference and eliminates the small variations in bandpass response which can be caused by small changes in stray capacities or other coupling mechanisms. This should be done for the second IF amplifier layout, where the IF filter is to be inserted between the first and second stages, because the coils have a definite susceptibility to strays and extraneous signals. An egg-crate-like arrangement of inter-stage shields was installed on the first IF layout, to facilitate bench experimentation, but it may not be needed in the final model, except around the first stages.

The layout for the signal processor circuitry is given in figure IV-31. It is possible that some significant changes may be needed in the remodulator circuitry, and so this board is likely to be relaid out also.

The layout of the discriminator is given in Fig IV-32. The short-circuiting soldered pin is not shown.

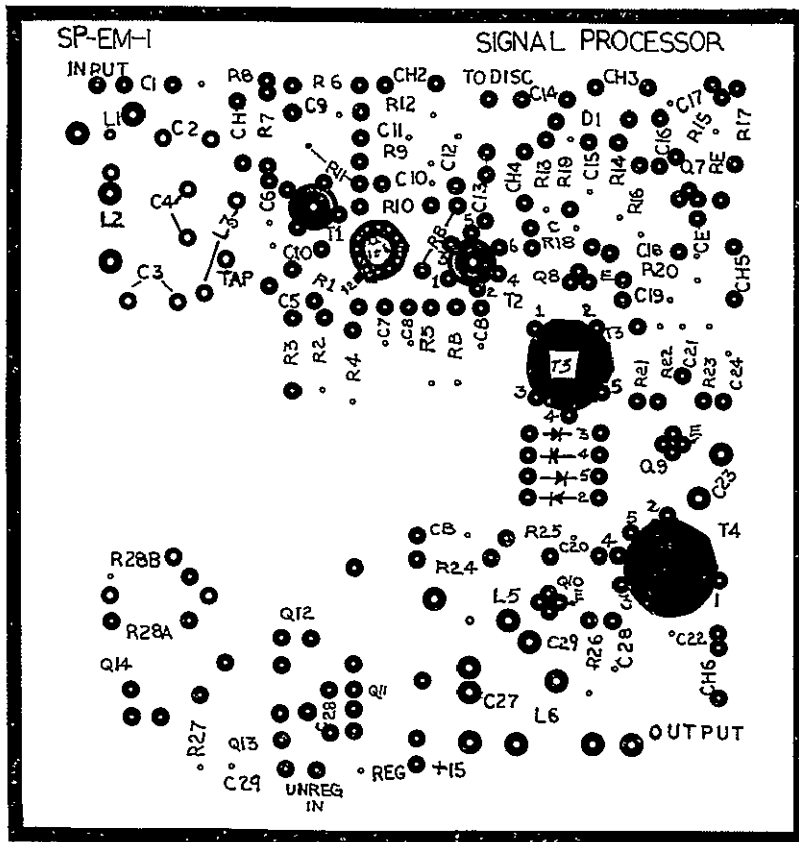
Performance of the IF, Limiter, Discriminator and Remodulator

Complete subsystem integration has not yet been accomplished. The local oscillator and mixer are working properly, but some work remains to be done with the front end, and is discussed in the next section on future work.

The IF amplifier has adequate bandpass and gain response, and needs only to have the first stage enclosed, as discussed in an earlier section.

The limiter provides uniform gain over the entire passband and over a 10 dB range of limiting, with an output power level at -5 dBm, this is slightly lower than originally desired, but is not critical and can be changed by rebiasing the constant current sources.

The discriminator-detector provides good linearity as measured by a static test, the result of which is shown in Fig. IV-20. A dynamic test using an FM signal should be performed to measure intermodulation distortion.



NOT REPRODUCIBLE

Fig IV-31. SIGNAL PROCESSOR BOARD LAYOUT

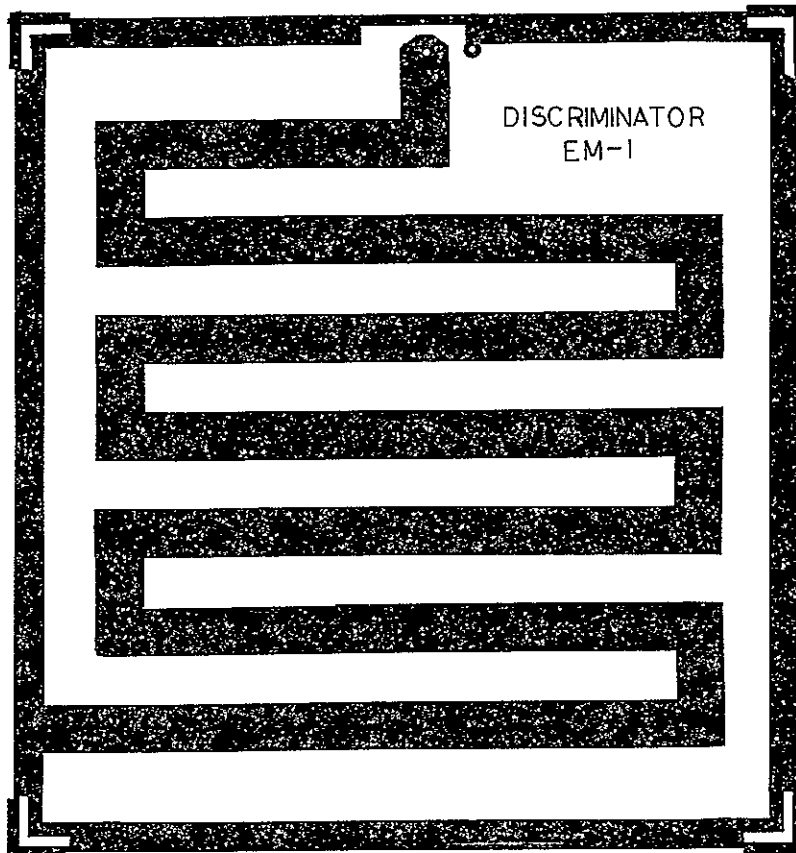


Fig. IV-32 DISCRIMINATOR BOARD LAYOUT.

The remodulator circuitry is very nearly complete, some minor circuit details must be attended to. Tests on the double balanced mixer indicate that adjustment is more critical than expected, and some attention could be given to the possibility of using active devices in a single balanced mixer instead of the present configuration.

Future Work

A great deal of the basic design is finished, and the concepts are justified, what remains for completion of this first prototype consists of attending to the details of subsystem integration, development work on the preselector filter (LO radiation trap), and impedance matching the mixer-feed to free space

Although this present prototype demonstrates the feasibility of a mass-producible, low-cost design, there are still a number of

changes in the layout which should be incorporated in a second prototype, along with the matching structures and preselector work, in order to move even closer to a final design. Similarly, the circuit boards should be relaid out to take account of the changes and improvements determined from the testing of the first engineering models. A local oscillator board with an LC oscillator should be fabricated, and a 167 MHz-X15 SRD multiplier should be investigated. In addition, development should be undertaken of the polarization converter needed to change the circularly polarized satellite signal into a linearly polarized signal. Since this front-end need not be broadband, two matching stubs mounted oppositely in the feed at 45° angles to the horizontal and spaced a quarter-wave apart, could be used, some experimental work with the original single-diode mixer is needed.

V COST ESTIMATES OF ELECTRONICS PACKAGE

The baseline design is taken from the working model configuration, with all of the modifications suggested in Section IV. The two major changes in the baseline design consist of a modification of the local oscillator configuration, which now employs a 250 MHz temperature compensated, LC oscillator instead of a crystal-controlled oscillator-multiplier, and the substitution of a 6 dB Noise Figure Schottky Barrier diode instead of the 5.5 dB diode previously used.

The method of costing this baseline design consists of obtaining a parts cost for several magnitudes of production. Then, empirically obtained assembly costs (given as a percentage of parts cost) are applied, with appropriate modifications to allow for differing module complexities. Finally, empirically obtained overhead and profit factors are included. It is assumed that manufacture of this equipment would be undertaken by established companies, and thus the start-up cost for producing a new product would be much less than if a new company were to be created. These start-up costs are not considered here.

A Origin of Costs

Brazilian component costs are used wherever applicable. They come from manufacturer price lists notably from a Phillips division IBRAPE which were obtained last year while one of the staff, Mr. Janky, visited Brazil. Most of the price quotes are for 100-lot prices. For Brazilian components, the reduction in price for large-quantity purchases is small, because the profit margin is set by Federal law.* This reduction may be expressed as the ratio of unit cost to 10^N -lot cost, when N is an integer. The sales price for each kind of component generally obeys a particular reduction rate as a function of quantity. However, the actual cost to produce that component may obey a much different trend. Both sales price and manufacturing price can be treated with a learning curve.

* Conversation with Amaden A. Machado, Director of Mialbras, an Italian-Brazilian capacitor manufacturer in Sao Paulo, Brazil, August, 1969.

B. Learning Curves

The learning curve is simply a name used to describe the geometric reduction in cost which occurs as volume increases. It is normally defined in terms of a percentage, such as 85%, and means that for each time the quantity produced is doubled, the new cost for an item is 85% of the old cost. This can be expressed mathematically as

$$\text{Cost (Q)} = \text{Unit Cost (learning curve \%)}^{\log_2 Q} \quad (1)$$

where Cost (Q) is the cost for Q items, given the unit cost and the desired learning curve percentage. A straightforward manipulation with logarithms yields

$$\text{Cost (Q)} = \frac{\text{Unit Cost}}{Q^{-\log_2 (\%)}} \quad (2)$$

which is better suited to our needs. The factor $Q^{-\log_2 (\%)}$ can be treated as a reduction factor. A graph of reduction factors versus quantity Q for various learning curve percentages is given in Fig V-1. Historically, manufacturing costs have generally followed an 85% learning curve [3]. However, a brief survey based on manufacturer quotes for components in this receiver indicate that sales prices generally follow a somewhat shallower learning curve. The reduction factors range from 92% for older technology components to 97% for new-technology items such as the microwave diodes. Wherever possible, direct quotes from manufacturers were obtained, especially for items which must be imported to Brazil. In order to fill in the blanks on such items as resistors, capacitors, and less sophisticated semiconductors, a 97% learning curve was applied for all Brazilian components. This shallow curve was used because of the previously indicated low markup to unit price on such components. It allows a 40% reduction in cost from the unit price to the 100,000 lot price. Many American-made components exhibit a much greater reduction for large-quantity purchases, for example, the single-lot cost of a KA35J3 Fenwal Thermistor is \$0.85, but the factory quote for 100,000 units is \$0.09, when purchases within one year. Thus the 10,000 unit parts cost is probably conservative.

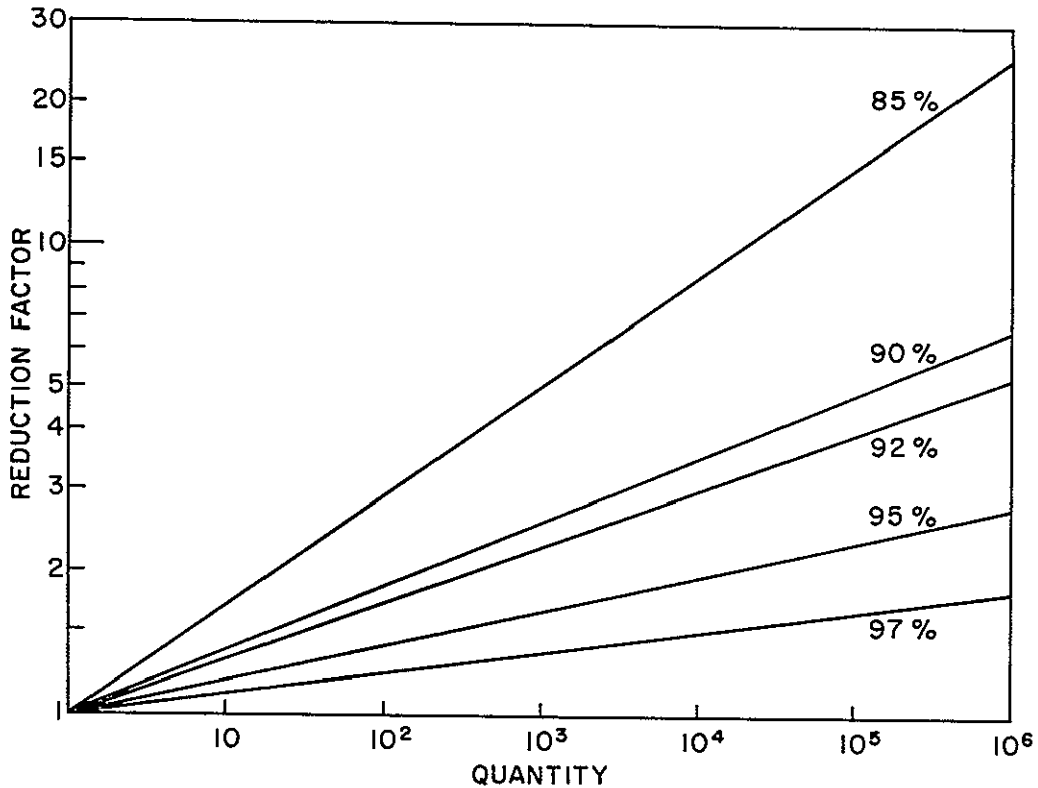


Fig V-1 REDUCTION FACTOR VERSUS QUANTITY

C Component Costs

All of the components used in the receiver are listed in Table V-I. The quantity used in each module is identified and totaled in the successive columns. The unit cost for quantities from 10 to 100,000 are listed, and the total cost for each quantity is tallied at the bottom. Small hardware items such as screws, wire, or rivets are accounted for in the miscellaneous entry. The table does not include the twin-line which would connect the electronics package to the power supply and television set, because there is sure to be a large variation in length from one installation to another, and should therefore be included as an installation cost.

Many of the semiconductor components listed are produced in both the U.S. and Brazil. However, the larger volume production in the U.S. of components, such as the 2N3866 power transistor, makes possible a much lower cost. For such cases, then, the U.S. cost is quoted. In the event

that full-scale production at the 100,000 unit level is planned, a substantial reduction in the Brazilian cost for such components should certainly occur, and a new estimate should be used. If, for other non-economic reasons, it is desirable to use Brazilian-made components regardless of cost, the parts cost would increase by \$3 00 at most, since the only components unavailable are the microwave mixer and step recovery diodes, the RCA3049 integrated circuit and the 3N159 Field Effect Transistor. All other components are available in Brazil, or could be produced.

The parts cost ranges from \$113 56 for 10 units to \$30 63 for 100,000 units. Inspection of the table indicates that the three most costly items are the two microwave diodes and the mixer-feed housing assembly. Because of their relatively high cost, it is worthwhile to examine these items in more detail.

D Mixer-Feed Housing

The method of fabricating the mixer-feed housing and the filter insert depend on the quantity desired. The mixer-feed housing pieces are most economically produced by sand casting for quantities from 2 to 3,500. At 3,500 units, the cost for die-casting is about the same as for sand casting, based on quotes from two American manufacturers. * We arbitrarily estimate that Brazilian costs should be approximately 3/4 of these costs, since labor and overhead costs are less in Brazil. ** The Brazilian purchase price is estimated at \$3 69 for 100,000 units. Table V-II lists the methods which could be used as a function of quantity. The cost for both sand-casting and die-casting is shown in Fig V-2.

* The sand casting quotes are from the Palo Alto Foundry and the die casting quotes are from Wells Die Casting Co, 1960 Carroll Ave, San Francisco, Calif.

** The large quantity die casting costs in Brazil may be estimated another way. For this case, the cost of the housing is essentially for the aluminum. The housing weighs 3 pounds, and aluminum is about \$0 47/pound, and so there is about \$1 50 worth of aluminum needed. Allowing 100% for an overhead-and-profit margin for a casting firm such as D F Vasconcellos, the casting cost should be about \$3 00. The larger figure of \$3 60 will be used in order to provide a conservative estimate.

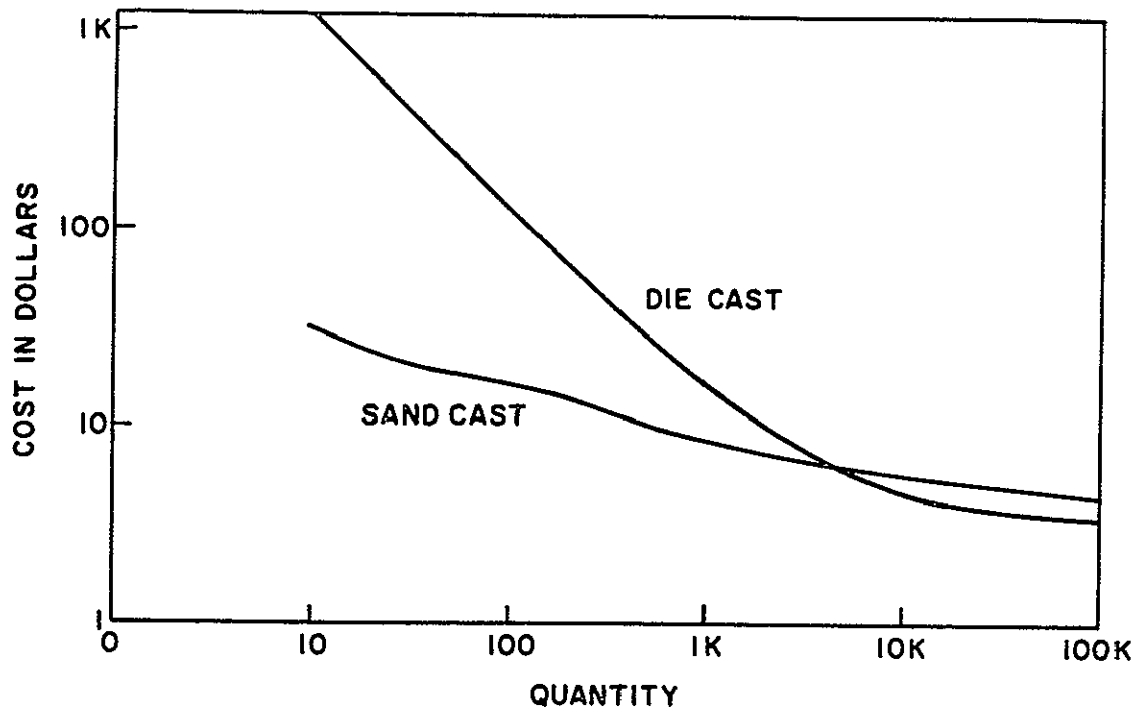


Fig V-2 PRODUCTION COST OF MIXER-FEED HOUSING VERSUS QUANTITY

for 100,000 units. Table V-II gives the methods and mold cost estimates for various quantities

Table V-II

MIXER-FEED HOUSING MOLD COSTS

Quantity	Method	Cost	
		American	Brazilian (3/4)
2-25	Sand cast, wooden double shrink master, family pattern	\$250 + \$16.75/unit	\$188 + \$12.50/unit
100	Sand cast, single shrink metal master, family pattern	\$900 + \$12.15	\$675 + \$9.12
1000	Sand cast, individual metal masters	\$1320 + \$9.50	\$990 + \$7.13
3,500-up	Die cast, two pieces	\$14,666 + \$4.75	\$11,000 + \$3.56

The filter insert should be machined if no more than 100 pieces are ever to be produced. But if total production needs are more than 100 pieces, and 100-lot quantities or more are needed, it will be more economical to die cast the insert. A graph of cost estimates obtained from an American manufacturer* is given in Fig. V-3, from the quotes given in Table V-III. Again, a factor of 75 is applied to obtain the estimate for Brazilian costs. This results in a conservative estimate for the smaller volume costs, and a fair estimate for the larger volume costs.

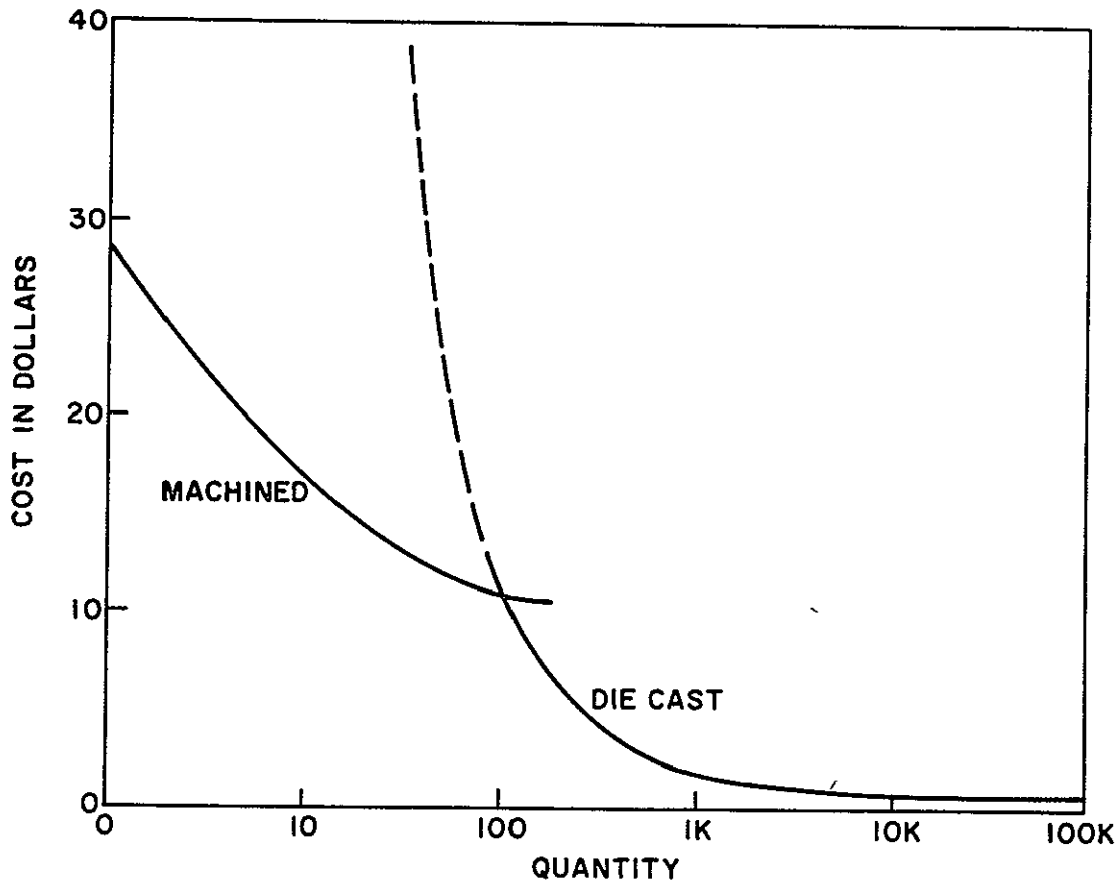


Fig. V-3 FILTER INSERT COSTS VERSUS QUANTITY

The costs for the diode mounting hardware follow a trend similar to that for the filter insert. A cost summary is given in Table V-IV.

As an indication of the conservative nature of the cost estimating, the total parts cost versus quantity is plotted on semi-log paper in

* Palo Alto Foundry, Palo Alto, Calif and Foster Precision Machinery, Mountain View, Calif

Table V-III

FILTER INSERT COSTS

	American	Brazilian
Die Cost	\$1337	\$1000
Piece Price		
50-100	\$2.50	\$1 88
100-1000	1 70	1 28
1000-10 K	1.01	0 76
10 K -100 K	1 00	0.72

Table V-IV

MIXER HARDWARE COST

Quantity	Cost
10	\$5 00
100	3 50
1000	1 50
10,000	75
100,000	50

Fig V-4 Curve A is the total parts cost, and reflects the dominant influence of the mixer-feed housing at low-production quantities. When this component cost is removed from the total cost, curve B results. This curve closely approximated a 94% learning curve, which is very conservative.

E Microwave Diode Costs

The large-quantity cost quotes from several manufacturers for various diode types is given in Fig V-5 as a function of stated noise figure. It has been previously discussed that the mixer diode noise figure should be 1 dB better than the overall receiver specification, or 6 dB.

Firm cost quotes can be obtained from diode manufacturers for 1000-lot quantities, beyond that, the price is subject to negotiation. There

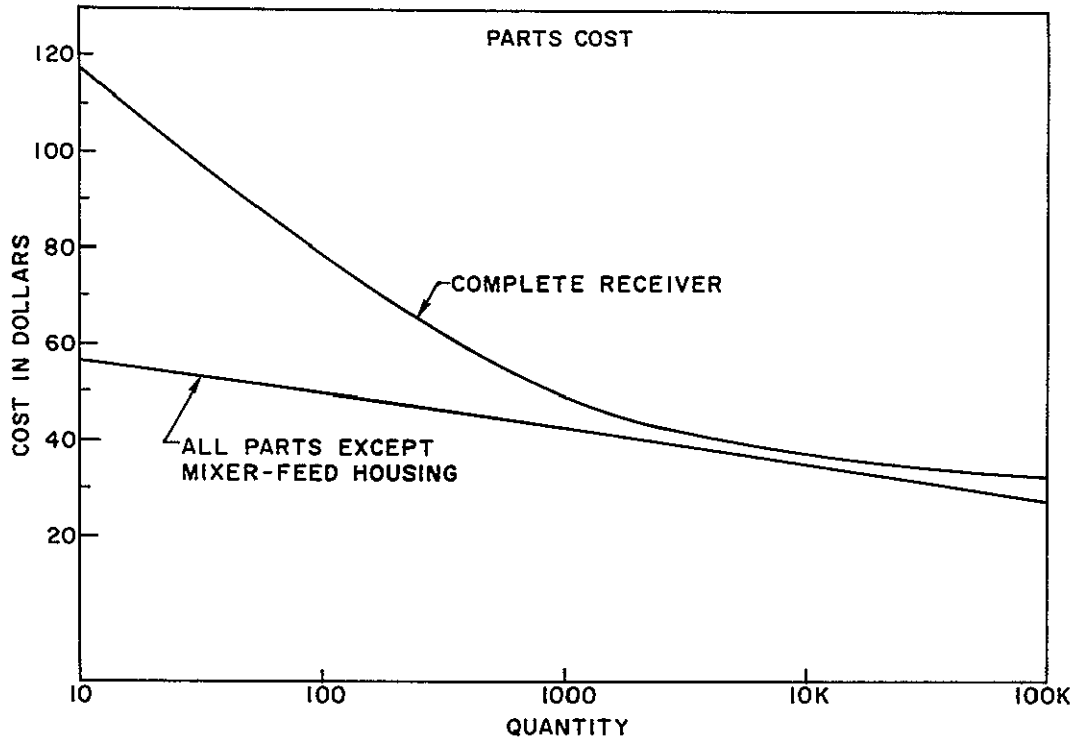


Fig V-4 PARTS COST VERSUS QUANTITY

has apparently never been such a large demand for these diodes from one customer to one vendor before and so there are no hard prices. In order to estimate a price, it is necessary to determine the cost contributions from the various operations needed to produce a diode.

The cost of fabricating the silicon junction is not substantially lower for the large-quantity requirement, since this process can be, or already is, automated. The cost of packaging the chip varies with the type of package, however, this process could also be automated to a large extent. Thus, almost any package could be specified for the large volume case. The major cost is incurred in the sorting and testing. For our application, the most important parameter to test for is the noise figure. If the worst of the production run is adequate for the needs of the application, then it is possible to gauge the cost for SB diodes by examining the cost for the worst point-contact diodes, the production of which is complete automated. In this case, the cost is \$0.60 for 100,000 units.* However, the worst noise figure generally

*The Sylvania quote for IN21 point contact diode is \$0.60 for large quantities.

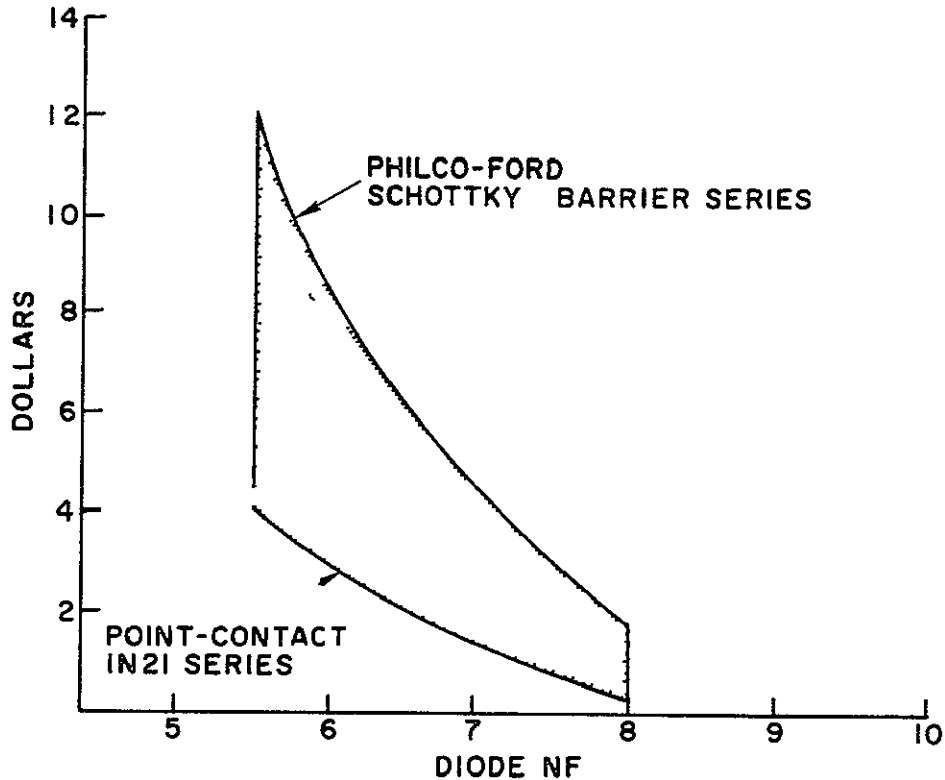


Fig V-5. PRICE RANGE OF MIXER DIODES VERSUS NOISE FIGURE

obtained from SB diodes below 3 GHz is about 7 dB, and the best is about 5.5 dB. To obtain 6 dB diodes, all of the diodes must be tested. If this test-and-sort procedure were automated, then the cost should increase by the amount needed for this operation. An automated noise figure testing machine should not cost more than \$100,000, and so the actual manufacturing cost should be less than \$1.50 per diode. If a 100% markup is allowed, then the 6 dB mixer diodes should cost no more than \$3.00 in very large quantities. At the present time, there is no demand for such quantities, and so there is no incentive to automate testing. Further, there are no doubt considerable R & D costs which must be recouped, and this inflates the price. But since there is considerable lead time available before full-scale production is scheduled, it is quite reasonable to assume that the diode costs will be at least as low as \$3.00 by 1975. However, the mid-1970 price for a large-quantity order, if delivered within one year's time, would be substantially

higher. Recent conversations with two manufacturers* indicate that \$6.00 is a reasonable estimate from which initial price negotiations could proceed. Consequently, that price is used for the large-quantity diode cost.

The possibility of using the Hewlett-Packard HP 2800 series Schottky-Barrier mixer diode is appealing because of the low-price of \$1.25 each in large quantities, but the typical noise figure is 6.3 dB at 2.6 GHz. If a 7-dB overall noise figure could be obtained with this diode, then it is definitely preferable to any other. Its present package is not quite suited to waveguide mounting, but that is a minor matter. It is felt that 6.0 dB noise figure diodes should be used in order to guarantee the 7 dB overall noise figure requirement, and so the \$6.00 price will be used. The question of the incremental costs for improving the receiver performance by using a 5.5 dB diode are discussed in the appendix on performance tradeoffs.

Because of the much larger production which has already occurred with point-contact diodes, a price of \$3.75 has been quoted by Sylvania for a 6 dB diode. The additional cost of \$2.25 for the Schottky Barrier diode is thus a very reasonable price to pay for the increased reliability and better temperature performance.

The future price for these diodes may also be estimated by simply applying a historical price trend. Conversations with several marketing representatives** indicate that a 20%/year decrease in the price for the next two years is a reasonable, conservative estimate. A 10%/year estimate is used for the next 3 years. The values are shown in Table V-V. The \$6.00 price is seen to drop to under \$3.00, as was previously estimated. After that, or perhaps slightly before 1975, the price may begin to increase because of inflation.

The D5817A is a Sylvania beamlead SB diode, which is supplied unpackaged from the vendor. The 1970 cost estimate is a firm quote. It is mentioned here because beamlead construction permits testing prior to packaging, this introduces the possibility of shipping the devices

* Sylvania and Philco-Ford

** Mr. Fran Udotch of Sylvania and Mr. L. Lieb of Hewlett-Packard

Table V-V

COST PROJECTIONS FOR MIXER DIODES

Device	Year	1970	1971	1972	1963	1974	1975
L8200B, D5221F		6 00	4.80	3 84	3.46	3.12	2 81
D5817A		2 65	2 12	1 70	1 53	1 38	1 24

to Brazil and packaging them there, with the consequent savings. The possibility of packaging the device in Brazil leads naturally to the next step of actually producing the complete device there. Since there are a number of semiconductor fabrication plants already in Sao Paulo, it is worth considering a discussion with those manufacturers there who are capable of producing Schottky Barrier diodes, such as Philco-Ford.

F Step Recovery Diodes

The December 1969 cost estimate of step-recovery diodes was \$5.00 for large quantities. The present 1-10 lot price for the suggested diode is \$8.20 (see Table V-I). The present estimate of \$4.00 is arrived at by application of a shallow (96%) learning curve, as described in a previous section. In light of the previous discussion on mixer diodes, it would appear that a substantial reduction in this price could be obtained by the time the project went into full production. A negotiated price less than \$3.00 should be feasible. The possibility of producing the diodes in Brazil is also worth considering, since microwave communications will certainly continue to expand and require such components commercially.

G Imported Components and Duty Considerations

Presently, a number of the components used in this radio are not manufactured in Brazil and therefore would have to be imported, unless plans are made to produce them in Brazil. These components are the mixer and step recovery diodes, the integrated circuit for the limiter, and the two field effect transistors. The power amplifier transistor

is available in Brazil, but at a much higher cost than from the U S In the interest of minimizing the receiver cost, it too should be imported, but there is normally a 100 percent duty on all imported electronic components, which increases the total parts price by the cost of these components, or \$13 70 If the duty were enforced, the total components cost would be \$44 33 However, this import duty could be waived, since the Brazilian government would be actively supporting and paying for the whole program Enforcing the duty would amount to inflating the equipment cost and needlessly spending money on red tape within the government

H Factory Costs Assembly, Overhead, Profit, and Taxes

Estimates for large-quantity factory costs will be given first, since this is the most interesting case, and statistical information is available to make reasonable estimates The method used in this first estimate should be applicable for production quantities of 10,000 units and more, but the numbers will of course change A method for estimating the factory cost for smaller quantities is then given None of these estimates account for start-up costs associated with training of personnel or buying new equipment, or any other initial investments All of these estimates assume that the development stage is reasonably complete, and at least 10 prototypes have been constructed in order to assess and remove any bugs

A sampling of the radio-television industry in Sao Paulo, where over 600,000 television sets were produced in 1969, indicates that the cost for assembly and adjustment is about 8 percent of the cost of parts Since all of the components needed for a television set are manufactured in Brazil, the cost of parts from which the 8 percent figure is derived are the total costs and include no extra costs for duty It therefore follows that the empirical 8 percent factor for estimating the assembly and adjustment costs should be applied to the duty-free total cost of \$30 63 This amounts to about \$2 50 and brings the production cost to \$45 50 If the duty was enforced, this production cost would be \$46 83

Overhead and profit in the radio-television industry in Sao Paulo ranged from 50 to 80 percent of the production cost This is much lower than in the United States and is due largely to the fact that little

remainder of the estimates, given for other quantities, will not include it. It has been given for this case simply as a reference.

I Alternative Configuration Costs

The 100,000 unit parts cost is broken down by module function and is shown in Table V-VII.

Table V-VII

MODULE PARTS COST (100,000 units)

Module	Cost \$
Mixer Diode, 6 dB	6 00
Mixer-Feed Housing	4 85
Local Oscillator	6 83
IF Amplifier	4 43
Limiter	2.25
Discriminator	0 62
Remodulator	2.05
Power Supply	2 57
Miscellaneous	<u>1 00</u>
TOTAL	\$30 63

Several alternative configurations, such as the use of a crystal-controlled local oscillator, have been costed and are included in Table V-VII for the sake of comparison.

It is very tempting to consider the possibility of obtaining the 7 dB specification with the much less expensive Hewlett Packard diode, since the parts cost would be reduced to \$25 63. However, the savings in parts cost could be partially reduced if more adjustments or more time is needed to obtain the performance.

J Low-Volume Production Cost Estimates

The problem of estimating the cost of assembly and test for small quantities is complicated by the lack of experience in actually building

Table V-VIII

ALTERNATIVE MODULE COSTS (100,000 units)

Alternative	Incremental Cost	New Total Parts Cost
5 5 dB diode	+ 3 00	\$33 63
HPA 2827 6 3 dB diode	- 5 00	25 63
Crystal Controlled LO	+ 2 16	32 79
Second Channel (filter, limiter, discriminator, remodulator)	+ 5 50	36.13
Crystal Control, 5 5 dB diode, and second channel	+10 66	41 29

and testing the receiver, since only one, the working model, has been built to date. A much better estimate could be made after several more engineering models were fabricated. However, some rough approximations can be made by comparing this receiver design to others of comparable complexity.

A very small sampling of receiver manufacturers in the Palo Alto area indicated that for quantities between 10 and 100 units of modules similar to those used in the present receiver, the breakeven price was six times the cost of parts. The production cost and the assembly and test costs can be estimated by working back from this ratio of factory cost/parts cost. If overhead is 100 to 125% of production costs, then production costs are $6/2 = 3$ or $6/2.25 = 2.67$ times the cost of parts. This means that the cost of assembly and test is 1.67 to 2 times the cost of parts.

This factor could also be derived by applying an appropriate learning curve in reverse; that is, we assume that the factor of 8% previously used for large quantity assembly cost estimates also obeys a learning curve. If it is further assumed that this 8% factor is based on an accumulated experience of at least one million units, then we calculate the assembly and test factor for 10 units by taking the ratio of the reduction factors for 100,000 units and 10 units from the appropriate learning curve. Using a standard 85% learning curve, the assembly and test factor becomes

$$\frac{26.3}{1.71} \times 8\% = 122\%$$

and so this estimate indicates that assembly and test costs amount to 1.22 times the cost of parts, for 10 units.

To obtain the empirically-observed assembly-and-test factor in the range from 1.67 to 2, an 83% learning curve must be used. Thus

$$\frac{41}{1.86} \times 8\% = 176\%$$

or an assembly and test factor of 1.76. Thus there appears to be a reasonable agreement between observed costs and costs estimated with a learning curve. While an actual measure of the time it takes to assemble and adjust the receiver would be more accurate, this method can be used for a first approximation. The assembly and test cost factors (expressed as a percent of the parts cost) are shown in Table V-IX.

Table V-IX

TOTAL FACTORY COSTS

Quantity	Parts Cost	Ass'y Cost Parts Cost	Production Cost	Overhead & Profit Production Cost	Factory Cost
10	\$114	200%	\$342	100%	\$684
10 ²	82	100	164	100	308
10 ³	52	45	75.50	100	151
10 ⁴	39	25	49	90	93
10 ⁵	31	8	33.50	80	60

These values are taken from the 85% learning curve and rounded off upward to the nearest convenient fraction in order to maintain a conservative estimate. The basic cost estimate of interest is the production cost, given in the fourth column and expressed as a percent of the parts cost. This production cost is the sum of the parts cost, assembly, and test costs. The overhead and profit factor, expressed as a percent of the production costs, is included as a rough indicator, but it should be remembered that very often this factor is inflated to cover other costs, such as R & D costs. It is assumed for the sake of discussion that all

of the necessary R & D is complete, and that a number of successful prototypes have been constructed. For small quantity-production, it is reasonable to expect that the overhead burden may be somewhat larger than for the large-quantity case, and so a 100% value is arbitrarily assigned for production rates up to 1000. The value gradually drops to the 80% figure quotes previously of overhead and profit in large-scale production in Sao Paulo. The resulting factory prices range from \$708 for 10 receivers to \$60 each for 100,000 unit. It bears repeating that the \$708 cost is essentially for the second group of 10 receivers, the first 10 prototypes could cost at least \$1000 each. The ratio of factory cost to parts cost ranges from 6 to 1.95, this wide spread indicates a very conservative estimate for the price of the receiver in small quantities.

K Cost Implications for a Brazilian Satellite Program

The estimated national annual educational budget in Brazil in the 1970's is \$400 million, approximately 11% of the annual Federal budget. The duty-free, state-taxed estimate for the antenna and adapter is \$111, in 1969 the factory costs plus taxes for a 23-inch television set in Sao Paulo were approximately \$170. Assuming that 152,000 schools should be equipped with these receivers, the cost for the hardware is \$43 million. In areas that are not yet electrified, an electric generator would be needed, and the cost would increase by less than \$2 million. Thus the total capital cost for all ground hardware is less than \$45 million. The rest of the hardware needed includes the satellite, the launch vehicle, the programming and transmitter facilities, and other miscellaneous items which have been estimated to cost \$36 million*. No more than one-third of the \$86 million capital cost would have to be financed during the first year of operation. This would require that the educational budget be increased by less than 7.5% in the base year. The additional capital expenditures could be financed over a 9-year period by increasing the educational budget by slightly more than 1% per year. Thus the cost of the equipment needed to bring an instructional television supplement to Brazil is very small in comparison with the projected budget.

The major expenses incurred in implementing such a system in addition to maintenance would be for salaries. People must write and produce

* ASCEND study, pp. 1-17.

the programing Teachers in the rural areas must be instructed in the use of the supplemental programing. A field support staff must be organized to gather information on the system operation in order to assess the problem areas as well as the successful aspects The ASCEND study estimates the annual operating cost at \$19.1 million for Brazil * This represents a small additional 5% of the projected budget

* ASCEND study, pp 2-90

VI. TRENDS FOR HIGHER FREQUENCIES

A. Configuration as a Function of Frequency Range

The present configuration is useable to approximately 6 GHz. Use of the single-diode mixer is possible to 6 or 8 GHz with very little change in concept. Of course, both mixer and step recovery diodes will be more expensive, assuming that the same 7 dB noise figure is required. Above 8 GHz, it may be very difficult to achieve a 7 dB noise figure in a mass-production design, 8 or 9 dB may be a much more reasonable goal. Beyond 6 GHz, it is expected that the fabrication and adjustment of the local oscillator will become much more difficult than it is worth, in comparison to other methods. Above 8 GHz, bulk-effect oscillators such as the Gunn diode mounted in a cavity could be used, if the 100 KHz guardband were inserted into the video signal prior to frequency modulation. There is a grey region from 6-8 GHz in which one could use an SRD multiplier of somewhat different design.

Use of the single-diode mixer is predicated on a low-AM noise level from the local oscillator, the AM noise properties of Gunn oscillators are usually much worse than those of SRD multipliers, and so a balanced mixer should be used with a Gunn oscillator. This is a less expensive alternative than using a lower-noise multi-stage SRD multiplier and a single-diode mixer, on the basis of cost and circuitry complexity. If a video guardband cannot be used, then a Gunn oscillator which is phase locked to a stable source through a lower-power SRD multiplier may be attractive, it should be investigated.

Dimensional tolerances become more severe in direct proportion to increasing frequency, thus the question of sensitivity becomes even more important at higher frequencies. This is most severe for the antenna surface. The present 10 segment 7-foot design is adequate to about 5 GHz, beyond that, a solid true parabola becomes more desirable, and at 12 GHz is a necessity. This will also mean an increase in cost, but by how much depends on the communication system specifications.

Preceding page blank

B. 12 GHz Communications System Specifications

A high-quality communications system at 12 GHz generally imposes more severe constraints on all specifications for both satellite and ground receivers. Frequency stability becomes more critical, as does the ability to keep the antenna pointed in the proper direction, since the beamwidth decreases for a given diameter as frequency increases. This implies that the satellite must be kept in the desired orbit location with much more precision than is necessary at 2.62 GHz. Station-keeping to 0.1° is feasible, and so this is not a serious problem.

One must allow an extra dB of signal strength as additional margin for the greater attenuation due to rain, and the one or two dB loss expected in the system noise temperature must also be accounted for. Given the exponential cost of antenna, and the large number of receivers being considered, it is felt that this 3-dB increase should be made up in the satellite ERP and not in the ground receiver figure of merit. Therefore, the following set of system parameters is proposed, as shown in Table VI-I. An antenna of 7 to 8 feet in diameter is assumed as the maximum which could be mass-produced by either stamping in one piece or by using a segmented method with doubly-curved petals, instead of singly-curved petals as in the 2.62 GHz design. Further tradeoff studies are needed to find the best allocation of A_e and T_e for a given figure of merit. But based on the use of a 7-foot diameter antenna and the cost analysis in ASCEND on antenna stamping, we suggest that such an antenna could be mass-produced for approximately \$80. The components for a 12 GHz adaptor and their costs are summarized in Table VI-II. The costs shown in this table for the front end are estimates only, and are not based on any existing hardware design.

We suggest that a crystal-controlled SRD-Multiplier be used to injection lock a Gunn oscillator, to provide adequate stability, if a wider IF bandwidth, and the resulting increase in satellite ERP, can be used, then this injection locking may not be needed for stability, and the local oscillator cost would be at least half as much. The mixer is double-balanced, and a waveguide realization is assumed. The remainder of the entries are the same as for the 2.62 GHz cost estimates. On the basis of the above configuration, we estimate that the cost of a 12 GHz

Table VI-I

12 GHz COMMUNICATION SYSTEM PARAMETERS

Effective Area of 7-foot Parabola (50% efficiency)		2 02 m ²
System Noise Figure		7 dB
System Noise Temperature		33 04 dB (2012°K)
Modified Figure of Merit A_e/T_e		-30 dB
Receiver Noise Bandwidth BW_{if}	$\beta = 2$	$\beta = 3$
	31 5 MHz	42 MHz
kBW_{if}	-153 65 dB	-152.38 dB
Required Carrier-to-Noise Ratio (4 dB rain margin, 3 dB beam edge margin)	17 dB	17 dB
Required Flux Density	-106 65 dBW/m ²	-105.38 dBW/m ²
Required Satellite ERP	55 70 dBW	56 97 dBW

Table VI-II

12 GHz RECEIVER COST ESTIMATES

Local Oscillator (injection locked Gunn Oscillator)	\$20 00
Mixer Assembly	20.00
Mixer-Feed Housing	6 00
Rest of Modules--same as for 2 62 GHz	<u>13.00</u> \$59.00
Assembly and Test 8%	4.80
Factory Cost	63.80 ~ 64.00
100% Overhead	128 00
Antenna Cost	<u>80 00</u>
TOTAL	\$208.00

receiver could be twice as high as the cost of a 2.62 GHz receiver. The extra 5 dB of satellite ERP required will increase the cost of the space segment by a substantial margin, and so the cost for 12 GHz direct broadcasting is quite a bit more expensive than at 2.62 GHz.

VII CONCLUSIONS

In the course of this contract, the requirements of a mass-producible microwave adaptor have been analyzed and a working model has been designed and fabricated. The existence of the prototype antenna of novel design and the 2.62 GHz integrated mixer-feed electronics housing are ample proof of the technical feasibility of such a receiver. See Section I for a more complete description of the adaptor characteristics. While the first prototype of the electronics package is not yet the ideal finished product, most of the changes needed to bring it closer to that ideal have been outlined, and require no radical departure from the present concept of the adaptor.

A cost estimate has been made for a range of quantities from 10 to 100,000 units, and is summarized in Table VII-I.

Table VII-I

FACTORY COST SUMMARY FOR ADAPTOR*

Quantity	10	10^2	10^3	10^4	10^5
Antenna	125	89	43	34	32
Electronics Package	684	308	151	93	60
Total Cost	809	397	194	127	92

* These estimates include parts, assembly and test, overhead, and profit, but no taxes, and is the price which a factory would charge to a buyer.

The large-quantity estimates (>1000) are of principal interest. They are based on conservative parts costs and large-quantity production costs estimates obtained by sampling the industry in São Paulo, Brazil.

Initial considerations for a 12 GHz adaptor indicate that such a receiver is more complicated because many requirements become more stringent and the microwave components become much more expensive as the receive frequency increases. The first cost estimates based strictly on a paper design indicates that the 12 GHz adaptor will cost about twice

as much as a 2 62 GHz adaptor, further development work is needed to make this estimate more concrete.

The most important conclusion is that microwave adaptors can be mass-produced, in both developed and developing nations, at a cost which makes satellite broadcasting economically feasible. However, this fact is no guarantee that such a system will be immediately incorporated into educational systems. Part of the reluctance to accept a technological innovation can be traced to such reasons as little knowledge of how to use it, uncertainty about how to implement it, and how to administer it. National planners should begin concentrating their efforts on solving the political and social problems of implementation, since an economically feasible hardware design is very nearly complete, and available.

APPENDICES

A PROGRAM FOR OPTIMIZING THE PETAL SHAPE, CALCULATING THE FEED HORN ILLUMINATION CONSTANTS, AND CALCULATING THE GAIN OF THE ANTENNA

The input data for this program are lines 2 through 6. The data are the antenna diameter in inches, focal length in inches, initial value for α (the feed horn illumination angle constant), the number of petals, and the frequency (GHz), respectively.

Lines 10 through 36 find the optimal $z_{\min}(y)$ for each y in 0.25 inch increments from the center of the antenna to the outside edge. The values of y and $z_{\min}(y)$ are written and punched on cards (by statements on lines 25 and 26) as Y , and ZS , respectively. The values for y and $z_{\min}(y)$ completely define the optimized petal shape.

Lines 37 through 46 calculate the feed horn illumination constants and the edge illumination.

Lines 69 through 71 index the value of α to search the range of $0.5 \leq \alpha \leq 1.4$ and to print out the gains for each α . This is done to find the optimum feed horn illumination pattern for the optimized antenna.

The printout, \$DATA, contains two columns which are, respectively, y and $z_{\min}(y)$. Following this, data printed out is arranged as follows:

```

0 15917  -1 36069
           0 36           35.50           31 04
etc

```

The number 0 15917 is the value of K in $K \cos^2 \alpha \theta$, the feed horn pattern, for $\alpha = 0.5$, the initial value for α . The number -1 36069 is the value of the edge illumination, i.e., down 1 36069 from the beam axis gain. The 0 36 is the antenna efficiency. The number 35 50 is the maximum gain if the feed and antenna were perfect. The number 31 04 is the actual gain.

```

1          DIMENSION Z(1000)
2          D=84.0
3          F=34.62
4          FEED=0.5
5          N=10
6          GHZ=2.62
7          AN=N
8          A=TAN(3.14159/AN)
9          WL=11.8/GHZ
10         Y=0.0
11         I=0
12         II=1
13         14 ZS=(Y*Y)/(4.0*F)
14         12 X=0.0
15         SUM=0.0
16         10 SIG2=(F+ZS=SQRT((F-ZS)**2 +Y*Y+X*X))**2
17         SUM=SUM+SIG2
18         X=X+0.1
19         IF(X=Y*A)10,10,18
20         18 IF(ZS=(Y*Y)/(4.0*F))21,21,16
21         21 GO TO 17
22         16 IF(SUM=SSUM)17,17,22
23         22 ZS=ZS+0.001
24         Z (II)=ZS
25         WRITE(6,75)Y,ZS
26         WRITE(7,75)Y,ZS
27         75 FORMAT(10X,2F10.5)
28         GO TO 13
29         17 SSUM=SUM
30         ZS =ZS+0.001
31         I=I+1
32         IF(I=99)12,12,13
33         13 Y=Y+0.25
34         II=II+1
35         I=0
36         IF(Y=D/2.0)14,14,15
37         15 SUM=0.0
38         TH=0.0
39         200 SUM=SUM+(COS(FEED*TH))**2*SIN(TH)*0.015708/FEED
40         TH=TH+0.015708/FEED
41         IF(TH=1.5708/FEED)200,200,201
42         201 FED=1.0/(6.28318*SUM)
43         FEDD=1.0/(6.28318*(1.0-COS(ATAN(8.0*F*D/(16.*F*D-D*D))))))
44         EDGF=ALOG10( (COS(ATAN(8.0*F*D/(16.*F*D-D*D))*FEED))**2)*10.0
45         WRITE(6,59)FED,EDGE
46         59 FORMAT(5X,2F10.5)
47         SUM=0.0
48         SUMM=0.0
49         J=1
50         195 Y=J
51         Y=Y/4.0
52         II=J+1
53         X=0.0
54         52 THETA=ATAN(SQRT(X*X+Y*Y)/(F-Z(II)))
55         GG= (COS(FEED*THETA))*SQRT(FED)
56         1*COS(6.28318*(F+Z(II)=SQRT((F-Z(II))**2+Y*Y+X*X))/WL)
57         1*0.0625

```

```

58      SUMM=SUMM+GGG
59      X=X+0.25
60      IF(X-(Y-0.125)*A)52,52,51
61      51  J=J+1
62      IF(Y-D/2.0) 195,196,196
63      196 SSUM=SUM*SUM/(SUMM*SUMM)
64      GM=(3.14159*D/WL)**2
        1*AN*0.5*D*A*0.5*D/(3.14159*D*D/4.0)
65      GMM=10.0*ALOG10(GM)
66      GAIN=10.0*ALOG10(SSUM*GM)
67      WRITE(6,53)SSUM,GMM,GAIN
68      53  FORMAT(10X,3F10.2)
69      FEED=FEED+0.1
70      IF(FEED-1.4)15,15,300
71      300 CONTINUE
72      RETURN
73      END

```

\$DATA

0.00000	0.00000
0.25000	0.00045
0.50000	0.00181
0.75000	0.00406
1.00000	0.00722
1.25000	0.01128
1.50000	0.01625
1.75000	0.02212
2.00000	0.02889
2.25000	0.03656
2.50000	0.04513
2.75000	0.05461
3.00000	0.06499
3.25000	0.07627
3.50000	0.08846
3.75000	0.10155
4.00000	0.11554
4.25000	0.13043
4.50000	0.14623
4.75000	0.17293
5.00000	0.19053
5.25000	0.20904
5.50000	0.22844
5.75000	0.24875
6.00000	0.26997
6.25000	0.29208
6.50000	0.31510
6.75000	0.33902
7.00000	0.36384
7.25000	0.38957
7.50000	0.41620
7.75000	0.45373

8.00000	0.48216		
8.25000	0.51150		
8.50000	0.54174		
8.75000	0.57288		
9.00000	0.60492		
9.25000	0.63787		
9.50000	0.67172		
9.75000	0.70647		
10.00000	0.75213		
40.25000	12.09886		
40.50000	12.25464		
40.75000	12.41132		
41.00000	12.55891		
41.25000	12.71739		
41.50000	12.86678		
41.75000	13.02707		
42.00000	13.17827		
0.15917	-1.36069		
	0.36	35.50	31.04
0.20386	-2.00932		
	0.43	35.50	31.80
0.25854	-2.82293		
	0.50	35.50	32.46
0.32253	-3.83587		
	0.56	35.50	32.97
0.39557	-5.10130		
	0.61	35.50	33.33
0.47750	-6.70629		
	0.64	35.50	33.54
0.56823	-8.80707		
	0.64	35.50	33.58
0.66774	-11.72698		
	0.63	35.50	33.46
0.77600	-16.33138		
	0.58	35.50	33.16
0.89297	-27.11288		
	0.52	35.50	32.66

B PETAL PLOTTING PROGRAM

The optimizing program output provided a regular printout and a deck of cards, each of which was punched with y and $z_{\min}(y)$. These cards are the input data for the Petal Plotting Routine and are read by statement 30 in a recursion method from $I = 1$ to $I = II$ where II is the number of input data cards. The values of y and $z_{\min}(y)$ are given the new variable names $y(I)$ and $z(I)$.

The petal dimensions $R(I)$ and $S(I)$ are computed as follows

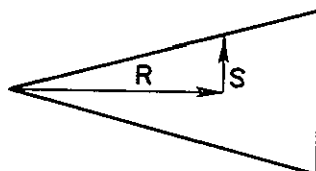


Fig. B-1. PETAL
DIMENSION ORIEN-
TATION

$$R(I) = \sum_{j=1}^I \sqrt{[Y(j) - Y(j-1)]^2 + [Z(j) - Z(j-1)]^2} \quad (B 1)$$

or

$$R(y,z) = \int_0^{R(y,z)} dy^2 + dz^2 = \int_0^{R(y,z)} 1 + \left(\frac{dz}{dy}\right)^2 dy \quad (B 2)$$

$$S(I) = Y(I) \times \left[\tan \left(\frac{180^\circ}{N} \right) \right] \quad (B 3)$$

These petal dimensions are then plotted on the 29 inch Cal Comp plotter. The petal computer plot is then used directly for petal fabrication.

Combining the Optimization Program and the Petal Plotting Program enables one to input four variables (diameter, focal length, number of petals, and frequency). In operation it takes only a few minutes to completely design the antenna petal and select the best feed pattern.

```

1          DIMENSION Y(3000),Z(3000)
2          CALL STRTP1(29)
3          N=10
4          AN=N
5          A=TAN(3.14159/AN)
6          II=169
7          I=1
8          30 READ( 5,20)Y(I),Z(I)
9          20 FORMAT(10X,2F10.5)
10         I=I+1
11         IF(I.GT.II)GO TO 25
12         GO TO 30
13         25 R=0.0
14         S=0.0
15         CALL PLBT1(20.0,14.0,23)
16         IPEN=3
17         I=0
18         10 I=I+1
19         IF(I.GT.3000)GO TO 100
20         IF(I.EQ.1)GO TO 40
21         GO TO 45
22         40 R=0.0
23         S=0.0
24         CALL PLBT1(R,S,IPEN)
25         IPEN=2
26         WRITE(6,101)I,R,S,Y(I),Z(I)
27         GO TO 10
28         45 R=R+SQRT((Y(I)-Y(I-1))**2+(Z(I)-Z(I-1))**2)
29         S=Y(I)*A
30         CALL PLBT1(R,S,IPEN)
31         IPEN=2
32         WRITE(6,101)I,R,S,Y(I),Z(I)
33         101 FORMAT(I10,4F15.5)
34         IF(I.EQ.II)GO TO 50
35         GO TO 10
36         50 IPEN=3
37         R=0.0
38         S=0.0
39         I=0
40         11 I=I+1
41         IF(I.GT.3000)GO TO 100
42         IF(I.EQ.1)GO TO 41
43         GO TO 46
44         41 R=0.0
45         S=0.0
46         CALL PLBT1(R,S,IPEN)
47         IPEN=2
48         GO TO 11
49         46 R=R+SQRT((Y(I)-Y(I-1))**2+(Z(I)-Z(I-1))**2)
50         S=Y(I)*A
51         CALL PLBT1(R,S,IPEN)
52         IPEN=2

```

```

53             IF(I.EQ.11)GO TO 100
54             GO TO 11
55             100 IPEN=3
56             WRITE(6,102)
57             102 FORMAT('END PROGRAM')
58             RETURN
59             END

```

C ANTENNA DIAMETER VS NOISE FIGURE TRADEOFF

Given a particular figure of merit A_e/T_e , it is desired to know the best size antenna and front end noise figure for a minimum cost. There is some kind of minimum, since a decreasing noise figure means an increasing cost, and a decreasing noise figure also means a decreasing antenna diameter and therefore a decreasing antenna cost. The cost information for microwave mixer diodes is given in Fig IV-5, the cost information for antennas is not quite as complete. We know that, in general, antenna costs follow an exponential function of diameter and reciprocal surface deviation, but in a small region from 6 to 10 feet and at a 2600 kHz frequency where mean deviations are not yet serious, a slightly more simple model could be used. Based on the present cost for a 7-foot antenna, and on an anticipated cost for a 10-foot antenna of similar design, the following cost model was constructed

$$\text{\$ Cost} = 8.55 D + 3.05 D^2$$

where D is the diameter in meters

Assuming $A_e/T_e = -27.61$ dB, one can construct a table of noise figures and the corresponding antenna diameters, the formula is $D = (T_e/227)^{1/2}$ the cost for each item is thus computed according to the formula, or taken from Fig V-5. The total cost is graphed versus the noise figure in Fig C-1. To obtain the stated noise figure, the diode used must be capable of 0.5 dB better noise figure. The data is given in Table C-I.

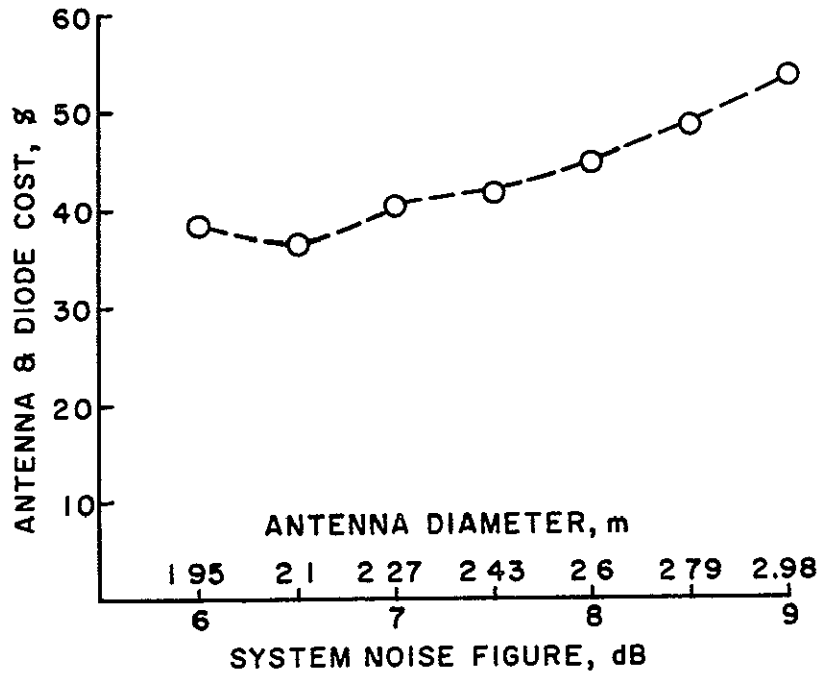


Fig C-1 ANTENNA AND DIODE COST VS SYSTEM NOISE FIGURE.

Table C-I

COSTS FOR VARIOUS ANTENNA-MIXER DIODE PAIRS FOR CONSTANT FIGURE OF MERIT

System Noise Figure dB	c	6.5	7	7.5	8	8.5	9
Antenna Diameter (m)	1.95	2.1	2.27	2.43	2.6	2.79	2.98
Diode Cost \$	10.00	6.00	5.00	3.00	2.00	1.00	1.00
Antenna Cost \$	28.30	31.50	35.10	38.80	42.90	47.60	52.50
TOTAL \$	38.30	36.50	40.10	43.80	44.90	48.90	53.50

D DELAY LINE OSCILLATOR

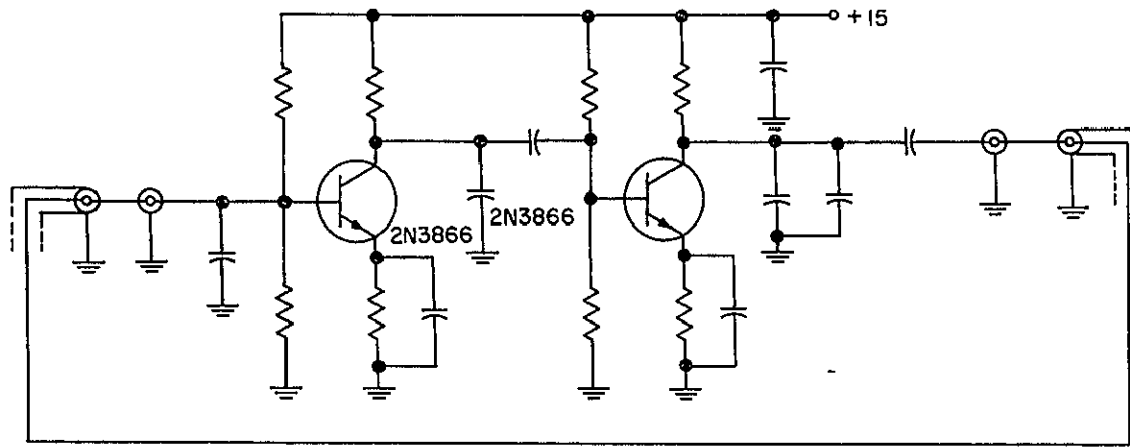
The original interest in the delay line oscillator stemmed from a desire to design an oscillator circuit which needed no adjustment whatsoever, the circuit would be assembled with components of a specified tolerance, and the resulting oscillation frequency would be within a

specified limit. The extent of this limit, called the fractional setting error (FSE) decreased as the receive frequency increased, for a fixed IF bandwidth. Originally, the extra bandwidth allowed was much larger than is presently permitted, thus making the FSE requirement quite loose. It was originally ± 4 MHz, which at 2500 MHz yields a FSE of 1.6×10^{-3} . If this amount is added to the 30 MHz 3-dB bandwidth of the IF, the total bandwidth becomes 38 MHz, and the noise bandwidth becomes about 40 MHz. This would require a 1 dB increase in carrier power to maintain the same carrier-to-noise ratio, and would require that much more of a linear region for the discriminator. Initial results indicate that this delay line oscillator could possibly meet the FSE requirement, but this oscillator is also slightly more expensive than a single-stage LC oscillator, including the cost of adjustment. Thus a much smaller allowable frequency variation and a factory-tuned LC oscillator would result in lower cost, lower satellite power, and a simpler discriminator. For these reasons, the delay line oscillator was set aside. But the fact that the delay line oscillator is much less sensitive to parameter variations than the lumped LC oscillator is worth reporting.

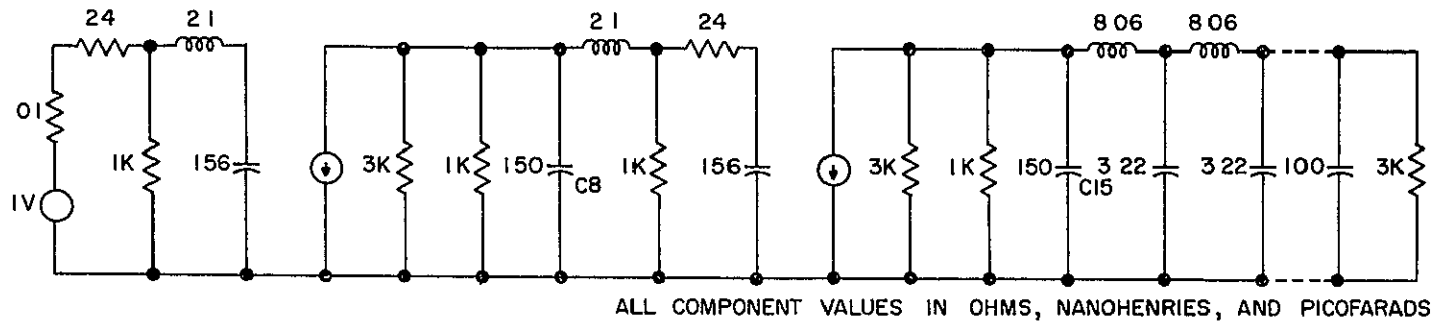
A delay line oscillator employing a two-stage amplifier and a length of transmission line has been analyzed with a computer program to determine its sensitivity to parameter variations. The schematic diagram and the equivalent circuit are given in Fig D-1, and the changes in resonant frequency for various changes in key parameters is given in Table D-1. This circuit provides more than an order of magnitude reduction in sensitivity to variations in shunt capacities.

This circuit reduces the sensitivity to component variations by using a distributed element to obtain the desired exact delay time and by using large shunt capacities to give close to 90° phase shift in each of the two amplifier stages. In each stage there is a phase shift due to capacitive loading of the output in addition to the 180° phase shift normally encountered. The magnitude of this phase shift is given by

$$\phi = \arctan(\omega RC)$$



a. Schematic diagram.



b Equivalent circuit

Fig D-1 TWO-STAGE DELAY LINE OSCILLATOR.

Table D-I

FRACTIONAL STABILITY FOR DELAY LINE OSCILLATOR $f_o = 270\ 338\ \text{MHz}$

Element, Nominal Value	Δ	Δf	$\Delta f/f_o$
C8 150 pf	+ 1 pf	- 1 3 kHz	$0\ 475 \times 10^{-5}$
	+10 pf	- 11 0 kHz	4.05×10^{-5}
C15 150 pf	+ 1	- 37.0 kHz	1.35×10^{-4}
	+10	-340 0 kHz	$12\ 4 \times 10^{-4}$
C40 150 pf	+ 1	- 36 8 kHz	$1\ 34 \times 10^{-4}$
	+10	-372 0 kHz	$13\ 8 \times 10^{-4}$
L1 8.06 nhy	+ 0081 nh	- 30 0 kHz	1.11×10^{-4}
	+ 081 nh	-256.0 kHz	$9\ 35 \times 10^{-4}$
	+ 1 0 nh	- 2.6 MHz	$95\ 0 \times 10^{-4}$

where ω , R and C are the oscillator frequency, the source resistance, and the loading capacitance. The derivatives of ϕ with respect to C and R are given by

$$\frac{d\phi}{dC} = \frac{\omega R}{1 + (\omega R C)^2} \approx \frac{1}{\omega R C^2} \quad \text{for } \omega R C \gg 1 \quad (\text{D-1})$$

$$\frac{d\phi}{dR} = \frac{\omega C}{1 + (\omega R C)^2} \approx \frac{1}{\omega R^2 C} \quad \text{for } \omega R C \gg 1 \quad (\text{D-2})$$

Expressed in terms of fractional changes of the components

$$d\phi \approx \frac{dC}{C} \left(\frac{1}{\omega R C} \right) \quad \text{for } \omega R C \gg 1 \quad (\text{D-3})$$

$$d\phi \approx \frac{dR}{R} \left(\frac{1}{\omega R C} \right) \quad \text{for } \omega R C \gg 1 \quad (\text{D-4})$$

Thus the dependence of ϕ on fractional changes in either output impedance or loading capacitance can be reduced by greatly increasing R or C , which, of course, increases the phase shift towards 90°

In the single stage oscillator the amplifier is intended to have only the 180° phase shift, i e., capacitive loading is to be kept to zero. Under these conditions a picofarad of capacitive loading causes a serious change in the phase shift. In the two-stage oscillator, each stage has the normal 180° change plus intentional phase change of nearly 90° due to heavy capacitive loading. An additional picofarad of load capacitance pushes it only a very small amount closer to 90°. The two stages thus can give a net phase change of very near 180° (plus the 360° due to stage inversion). This phase change is relatively independent of capacitive loading and frequency. The delay line then provides the remaining 180° phase shift. Since this line shift is a function of line length and frequency, the line length chosen is the predominant frequency determinant.

The sensitivities given in Table D-I were derived from a computer program called ECAP* This program computes the magnitude and phase of each voltage and current in each node and branch at a specific frequency. When the phase at the last node just crosses through zero degrees (with respect to the input), oscillation would occur when output and input are joined. The program is run over a series of frequencies to determine the crossover point. The size of the frequency increments is successively reduced to 5 kHz and the crossover frequency is finally obtained by linear interpolation. In the program the circuit model used for the 2N3866 transistor, shown in Fig. D-1, is derived from the impedance vs frequency information on the transistor data sheet. The circuit closely approximates the data sheet information over the 200 to 300 MHz range, but for lower frequencies would have to be modified.

By way of comparison, the sensitivity of the LC oscillator will be presented. The frequency of oscillation for the circuit given previously in Fig. IV-9 is

$$\omega_o^2 = \frac{LG_1G_2 + C_1 + C_2}{LC_1C_2} \quad (D-5)$$

The approximation is given by

* Available from IBM

$$\omega_o \cong \frac{C_1 + C_2}{LC_1 C_2} \quad (D-6)$$

The sensitivity of this oscillator to parameter variations is given by

$$\frac{\Delta\omega}{\omega_o} = -\frac{1}{2} \left(\frac{\omega_1}{\omega_o} \right)^2 \frac{\Delta L}{L} \approx -\frac{1}{2} \frac{\Delta L}{L} \quad (D-7)$$

$$\frac{\Delta\omega}{\omega_o} = -\frac{1}{2} \left(1 - \frac{1}{\omega_o^2 LC_1} \right) \frac{\Delta C_1}{C_1} \quad i = 1, 2 \quad (D-8)$$

$$\frac{\Delta\omega}{\omega_o} = \frac{G_2 \Delta G_1}{2\omega_o^2 C_1 C_2} \quad \text{or} \quad \frac{G_1 \Delta G_2}{2\omega_o^2 C_1 C_2} \quad (D-9)$$

It can be seen that for a given assumed variation of ΔL , ΔC_1 , the sensitivities increase as frequency increases, since both L and C are decreasing with frequency. If we assume that $C_1 \approx C_2$, then Table D-II gives the Fractional Setting Error for 1 pf and 1 nh variations from the ideal.

Table D-II

FRACTIONAL SETTING ERROR FOR OSCILLATOR IN FIG IV-9
FOR $\Delta L = \pm 1$ nh, $\Delta C = \pm 1$ pf

Frequency f_o	L_1 nh	$\Delta f/f_o$	C_1 , pf	$\Delta f/f_o$
50 MHz	100	5×10^{-3}	200	1.9×10^{-3}
100 MHz	50	10×10^{-3}	100	3.8×10^{-3}
250 MHz	25	20×10^{-3}	32	11.7×10^{-3}

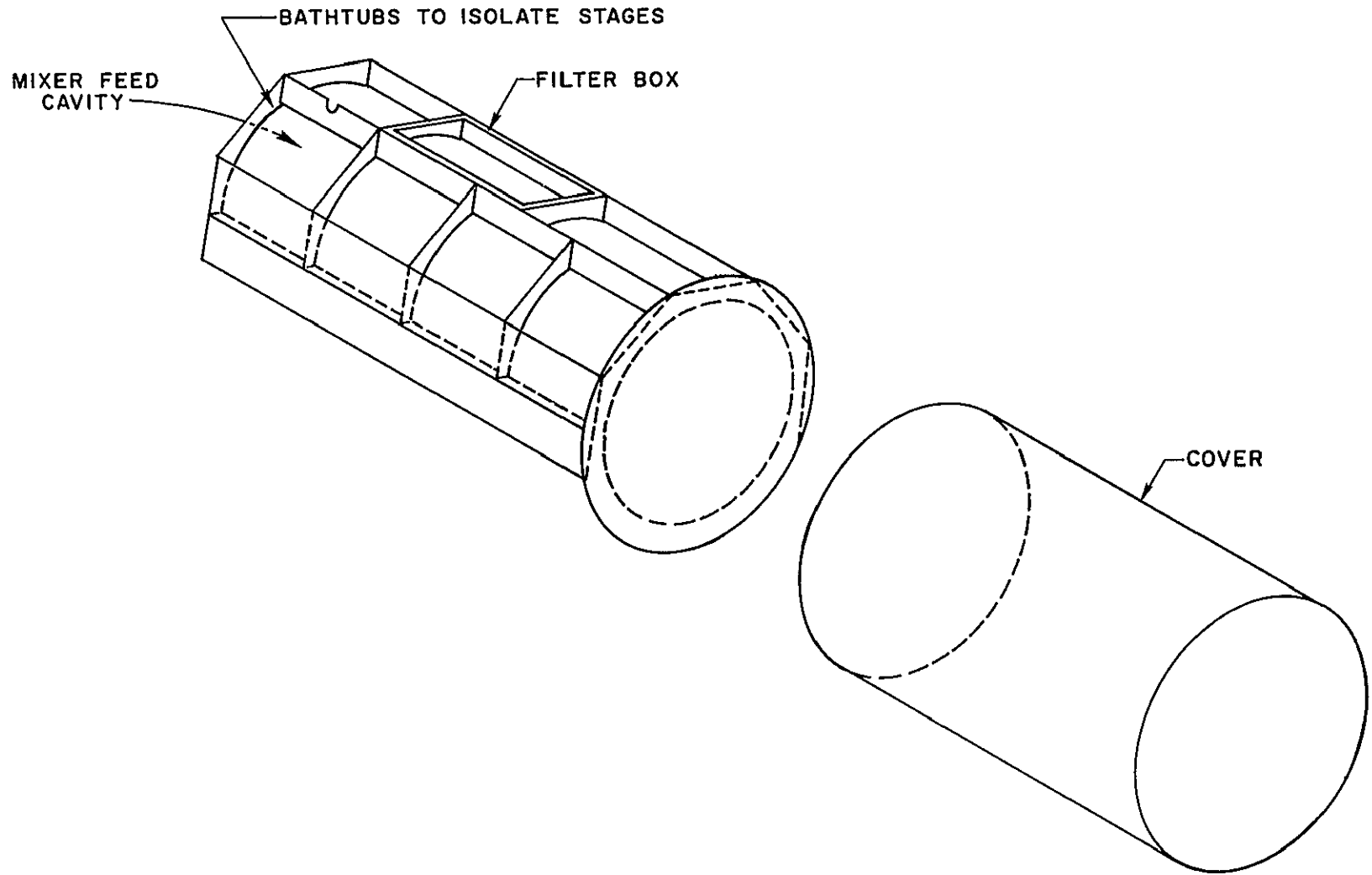
It can be seen from this table that a given percentage variation in these components gives a comparable error in the frequency. Obviously lumped circuit components could not be used with the normal tolerances, without adjustments.

E. ALTERNATE LAYOUTS FOR MIXER-FEED HOUSING

The basic ideas of several alternate layouts are shown in Figs E-1, E-2, and E-3. In the first case, it was thought that the various circuit boards could be long and thin, and that isolation compartments could be provided for one or two circuits at a time by casting them on the outside of the mixer-feed, as shown in Fig E-1. There would be very little problem with interconnections. The configuration is still a reasonable one, but it was set aside in favor of the present layout because there was not enough time to proceed with the layout of the individual circuit boards for this arrangement, this was necessary in order to determine the position of compartments and the details of interconnections so that a good working model could be made. The present layout offers more flexibility in choice of circuit board position and circuit allocation, and may be less expensive to cast than the housing in Fig E-1.

The other two layouts are only variations on the present layout. In Fig. E-2, the electronics circuit box and the upper half of the housing are cast as one piece, in order to avoid having to use RF gasket material at the joints of each of the isolation webs, as will have to be done with the present layout. But the casting is a little more difficult because of the extra depth, and the mixer-diode-to-IF amplifier interconnection problem is not easily handled, even if the circuit boards are rearranged so that they all are parallel to the axis of the cylindrical cavity. The half cylinder is needed in order to mount the mixer diode and the matching stubs.

The third alternative, as shown in Fig. E-3, shows the circuit boards stacked in horizontal planes, with the LO and IF boards on the top half, and the signal processor and discriminator boards on the bottom. This configuration would still require a top cover for the filter insert. Although the filter insert could be put in from a hole in the rear wall of the electronics box, it would have to be a press fit to insure good electrical contact between the support ring and the two ground planes, in the present configuration, this good contact is insured by screwing down the top cover to the circular cavity. (It should



173

Fig E-1 WRAPAROUND CONFIGURATION

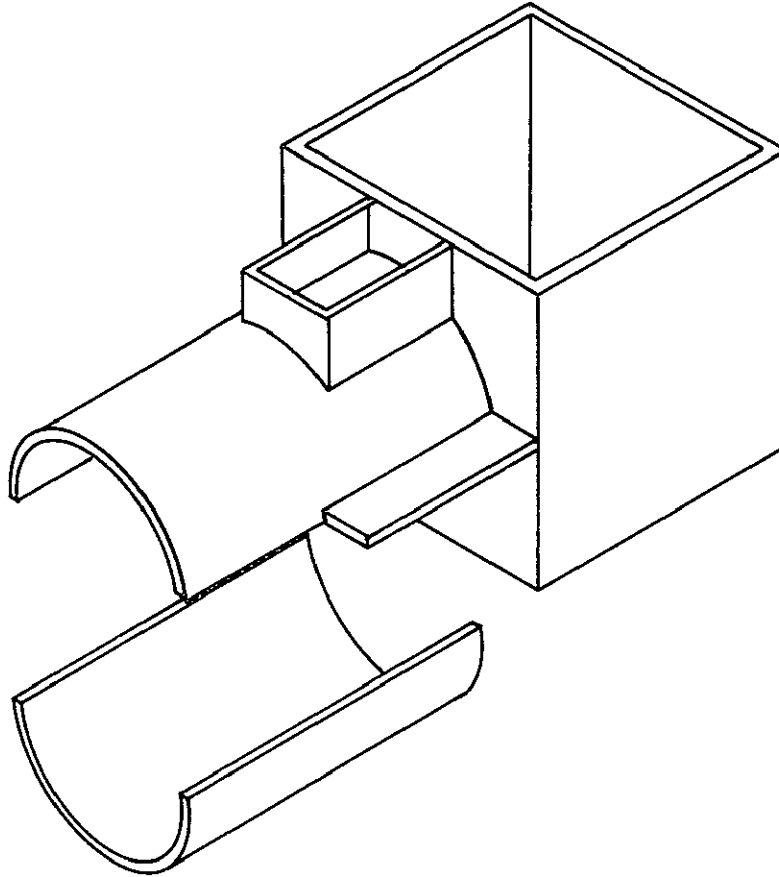


Fig E-2 COMPLETE ELECTRONICS COMPARTMENT, HALF CYLINDER

be riveted in production) The same thing should be done with this alternate configuration This configuration is the easiest to modify the size of circuit boards with the least effect on the housing.

It is the best alternative to date It is not rejected, but there are no major stumbling blocks with the present configuration which this one solves

F. CIRCULAR WAVEGUIDE ACCESSORIES AND THE "PERFECT" TRANSITION

The mode of propagation selected for the mixer-feed is the Transverse Electric (TE_{11}) mode, this mode is easily excited by a radial

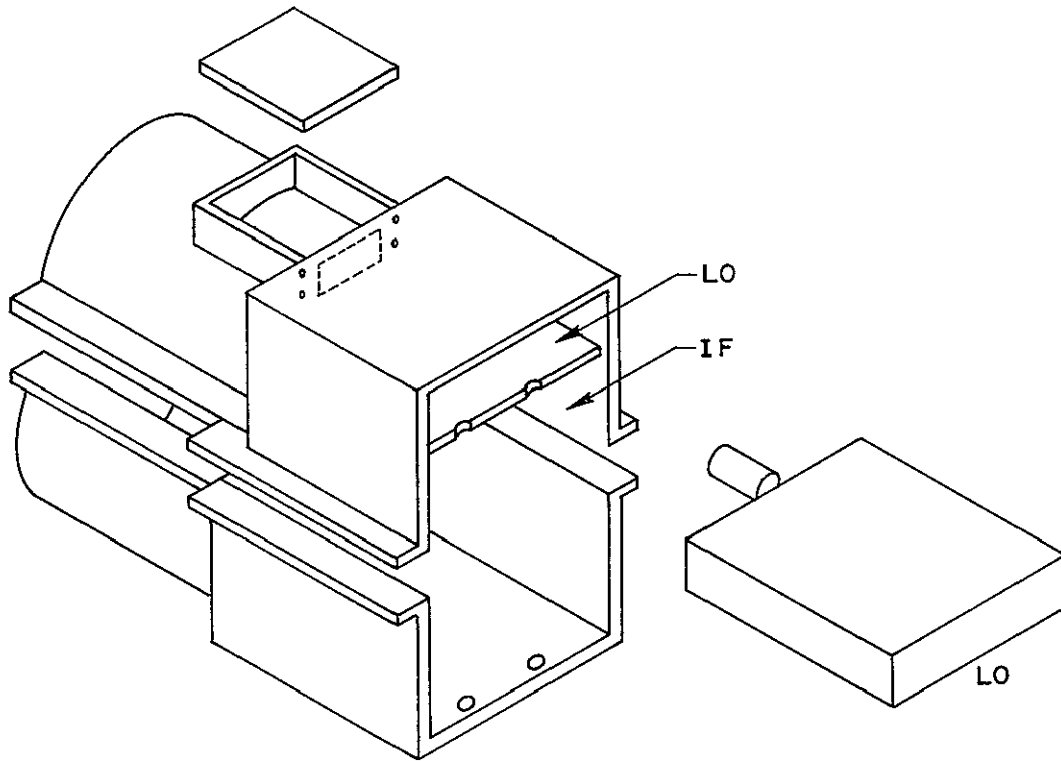


Fig. E-3 SPLIT HOUSING WITH CIRCUIT BOARDS MOUNTED IN A HORIZONTAL PLANE.

probe mounted some distance away from the wall of the circular waveguide, as shown in Fig F-1. The probe is cylindrical and rounded at both ends to reduce the amplitude of the degenerate modes which exist to match the boundary conditions. The basic arrangement shown in Fig F-1 was modified by making the probe position adjustable and the rear wall adjustable by using a plunger with small finger stock around it to form a good electrical contact.

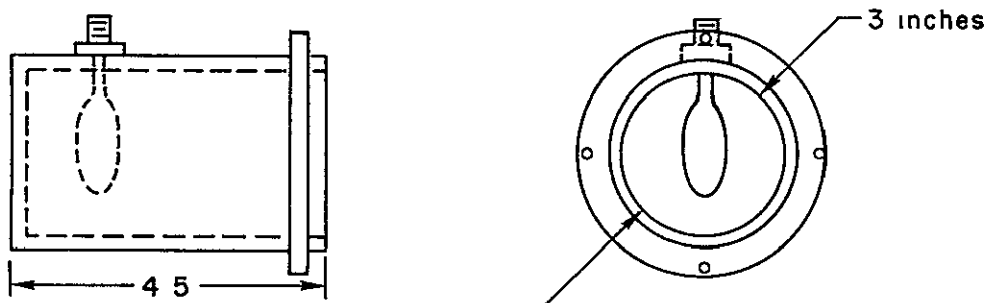


Fig. F-1. COAX-TO-WAVEGUIDE TRANSITION

The experimental mixer relied on matching the 2620 MHz signal source from coax to the waveguide with a double stub tuner, in the final installation, there would be no coax-to-waveguide transition, only a waveguide-to-free space transition. Therefore it is necessary to do all the impedance-matching within the waveguide. It is desirable that the matching structures designed and tested in the laboratory also be usable in the final waveguide to free-space assembly at the antenna. Therefore a perfect transformer which matches 50-ohm coax systems to the waveguide impedance is necessary. Complete adjustment of the mixer-feed at the antenna will have required two matching operations one to match the waveguide to free space, and one to match the mixer diode to the waveguide for best noise figure. Because we are working in the laboratory first, matching the diode to the waveguide has been done first. Matching of the entire mixer-feed cavity to free space will be done presently.

The perfect transformer was constructed as follows. A conical waveguide load was first constructed by pouring an iron-filled epoxy (castable-F Resin) into a mylar cone supported in sand. The load was then used to terminate a 7-foot length of circular waveguide, as shown in Fig F-2. A short distance from the load, 5 probes were inserted into the guide to sample the E-field at eighth-wave intervals. This method was used instead of the slotted line because our slotted line

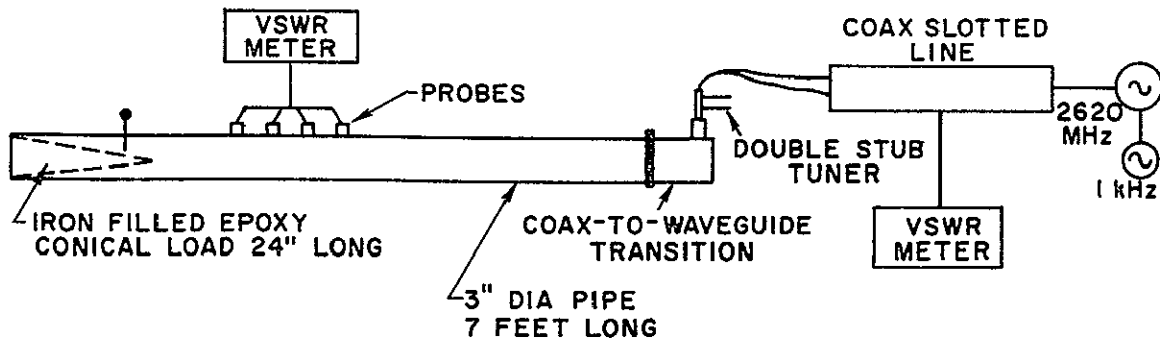


Fig F-2 ALIGNMENT SETUP FOR THE "PERFECT" TRANSITION

was too short and suffered from slot effects * A tuning screw was installed in the waveguide near the apex of the conical load, and was adjusted until there was less than a 0.5 dB variation in probe readings. This provides a near-perfect, reflectionless load. A perfect transformer is obtained from the probe-launch assembly by adjusting the double-stub-tuner for minimum VSWR on the coaxial slotted line. All the positions and critical dimensions are noted and maintained.

This perfect transformer is now installed on the mouth of the mixer-feed cavity. When the load at the end of the mixer cavity, namely the diode, is matched to waveguide impedance (1066 ohms), this perfect transformer couples all the signal power into the guide. The diode support structure has been matched to the waveguide by this method with a short rod (0.85 inches) mounted 0.90 inches in front of the diode structure.

G THE 2.62 GHz WIDEBAND FM TEST SIGNAL SOURCE

A 262 MHz oscillator capable of ± 1.5 MHz frequency deviations at high modulation rates has been built using a field effect transistor for the modulator and a voltage-variable capacitor in a common-base Colpitts bipolar oscillator. The circuit diagram is shown in Fig. G-1. A Field Effect Transistor is used as a buffer output stage.

This oscillator-buffer drives a 3 stage power amplifier chain which in turn drives a Hewlett-Packard step-recovery diode module. The 10th harmonic is selected in an interdigital filter similar to the one used in the Local Oscillator chain. The result is a ± 15 MHz deviation at 2620 MHz, at modulation rates to 6 MHz, which is adequate.

* E. M. Purcell, "Measurement of Standing Waves," Technique of Microwave Measurements, M.I.T. Rad Lab Series, Edited by C. G. Montgomery, Boston Technical Lithographers, Inc., Lexington, Mass., 1963, p. 482.

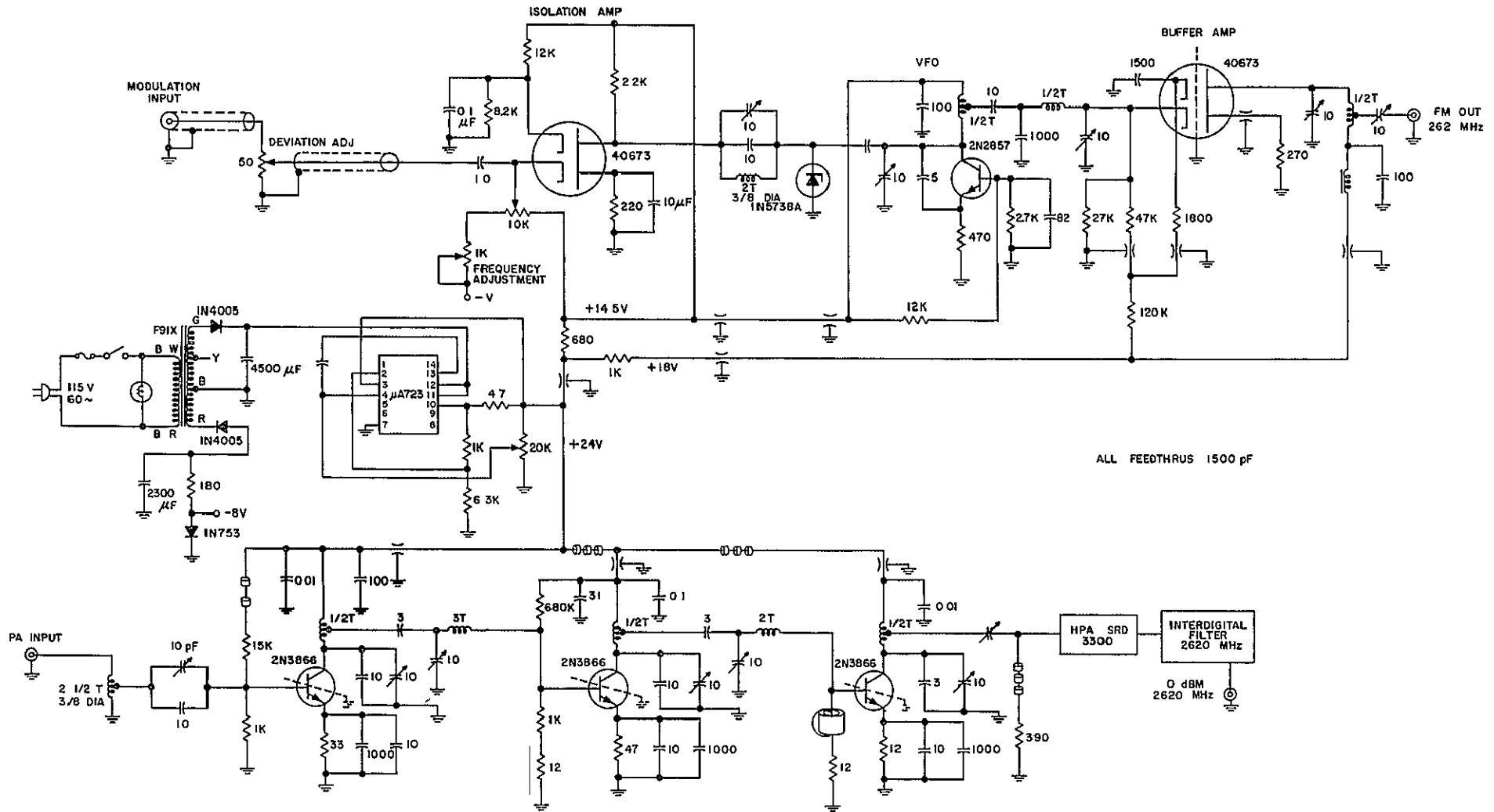


Fig G-1 SCHEMATIC DIAGRAM FOR THE 2.62 GHz WIDEBAND FM TEST SIGNAL SOURCE

H DISCRIMINATOR DESIGN

The circuit diagram for the transmission line discriminator is given in Fig. H-1. The transfer function may be derived as follows

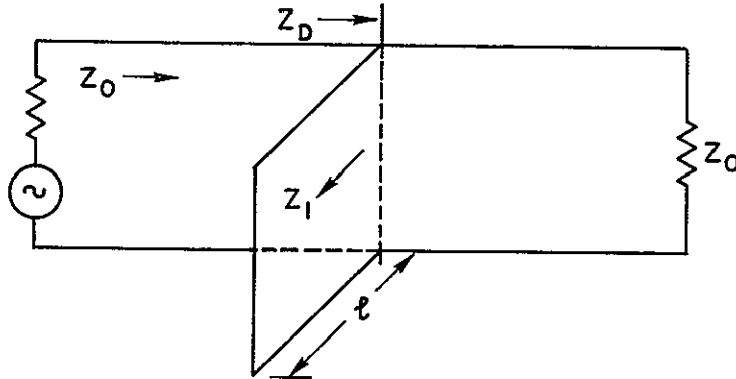


Fig H-1. CIRCUIT DIAGRAM OF THE TRANSMISSION LINE DISCRIMINATOR.

The impedance at the discontinuity is Z_D , the parallel combination of Z_1 and Z_0 . The voltage transmitted to the total impedance discontinuity is proportional to

$$\frac{E_t^+}{E_{\text{Incident}}^+} = \frac{2Z_D}{Z_D + Z_0} = \tau \quad (\text{H-1})$$

Knowing that the shunt load Z_1 will be a shorted or opened line and will thus not dissipate any power, this transmission coefficient will represent the total amount of power delivered to the matched load arm of the discontinuity. Thus we may write

$$E_{\text{Load}} = \tau E_{\text{Incident}}$$

or

$$E_L = \frac{2}{1 + \frac{Z_0}{Z_D}} E_{\text{IN}} \quad (\text{H-2})$$

since

$$Z_D = \frac{Z_1 Z_0}{Z_0 + Z_1}$$

$$\begin{aligned} \frac{E_L}{E_{IN}} &= \frac{2}{1 + \frac{Z_0(Z_0 + Z_1)}{Z_0 Z_1}} \\ &= \frac{2Z_1}{2Z_1 + Z_0} \\ &= \frac{E_{IN}}{1 + \frac{Z_0}{2Z_1}} \end{aligned} \tag{H-3}$$

since $Z_1 = jZ_0' \tan \beta l$ for a shorted line,

$$\frac{E_L}{E_{IN}} = \frac{1}{1 - j \frac{Z_0}{2Z_0'} \cot(\beta l)} \tag{H-4}$$

We are interested in the actual voltage measured, and by taking the absolute value, we have

$$\left| \frac{E_L}{E_{IN}} \right| = K_1 \left[1 + K_2^2 \cot^2 \frac{2\pi \ell}{c} f_1 \right]^{-1/2} \tag{H-5}$$

where

K_1 = Detector Efficiency Constant

$K_2 = Z_0 / 2Z_0'$

ℓ = Line Length

c = Velocity of Propagation

f_1 = Frequency of Input Signal

Discriminator action is more clearly represented if Eq. (H-5) is rewritten as

$$\frac{E_L}{E_{IN}} = K_1 \left[1 + K_2^2 \cot^2 2\pi \left(\frac{N}{8f_o} \right) f_1 \right]^{-1/2} = E(f) \quad (H-6)$$

where

$$\frac{\ell}{C} = \frac{N}{8f_o}$$

The ℓ/C term corresponds to a particular period τ or frequency f_o at which the line is a wavelength long. However, we wish to operate at a frequency f_o for which the line length is some odd multiple of $\lambda/8$ in order to be on the most linear portion of the characteristic. It will be shown that the sensitivity of the discriminator increases as N increases, but for a constant peak deviation of ± 12.5 MHz about a fixed IF of 120 MHz, the linearity decreases. Thus we pick the largest N (greatest length) which gives a distortion less than some arbitrary upper limit, such as 3%.

The linearity of the discriminator can be adjusted by varying the characteristic impedance Z_o' of the line. The optimum value is defined as that Z_o' which gives the least variation in the first derivative of $E(f)$ over the largest frequency range. It can be determined in the following manner:

The line length is such that the operating frequency f_o is midway between the extrema of the discriminator characteristic. We require that the discriminator characteristic be as linear as possible through the operating point, this implies that the first derivative $dE(f)/df$ be as constant as possible. [In other words, if we were expressing $E(f)$ in a power series about f_o , we would want the coefficients of all terms of second order and higher to be as small as possible. They

will never be zero, since $E(f)$ is infinitely differentiable, but they can be minimized] This can be done by requiring that the point of inflection of $E(f)$ also occur at f_0 . The point of inflection is given by $d^2E(f)/df^2 = 0$. When this is done, the first derivative is symmetric about f_0 and the variation over any symmetric range is the smallest possible. We now find K_2^2 from the condition $d^2E(f)/df^2 = 0$. The first derivative is given by

$$\frac{dE(f)}{df} = \frac{K_1 K_2^2 (2\pi N/8f_0) \cot 2\pi \frac{N}{8f_0} f_1 \operatorname{CSC}^2 2\pi \frac{N}{8f_0} f_1}{\left[1 + K_2^2 \cot^2 2\pi \left(\frac{N}{8f_0}\right) f_1\right]} E(f) \quad (\text{H-7})$$

After substituting $\tau = 2\pi N/8f_0$, the second derivative is given by

$$\frac{d^2E(f)}{df^2} = \frac{K_1 K_2^2 \tau^2 E(f)}{\left[1 + K_2^2 \cot^2 \tau f_1\right]^2} \left[K_2^2 \cot^2 \tau f_1 \operatorname{CSC}^2 \tau f_1 (3\operatorname{CSC}^2 \tau f_1 - \tan^2 \tau f_1 \operatorname{CSC}^2 \tau f_1 - 2) - 2 \cot^2 \tau f_1 \operatorname{CSC}^2 \tau f_1 - \operatorname{CSC}^4 \tau f_1 \right] = 0 \quad (\text{H-8})$$

At $f_1 = f_0$, $\cot^2 \tau f_1 = 1$, $\operatorname{CSC}^2 \tau f_1 = 2$, $\operatorname{CSC}^4 \tau f_1 = 4$, solving for K_2^2 , we have

$$K_2^2 = 2$$

or

$$Z_0' = \frac{Z_0}{2\sqrt{2}}$$

We must now specify the length of the line to get the greatest sensitivity without exceeding an arbitrary 3% distortion limit. Distortion is given by

$$\% \text{ Distortion} = \frac{E(f_1) - E(f_2) - \frac{dE(f_o)}{df} (2\Delta f_{\max})}{E(f_1) - E(f_2)} \times 100 \quad (\text{H-9})$$

where

$$f_1 = f_o - \Delta f_{\max}$$

$$f_2 = f_o + \Delta f_{\max}$$

$$\frac{dE(f_o)}{df} = \text{the slope of } E(f) \text{ evaluated at } f_o$$

The maximum deviation is ± 12.5 MHz. The distortions for line lengths of $\lambda/8$, $3\lambda/8$, and $5\lambda/8$ are given in Table H-I. ϕ_1 and ϕ_2 are the angular equivalents of f_1 at the extremes of frequency excursion.

Table H-I

N	ϕ_1	ϕ_2	$\Delta\phi$	$\frac{dE(f_o)}{df}$	$\frac{(12.5)}{10^6} \cdot E'(f_o)$	$\frac{E(f_1) - E(f_o)}{E(f_o)}$	$\frac{E(f_2) - E(f_o)}{E(f_o)}$	Ave % Distortion
1	40.4	49.6	9.2	503×10^{-9}	.063	-0.063	+0.062	1.6%
3	121	149	28	15.1×10^{-9}	.189	.185	-0.186	1.89%
5	202	249	47	25.2×10^{-9}	.315	-.292	.303	5.91%

The best choice is for $N = 3$, with a distortion of 1.89% and a relative sensitivity of 15.1×10^{-9} V/Hz.

It remains only to specify the impedances Z_o and Z_o' . 17 ohms is obtainable with wide strips, and so a 50 ohm Z_o is feasible.

PRECEDING PAGE BLANK NOT FILMED

REFERENCES

- 1 Bayless, R E , et al , "Comparative Analysis of Point-Contact and Schottky Barrier Diodes," Microwave Exposition, New York, New York, June 7, 1967
- 2 Blaser, L , and J S MacDougall, "Applications of the Silicon Planar Field Effect Transistor," Fairchild Applications Bulletin, December 1964
- 3 Conley, P , Experience Curves as a Planning Tool, IEEE Spectrum, June 1970.
- 4 Cote, A J., Matrix Analysis of Oscillators and Transistor Applications, IRE PGCT, September 1959
- 5 Feldman, N , Communications Satellite Output Devices, 8 Microwave J , December 1965
- 6 Getsinger, W J , Coupled Rectangular Bars Between Parallel Plates, MTT-10, January 1962
- 7 Hakim, S. S , Feedback Circuit Analysis, John Wiley and Sons, New York, New York, 1966
- 8 Harvey, A F , Mechanical Design and Manufacture of Microwave Structures, PG-MTT, October 1959
- 9 Hewlett-Packard, "Harmonic Generation Using Step Recovery Diodes and SRD Modules," Application Note 920, Palo Alto, 1968
- 10 International Radio Consultative Committee, Documents of the XIth Plenary Assembly in Oslo, 1966, Vol IV, Part 2, Space Systems and Radioastronomy, International Telecommunications Union, Geneva, 1967
- 11 International Telephone and Telegraph Corp , Reference Data for Radio Engineers (4th Ed. H. P. Westman 1956)
- 12 Janky, J M , Low-Cost Receivers and the Use of Direct Broadcast Satellites for Instructional Television, Stanford Journal of International Studies, Vol 5, June 1970
- 13 Jasik, H (Ed), Antenna Engineering Handbook, McGraw-Hill Book Co , Inc , New York, 1961
14. Lee, C W , An Analysis of a Super Wide-Band FM Line Discriminator, Proc IEEE, September 1964
- 15 Lerner, R M , Bandpass Filters with Linear Phase, Proc IEEE, March 1964

Preceding page blank

- 16 Linvill, J. G , and J Gibbons, Transistors and Active Circuits, McGraw-Hill Book Co , Inc., New York, 1961
17. Matthaei, G. L , Interdigital Band-Pass Filters, MTT-10, November 1962.
- 18 Mouw, R B , and S M. Fukuchi, Broadband Double-Balanced Mixer/Modulators, Part I, 12 Microwave J , March 1969
- 19 Pope, D. L , Parametric Representation of Ground Antennas for Communications Systems Studies, BSTJ, December 1968
- 20 Pound, R V., Microwave Mixers, MIT Radiation Laboratories Series No. 16, Boston Technical Publishers, Lexington, Mass., 1947
21. Pyle, J R , Design Curves for Interdigital Band-Pass Filters, MTT-12, September 1964
22. Ramo, Whinnery, and Van Duzer, Fields and Waves in Communication Electronics, John Wiley and Sons, New York, New York, 1965.
23. Ruthroff, C L , Some Broadband Transformers, Proc IRE, August 1959
- 24 Ruze, J , Antenna Tolerance Theory - A Review, Proc. IEEE, April 1966
25. Schwartz, Mischa, Information, Transmission, Modulation, and Noise, McGraw Hill Book Co., New York, New York, 1959
- 26 Slurzburg, M , W Osterheld and E. N Voegtlin, Essentials of Television, McGraw-Hill Book Co., Inc , New York, 1956
27. Stanford School of Engineering, Advanced System for Communication and Education in National Development, Stanford University, June 1967.
28. Strum, P. D., Some Aspects of Mixer Crystal Performance, Proc IRE, Vol. 41, July 1953.
- 29 Sunde, E D , Communications Systems Engineering Theory, John Wiley and Sons, New York, 1969.
30. Texas Instruments, Inc , Circuit Design for Audio, AM/FM, and TV, McGraw-Hill Book Co , New York, 1967
31. Torrey, H C , and C A Whitmer, Crystal Rectifiers, MIT Radiation Laboratory Series, No. 15, Boston Technical Publishers, Lexington, Mass , 1947
- 32 Vossburg, W. A., Stripping the Mystery from Strip-Line Laminates, Microwaves, January 1968

33. Wright, R T and S. T Smola, "Performance Characteristics of Philco-Ford Microwave Schottky Barrier Diodes," Microelectronics Applications Report No. 300, Blue Bell, Pennsylvania, July 1968

REPORT DISTRIBUTION LIST
Contract NAS 12-690

<u>No of Copies</u>		<u>No of Copies</u>	
	NASA Headquarters		Hughes Aircraft Company
	Washington, D C 20546		Space Systems Division
1	Attn SA/L Jaffe		1194 W Jefferson Blvd
1	SC/R B Marsten		Culver City, Calif , 90230
1	SCC/A M G Andrus	1	Attn R W Walp
1	SCE/D Silverman		
	NASA Lewis Research Center		Communications & Sys , Inc
	21000 Brookpark Road		6565 Arlington Boulevard
	Cleveland, Ohio 44135	1	Falls Church, Virginia 22046
1	Attn C. C Conger (M S 54-1)		Attn J Bisaga
1	R E Alexovitch (M S 54-5)		
1	P W Kuhns (M S 54-5)		TRW Systems
1	E H Davison (M S. 54-5)		One Space Park
	Technology Utilization	1	Redondo Beach, Calif , 90278
1	Officer (M.S. 3-19)		Attn J Jansen
1	Library (M S 60-3)		
	Report Control Office		Rand Corporation
1	(M S 5-5)		1700 Main Street
1	N T Musial (M S. 500-311)	1	Santa Monica, Calif , 90404
	Rockets & Spacecraft		Attn Dr J Holt
	Procurement Section		
1	(M S 500-313)		Fairchild-Hiller
	NASA Goddard Space Flight Center		Space & Electronics Sys Div
	Greenbelt, Maryland 20771	1	Sherman Fairchild Tech Center
	Attn 733/John E Miller		Germantown, Maryland 20767
1	Library		Attn Samuel Folley
	NASA Ames Research Center		Communications Satellite Corp
	Moffet Field, California 94035	1	1835 K Street, N W
	Attn OART-MAD/E. VanVleck		Washington, D C. 20036
1	(M S 202-6)		Attn Dr. W Pritchard
	NASA Scientific and Technical		U S Information Agency
	Information Facility	1	25 M Street, S W
	Box 33		Washington, D C 20547
	College Park, Maryland 20740		Attn IBS/EF/G Jacobs
3	Attn NASA Representative		
	General Dynamics/Convair Div	1	Federal Communications Comm
	P. O Box 1128		521 12th Street
	San Diego, California 92112		Washington, D C 20554
1	Attn J A. Fager		Attn H Fine
		1	Communication Research Cent
			Department of Communications
			Ottawa, Canada
		1	Attn Collin Franklin, Library

No of
Copies

No of
Copies

1	General Electric Company Space Division Valley Forge Space Technology Center P O Box 8555 Philadelphia, Penn 19101 Attn R Hesselbacher	1	Mr Robert Bruce Director of Policy Planning Public Broadcast Service 955 L'enfant Plaza, S.W Washington, D C
1	General Electric Company Electronics Park Syracuse, New York 13201 Attn J P Hesler Bldg 3, Rm 119	1	Mr Arthur D Morse Executive Director International Broadcast Inst Via del Corso, 525 00186 Rome, Italy
1	Executive Office of the President Office of Telecommunications Management Washington, D C 20504 Attn ODTM/Donald Jansky	1	Dr Edward F Miller National Aeronautics and Space Administration Lewis Research Center--M.S 54-5 21000 Brookpark Road Cleveland, Ohio 44135
1	Agency for International Dev Room 2485 21st and Virginia Avenue, N.W Washington, D C 20523 Attn Dr Cliff Block		
1	National Library of Medicine Bethesda, Maryland 20014 Attn Dr Ruth Davis		
1	International Development Technology Program Washington University Box 1140 Saint Louis, Missouri 63130 Attn Dr R. P. Morgan		
1	Mr. Edward W. Ploman Director, International Relations Swedish Broadcasting Corporation Stockholm 1, Sweden		
1	Professor Iskandar Alisjahbana Head, Department of Electrotechnical Engineering Bandung Technical Institute Dj Sangkuriang 26 Bandung, Indonesia		